The prediction of the NO_x emissions of a 4-stroke marine diesel engine equipped with exhaust gas recirculation

Using a mean value simulation model

M.A.J. van Riet

Delft University of Technology
SDPO.18.035.m

TU Delft

JUMBO

The prediction of the NO_X emissions of a 4-stroke marine diesel engine equipped with exhaust gas recirculation

Using a mean value simulation model

by

M.A.J. van Riet

to obtain the degree of Master of Science
at the Delft University of Technology,
to be defended publicly on Tuesday August 28, 2018 at 10:00 AM.

Student number:	1512013	
Report number:	SDPO.18.035.m	
Project duration:	May 1, 2017 – August 28, 2018	
Thesis committee:	Ir. K. Visser, Rear-Admiral(ME) ret.,	TU Delft, Chairman
	Ir. P. de Vos,	TU Delft, Supervisor
	Ir. K. van der Heiden,	Jumbo Maritime, Supervisor
	Ir. M.B. Duinkerken,	TU Delft, External

An electronic version of this thesis is available at http://repository.tudelft.nl/.

TU Delft JUMBO

Preface

With this thesis, I complete my Master's programme Mechanical Engineering at the Delft University of Technology. More than a year of hard work at the Jumbo Maritime office, the university and at home have resulted in this work. And I couldn't have done it all by myself.

I would like to thank Peter de Vos for being my daily supervisor for this project. I learned a lot from him during our meetings and when I was stuck, he always came with a different angle of approach to point me in the right direction. I also want to thank Klaas Visser for being the head of my graduation committee. We only had a few meetings together, but thanks to his input these meetings were really productive. Finally, I want to thank the external committee member, Mark Duinkerken, for taking the time to be a part of my graduation committee.

Then I want to thank Jumbo Maritime for giving me the opportunity to conduct my research there. From Jumbo Maritime, I would especially like to thank Kasper van der Heiden, my other supervisor, for providing me with guidance during every step of my research and also for his input and vital insights. Special thanks go out to my fellow students at Jumbo Maritime, Duke, Joeri, Sjoerd, Lex and Kostas. I want to thank them for their support, their company and most of all for the fun and coffee breaks we had together.

Last but certainly not least, I want to thank the people who have always supported me unconditionally. Of course, I am talking about my parents and my brother and sister. Thanks for the support, the nice homecomings, and always being there for me.

Michel van Riet
Delft, August 2018

Abstract

Due to their efficiency and high power density, large-bore diesel engines are widely used in ships and power plants even though they produce high amounts of polluting emissions. Therefore the regulations regarding polluting emissions are becoming more and more stringent. One of the latest regulations is the IMO Tier III legislation, which entered into force in 2016 and it requires a reduction of NO_x emissions of 70% compared to the Tier II legislation. This most recent legislation is intended for all ships sailing in so-called NO_x Emission Control Areas (NECA). Existing NECA's are the North American and U.S. Caribbean emission control areas, but IMO has already designated the Baltic Sea and the North Sea as emission control areas for nitrogen oxides for ships with keel-laying on or after 1 January 2021. In order to meet the NO_x requirements several compliance methods are available.

One method to comply with the new legislation is exhaust gas recirculation (EGR), which is already a mature technology in the automative and land-based industry. The formation of NO_x requires a high amount of oxygen and a high temperature. The working principle of EGR is based on lowering the concentration of oxygen in the combustion chamber and increasing the specific heat of the combustion mixture. This is achieved by recirculating part of the exhaust gas, which consists mainly of inert gases and a low percentage of oxygen, back into the combustion chamber. If low-pressure EGR is applied, the exhaust gas is expanded through the turbine and after it has been cooled, it is mixed with the fresh air entering the engine. If a high-pressure EGR configuration is implemented the EGR loop already starts upstream of the turbine and re-enters the engine cycle after the compressor.

This research focusses on two main objectives: the first one is to gain insight in the behaviour of 4-stroke marine diesel engine equipped with EGR. Secondly predictions will be made of the NO_x emissions after the implementation of EGR. In order to achieve these objectives an extensive literature study has been conducted to review the formation of NO_x in diesel engines, the reaction kinetics and the factors that influence the NO_x emissions. A mean value first principle model in the MATLAB/Simulink environment is used to simulate the implementation of the two different EGR configurations.

The effects of EGR were different than expected. The amount of oxygen in the engine is described by the flow of fresh air into the engine and the air excess ratio. With the implementation of EGR these engine parameters showed decreases up to 40% for an EGR rate of 50%. The other important factor for the formation of NO_x is the maximum combustion temperature. Despite an increasing EGR rate, causing an increase in specific heat for the combustion mixture, the temperature only showed a small decrease for the high-pressure EGR configuration. The low-pressure configuration even showed a small temperature rise. The reason for the temperature rise is the control strategy of the diesel engine model. The speed of the engine is kept constant at 600 rpm and the load is varied from 10% to 100%. If the desired power output is not reached, more fuel is injected to still achieve the desired power. This results in more heat release and as a result also a small temperature rise. A different control strategy, which could be dependent on speed and fuel, would result in a temperature drop.

The second objective is to predict the NO_x emissions of the engine when it is equipped with EGR. In order to achieve this a nonlinear regression model was used to fit the available emission data with a specific set of engine parameters. The implementation of EGR causes changes in the engine parameters and this way the fits can be used to make an estimate of the NO_x emissions. Reductions up to 70% are achieved for an EGR rate of 50%. What must be kept in mind is that no observational NO_x emission data is available for a similar engine equipped with EGR. Until such data becomes available the predictions cannot be estimated. Altogether it can be concluded that the use of an nonlinear regression model is an excellent method to fit a set of emission data with diesel engine parameters. The predictions look promising although they are not validated yet.

Contents

List of Figures

List of Tables

Nomenclature

Roman variables

Symbol	Name	Unit
afr	Air/fuel ratio	-
$bmep$	Brake mean effective pressure	bar
$bsfc$	Brake (power) specific fuel consumption	g/kWh
c	Specific heat polytropic process	kJ/kgK
c_p	Specific heat at constant pressure	kJ/kgK
c_v	Specific heat at constant volume	kJ/kgK
D_B	Bore diameter	m
h^L	Lower heating value	kJ/kg
i	Number of cylinders	-
k	Number of revolutions per cycle	-
L_S	Stroke length	m
M	Torque	Nm
m	Mass	kg
$\dot{m}$	Mass flow	kg/s
n	Engine speed	rpm or rps
P	Power	kW
p	Pressure	kPa or bar
R	Gas constant	kJ/kgK
S	Entropy	kJ/K
s	Slip factor	-
sfc	Specific fuel consumption	g/kWh
T	Temperature	K
X	Fuel rack position	mm
x	Air mass fraction	kg/kg

Greek variables

Symbol	Name	Unit
ϵ	Geometric compression ratio	-
η	Efficiency	-
κ	Isentropic index	-
λ	Air excess ratio	-
σ	Stoichiometric air to fuel ratio	-

Subscripts

Symbol	Name
a	air
a	at compressor inlet (air filter outlet)
amb	ambient
B	bore
b	at compressor outlet (charge-air cooler inlet)
c	at inlet receiver (charge-air cooler outlet)
cyl	cylinder
d	at exhaust receiver (turbine inlet)
e	at turbine inlet (exhaust silencer inlet)
eng	engine
EGR	Exhaust Gas Recirculation

f	fuel
fresh	fresh air entering cylinder
g	gas
in	total into the system
inl	at inlet duct
is	isentropic
max	maximum average
min	minimum
nom	nominal
S	Stroke
sg	stoichiometric gas
slip	slip flow

Abbreviations

CFD	Computational fluid dynamics
CIMAC	Conseil International des Machines A Combustion
CO	Carbon monoxide
CO_2	Carbon dioxide
COM	Compressor
CYL	Cylinder
ECA	Emission Control Area(s)
EIAPP	Engine International Air Pollution Prevention
EGR	Exhaust gas recirculation
FAT	Factory acceptance test
HAM	Humid Air Motor
HCCI	Homogeneous Charge Compression Ignition
HFO	Heavy Fuel Oil
HC	Hydrocarbons
IMO	International Maritime Organisation
IR	Inlet Receiver
LSF	Low-Sulphur Fuel
MARPOL	Marine Pollution (Treaty)
MDO	Marine Diesel Oil
MGO	Marine Gas Oil
MEPC	Marine Environment Protection Committee
MVFP	Mean Value First Principle
NO_x	Nitrogen oxides
OR	Outlet Receiver
PM	Particulate matter
RMSE	Root Mean Squared Error
SCR	Selective Catalytic Reduction
SSE	Sum of Squares due to Error
SSR	Sum of Squares of the Regression
SST	Total Sum of Squares
TC	Turbocharger
TUR	Turbine
VGT	Variable Geometry Turbocharger
VVA	Variable Valve Actuation

1 Introduction

1.1. Research background and relevance

Due to their efficiency and high power density, large-bore diesel engines are widely used in ships and power plants. Due to their high efficiency, diesel engines emit a relatively small amount of carbon dioxides. The downside is that they produce relatively high amounts of harmful emissions, in particular NO_x. These pollutant emissions can cause serious harm to the ecological environment and human health.

Because of these effects this has been an issue of high concern for the International Maritime Organization (IMO), the Marine Environmental Protection Committee(MEPC), the World Health Organization and other agencies and governments. In was already in 1997 that the IMO adopted an international convention protocol to reduce the polluting emissions from ships in order to achieve a sustainable maritime development[18]. The protocol has been approved by 15 member countries an it came into force in 2005. From then on pollutants emitted from ships, like nitrogen oxides, volatile organic compounds, sulphur oxides etc. will be regulated by that convention through ship inspections and issuance of certificates.

For the successful implementation of these safeguards, legislative support is necessary. It is therefore suggested that the administration of both navigational and environmental protection cooperate in the revision of relevant federal laws, to implement the provisions of the MARPOL(Marine Pollution) convention. MARPOL arose in the 1970's out of the efforts of the IMO to protect the environment from pollution from ships. Since the 1970's, a number of conventions have been adopted and the six annexes have been developed, all addressing specific areas of concern to international maritime pollution problems. Annexes I to V contain the prevention of pollution by oil, harmful substances, sewage and garbage. Annex VI was adopted to prevent the air pollution from ships. These annexes ensure that the pollutant emissions from ships can be effectively controlled.

But controlling the air pollution from ships is more difficult than it sounds. It is known that more than 50% of a vessel's operating expenses consist of the cost of fuel oil. Most of the world's shipowners use degraded residue heavy fuel oil to propel their ships. These heavy fuel oils, or HFO's, contain high levels of asphalt, carbon residues, sulphur and certain metallic compounds. When they are burned, HFO's produce significant amounts of carbon dioxide (CO_2), carbon monoxide (CO), sulphur oxides (SO_x), nitrogen oxides (NO_x), unburned hydrocarbons (UHC) and particulate matter (PM). These pollutant emissions enhance the greenhouse effect, contribute to the depletion of the ozone layer, produce acid rain and they are harmful to the health of living beings. Therefore they have attracted a great deal of public concern.

Jeremy Plester, from The Guardian[47], notes that shipping accounts for 13% of the annual sulphur oxide emissions worldwide. Heavy fuel oil contains 2700 [30] to 3500[47] times more sulphur than road fuel and besides that it also contributes to the formation of particulate matter. That is why the maximum amount of sulphur a fuel can contain is also limited and the regulations are becoming more and more strict. Starting in 2020 the maximum amount of sulphur in marine fuels is only 0.5%, where it still was 4.5% in 2012. In emission control areas or ECA's, the limit will even be tightened to 0.1%.

The same applies to other pollutant emissions, like the nitrogen oxides: shipping emissions also make 15% of the global NO_x emissions[53]. It has already been ten years since the Marine Environment Protection Committee has defined three levels of IMO emissions regulation systems for marine diesel engines. The Tier II regulation was already implemented in 2011 and the Tier III emissions regulation came into effect in 2016. The Tier III regulation requires a 80% reduction in nitrogen oxides (NO_x) in comparison with the Tier I regulation.

The new regulations have a big impact on diesel engine manufacturers and shipowners. There are different tiers or levels of NO_x control based on the ship construction date and within each tier the actual limits are determined from the engine's rated engine speed. A table with the different revisions of the NO_x emissions limit can be seen in table 1.1. Figure 1.1 shows the same data, but gives a better visualisation for the different engine speeds.

Tier	Date	NO_x Limit (g/ kWh)		
		n < 130	130 ≤ n < 2000	n ≥ 2000
I	2000	17.0	$45n^{(-0.2)}$	9.8
II	2011	14.4	$44n^{(-0.23)}$	7.7
III	2016	3.4	$9n^{(-0.2)}$	2.0

Table 1.1: MARPOL Annex VI, NO_x regulations[26]

The NO_x control requirements do not apply on all ships, they only apply to installed marine diesel engines of over 130 kW output. It also excludes ships that are solely used for emergency purposes irrespective of the tonnage of the ship onto which such engines are installed. This means that rescue vessels do not need to meet the Annex VI requirements.

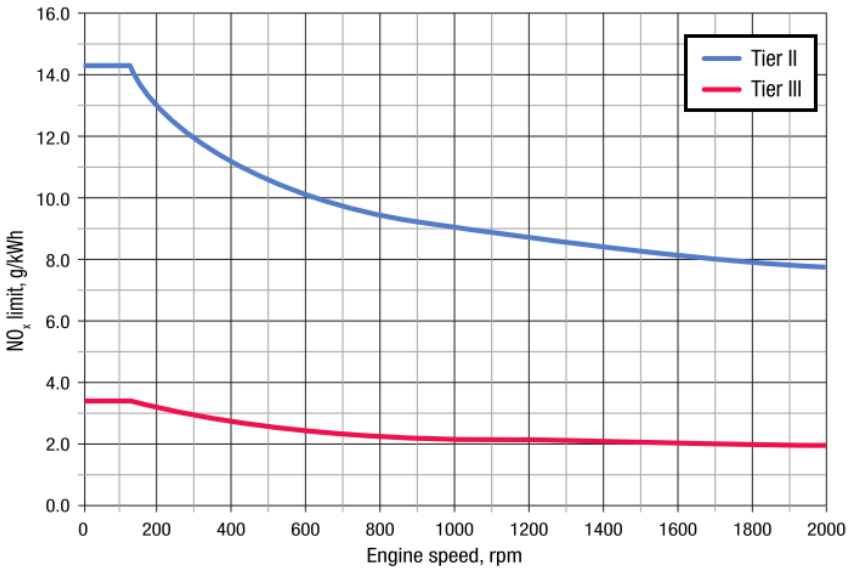

Figure 1.1: NO_x Emission limits according to MARPOL Annex VI[39]

Jumbo Maritime is a company that faces the same issue regarding new-built ships. Just as every other shipowner they have to comply with the latest regulations. Jumbo Maritime[28] is a heavy lift shipping and offshore transportation and installation contractor. Jumbo has already been developing pioneering solutions for ocean transportation for more than 50 years. Today they operate a fleet of versatile and in-house designed heavy lift vessels with lifting capacities between 500 and 3.000 tonnes. Jumbo Maritime is always thinking about the future and this also means thinking about expanding their fleet. Therefore Jumbo is also interested in finding a solution to this difficult problem.

Today's diesel engine technology is not capable of reducing the emissions to within the new limits without making alterations the engine itself. The Tier II levels could be achieved by tuning the engine, but to comply with the Tier III legislation ships shall have to be fitted with systems that can reduce NO_x to below the Tier III standards. There are multiple options to reduce the NO_x emissions to below the new standards. A number of different abatement methods have already been presented by van Riet[60].

According to Lamas and Rodríguez[32] a distinction can be made between two procedures when it comes to reducing NO_x, namely primary and secondary measures. The primary measures focus on reducing the amount of NO_x formed during combustion. This can be done by optimizing certain engine parameters with respect to the harmful emissions. Because the main factors influencing the formation of NO_x are high temperatures, residence time and the availability of oxygen, the primary methods focus on lowering these factors. The secondary measures aim to remove the already formed NO_x from the exhaust gas stream by a number of abatement methods. The most promising methods will be more thoroughly discussed in chapter 2.

One of the options is the use of an after-treatment system like Selective Catalytic Reduction(SCR). The working principle of SCR is a catalyst that converts the NO_x emissions with the help of a selective reducing agent. Ureum or ammonia is injected into the exhaust gas piping upstream of the reactor to convert the NO_x to non-critical products of nitrogen and water vapour. The degree of NO_x removal depends on the amount of ammonia added. The big advantage of SCR is that it removes NO_x by 80 to 90%. The downsides of SCR are the high investment costs, the high operating costs and the costs for maintenance. The investment costs for the entire SCR plant can be as high as 50 to 100% of the engine costs and the catalyst costs can be as high as 10% of the fuel costs. Besides the high operational and investment costs, one of the biggest downsides of SCR is the large spatial requirement.

Instead of using an after-treatment system to comply with the NO_x emissions legislation, it is also possible to avoid the formation of NO_x during combustion. This can be done by modifying the combustion cycle and means that the emissions are reduced in the combustion chamber and no after-treatment systems are needed.

One method to effectively reduce the NO_x formation in the cylinder is Exhaust Gas Recirculation or EGR. EGR already is a mature technology which is already used in automotive engines for several decades. As the name already mentions exhaust gas is recirculated back into the engine to displace a part of the fresh air entering the combustion chamber. Exhaust gas mainly consists of carbon dioxide(CO_2), water(H_2O) and nitrogen(N_2) and this mixture has a higher specific heat compared to the fresh air drawn into the combustion chamber. This slows the combustion and reduces the combustion temperature, which lowers the NO_x formation.

The aim of this thesis is to look into the reduction of NO_x emissions of marine diesel engines by using exhaust gas recirculation. EGR is chosen over SCR, because SCR is already a proven technology. EGR on the other hand is already widely used in the automotive industry, but has not yet made its impact in the maritime industry. EGR just might be the way to comply with the latest NO_x emission limits.

1.2. Research objectives

The proposed thesis not only investigates the effects of exhaust gas recirculation on the NO_x emissions of a 4-stroke marine diesel engine, but it also focusses on correctly matching engine emission data with an existing diesel engine model and correctly predicting the NO_x emissions. A 4-stroke engine is chosen because the majority of Jumbo's vessels is powered by 4-stroke marine diesel engines. The four newest ships are all powered by two MaK 9M 32C Caterpillar engines delivering a combined power output of 9000 kW. Because this engine has not changed a lot over the years and emission data is available, this engine will form the basis for this research.

With the known engine and emission data, acquired from the factory acceptance test (FAT) records, the Engine International Air Pollution Prevention (EIAPP) certificate (and supplement) and the engine product guide, a mean value first principle(MVFP) DE-model can be calibrated to match the 9M 32C MaK engine. A

MVFP DE-model can simulate a complete turbocharged diesel engine system rapidly and efficiently and is often used for diesel engine system studies. Other similar studies were already conducted by Linden[33] and Galindo Lopez[20] and they used two- and three-zone in-cylinder models respectively. Those type of models might have a higher fidelity, but both Linden and Galindo Lopez had problems with making reasonable predictions of the NO_x formation. The model choice will be further evaluated in chapter 3.

The next step in this research is to match the available NO_x emission data with the calibrated engine model. First, the available emission data will be evaluated on usability. After that a number of fits, depending on certain engine parameters, will be used to match the NO_x data. These fits will be made using a nonlinear regression model. Such a model can use a number of variables to match the engine parameters with the available NO_x emission data. After the implementation of exhaust gas recirculation, the same fits can be used to predict the impact of the EGR on the emissions.

Once the engine is calibrated correctly and the NO_x fits have been made, the next step is to implement the different EGR configurations into the model. The used configurations are low and high-pressure EGR. Once implemented, the configurations will be evaluated and the effects of the implementation on certain engine parameters will be discussed. Finally, a NO_x emission prediction will be made using the NO_x fits and the changed engine parameters.

The above mentioned research objectives can be summarized in the following research question:

How can the NO_x emissions of a 4-stroke marine diesel engine be predicted after the implementation of exhaust gas recirculation and with the use of a mean value simulation model?

In order to achieve the objectives and solve the problem described above, the following steps are necessary:

- Investigate the NO_x formation in diesel engines and determine the most important factors that influence the formation.
- Determine which engines are used on Jumbo Maritime's vessels and select an appropriate simulation model which can be calibrated with the available engine data.
- Evaluate the available NO_x emission data and use certain engine parameters to fit this data.
- Explain the working principle of exhaust gas recirculation and implement multiple EGR configurations into the calibrated diesel engine model.
- Evaluate the effects of the implementation of the different EGR configurations on the diesel engine model.
- Use the developed NO_x fits to predict the NO_x emissions of the diesel engine equipped with EGR.
- Analyse the results of the implementation of EGR and the NO_x predictions and draw conclusions.

If all these steps are taken the thesis can be concluded and recommendations for future research can be given.

1.3. Thesis outlines

This thesis consists of seven chapters and four appendices. This chapter has already given a short introduction to the research background and the relevance of this research. It explained the use of diesel engines for marine applications and the polluting effects that comes with the burning of fossil fuels. This is mainly due to the type of fuel that is used for marine diesel engines. The residual fuel oil cannot be used for many other applications than the marine industry. For now the shipping sector still relies on fossil fuels and that is why governing bodies try to reduce the polluting impact of burning fossil fuels with new regulations. Resulting from this follows the problem definition on how to cope with these new regulations. The research objectives show what is needed to solve this problem. And then this chapter is concluded with the thesis outlines, which present the structure of this research.

Chapter 2 succeeds an already conducted literature study and will present the necessary fundamentals for this research. It starts with an elaboration on the formation of NO_x in diesel engines. Therefore three

NO_x formation principles will be discussed: thermal NO_x formation, fuel NO_x formation, prompt NO_x formation and their accompanying reaction kinetics and equilibrium reactions.What follows from the formation principles and reactions are the factors that influence the formation of NO_x. These are relevant and necessary for a successful execution of this research. That chapter continues with a number of NO_x abatement methods and it will be explained why EGR is chosen out of all options.

Chapter 3 focusses on the choice of the diesel engine modelling concept. A lot of different models are available and can be used to simulate a marine diesel engine. It will be explained why the mean value first principle Diesel A-Modular model is chosen to conduct this research and the model will be explained in further detail. One of the most important parameters of the Diesel A-Modular model is the air mass fraction. This fraction is defined as the part of the total mass that consists of air. This fraction is also used to determine the air excess ratio and the specific heat of the air and stoichiometric combustion gas mixture. After that a general description of the used diesel engine will be given. For this research the 9M 32C MaK diesel engine is used and its specifications will be given. The final part of this chapter focusses on combining the chosen model with the 9M 32C diesel engine by using data from the factory acceptance test and an EIAPP report. The chapter will be concluded with an evaluation on how well the model simulates the actual diesel engine.

The fourth chapter will elaborate on the fitting of the NO_x emission data. It kicks off with a discussion on the available NO_x emission data. Because the available data set is quite limited, the origin and usefulness of the data will be discussed first. The data is extracted from the EIAPP report of the parent engine of the 9M 32C MaK engine and is the result of a set of test cycles which are specific for the application of the engine. Because Jumbo's vessel are equipped with controllable pitch propellers, the used test cycles are for the "constant-speed main propulsion" application and the "constant-speed auxiliary engine" application. The outliers in the emission data will be discussed, followed by the factors that influence the formation of NO_x. Then the actual fitting can begin: a nonlinear regression model is used to fit certain engine parameters with the NO_x emission data(kg/h and g/kWh). This chapter is concluded with an evaluation of the NO_x emission fits using a set of goodness of fit statistics.

Chapter 5 introduces the working principle of exhaust gas recirculation and what the benefits and disadvantages of EGR are. Then the two different EGR configurations that will be used for this research will be discussed in more detail: low-pressure and high-pressure exhaust gas recirculation. The next step is to implement both configurations in the calibrated diesel A-Modular model. The difficulties and changes to the model which arose during the implementation of these configurations are then evaluated.

Chapter 6 will present the results of this research. First, the effects of the implementation of EGR on the most important engine parameters will be discussed. These are the parameters that are also used for the fitting and focus on the availability of oxygen and the maximum combustion temperature. Once these parameters have been discussed the actual prediction of the NO_x emissions will be evaluated. Due to the change in certain engine parameters, the fits are used to predict the NO_x emissions with EGR enabled. The final chapter concludes this thesis and recommendations for future research will be given.

2

NO_x formation and abatement methods

2.1. Introduction

This chapter will give an overview of the relevant literature for the proposed thesis work, starting with a more thorough explanation of the formation of NO_x in diesel engines. Three NO_x formation principles will be discussed: thermal NO_x formation, fuel NO_x formation, prompt NO_x formation and their accompanying reaction kinetics and equilibrium reactions. What follows from the formation principles and reactions are the factors that influence the formation of NO_x. These factors are relevant and necessary for a successful execution of this research. Once the formation of NO_x has been discussed, the chapter continues with discussing different methods to reduce the NO_x formation and NO_x emissions. This chapter will be concluded with the substantiation of the choice to use exhaust gas recirculation to reduce the formation of NO_x.

2.2. NO_x formation in diesel engines

Tis section will elaborate a bit more on the NO_x formation in diesel engines. For the combustion in a diesel engine, intake air is needed. Almost all the engine intake air, 99%, consists of nitrogen(N_2) and oxygen(O_2). A large part of the nitrogen does not react in the diesel engine combustion process, but a small percentage is oxidised to form exhaust gases containing various oxides of nitrogen. These oxides of nitrogen are nitrogen monoxide(NO), nitrogen dioxide(NO_2) and a minor concentration of nitrous oxide(N_2O). The nitric oxides and nitrogen dioxides are both considered as nitrogen oxides or NO_x. N_2O is not regarded as a NO_x component, but it is considered as a strong greenhouse gas which contributes to the detrimental effect on the ozone layer in the upper atmosphere.[12]

Nitrogen oxides are formed during the diesel engine combustion process within the burning fuel sprays. Because of the high temperatures due to flames and combustion, nitrogen reacts with the oxygen within the engine intake air. This way, nitric oxide(NO) and nitrogen dioxide(NO_2) will be formed. At a later stage in the combustion process, during the expansion and in the exhaust system, part of the NO will convert to form nitrogen dioxide. The formation of NO_x is controlled by local conditions in the spray. Temperature and oxygen concentration are of most influence on the formation and besides that pressure and time also play a role. The higher the temperature and the longer the residence time at this high temperature, the more NO_x will be formed[36, 43, 56].

During combustion, the amount of NO formed is substantially higher than the amount of NO_2 formed. The other oxides of nitrogen, like dinitrogen oxide(N_2O), dinitrogen tetrooxide(N_2O_4) and dinitrogen pentoxide(N_2O_5) occur in very small quantities. The formation of NO_x can be divided into three different kinds of formation. These are thermal NO, which is formed among the combustion products at high temperatures according to the Zeldovich mechanism from atmospheric nitrogen, so-called prompt NO, which already develops in the flame front from air nitrogen and fuel NO, which is produced by nitrogen portions in the fuel. These different kind of formations will be further evaluated below.

Thermal NO_x formation

Thermal NO formation proceeds "behind" the flame front and is the process where combustion air bound nitrogen, N_2, reacts with the oxygen, O_2, in the combustion air to produce NO. A very high temperature is required for the formation of thermal NO and the formation is exponentially dependent on temperature. This is shown in figure 2.1, where it can be seen that the NO formation rises steeply from around 2000°C.

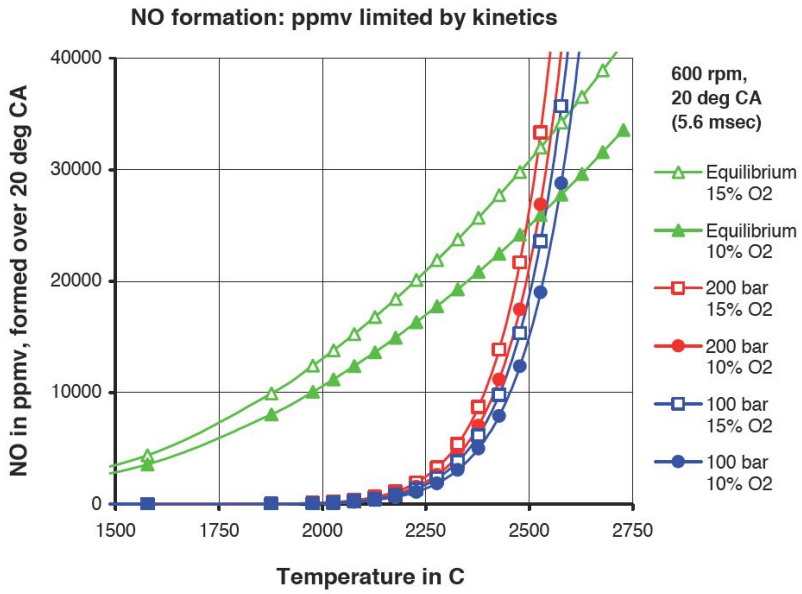

Figure 2.1: NO formed in time available in typical medium speed diesel engine[56]

Considering that the mean bulk temperature in a diesel engine does not exceed 2000°C, so-called hot spots or local areas with a higher than average temperature, are the main contributors to the formation of NO_x according to Yfantis et al.[66]. Therefore it is very difficult to model the formation of NO_x accurately. Other important factors that are important for the formation of NO_x are the residence time and the local availability of oxygen. The process is mainly governed by the so-called extended Zeldovich mechanism which consists of three equilibrium reactions, as been used by Hebbar[23], Turns[58] and Marissal[41].

$$N_2 + O \overset{k_1}{\longleftrightarrow} NO + N \tag{2.1}$$

$$N + O_2 \overset{k_2}{\longleftrightarrow} NO + O \tag{2.2}$$

$$N + OH \overset{k_3}{\longleftrightarrow} NO + H \tag{2.3}$$

These equations show that the thermal nitric oxide formation is determined by only five chemical species, namely O, H, OH, N and O_2. This also means that for the thermal NO_x formation no fuel is being used. Equation 2.1 shows how the strong and stable triple bond of air-bound nitrogen molecule is decomposed. This requires a very high activation or temperature. With a high temperature also comes a significantly fast reaction[44, 52, 54, 56]. The speed constants k_i are experimentally determined, but according to Imperato[25] they have an exponential temperature dependence. Although the Zeldovich mechanism is one of the most investigated reaction mechanisms, there still is a lot of uncertainty concerning the choice of speed constants. This means that deviating values are suggested for this in literature.

Fuel NO_x formation

Schwerdt[52] described fuel NO_x formation as the process where the nitrogen in the fuel reacts with the oxygen in the combustion air in order to form NO_x. There is a difference in nitrogen content between gaseous fuels compared to liquid and solid fuels, like marine diesel oil and coal. Gaseous fuels have a relatively low amount of fuel-bound nitrogen and therefore this results in a low amount of NO_x being produced. Coal and oil have a higher amount of fuel bound nitrogen and thus the NO_x formation will be larger.

Winnes and Fridell[63] explain that when a marine diesel oil (MDO) or marine gas oil (MGO) is used, the fuel NO_x formation is really small due to the small amount of fuel bound nitrogen. This is confirmed by De Nevers[16] and Nam[45] who state that fuel NO_x accounts for only about 10 to 20% of the total NO_x emissions. Thermal NO_x is the main contributor to the NO_x emissions. The available EIAPP certificate[10] also states that the amount of nitrogen in the test fuel is only 29 ppm, which is a lot lower than the resulting NO_x emissions, which are over 700 ppm at their lowest value.

Despite not being fully understood, the following two equations show the mechanism for the fuel NO_x formation:

$$N_{Complex} + OH \longleftrightarrow NO + X \tag{2.4}$$

$$N_{Complex} + NO \longleftrightarrow N_2 + X \tag{2.5}$$

The X in both equations symbolizes other products where the mechanism is not fully understood. For this research the most important NO_x formation is the thermal NO_x formation.

Prompt NO_x formation

The last process describing NO_x formation is the prompt NO_x formation or Fenimore mechanism and this process describes the formation of prompt NO in the flame front itself. This process describes how the nitrogen is decomposed en formed into radical hydrocarbons during the combustion of fuel. On their turn, these radicals are quick to react with the nitrogen from the combustion air to form transition substances which then oxidises to NO_x. The first step in this process is as follows:

$$CH + N_2 \longleftrightarrow HCN + N \tag{2.6}$$

In this equation, HCN is the transition substance which converts to atomic nitrogen through a number of steps, namely:

$$HCN \longrightarrow NCO \longrightarrow NH \longrightarrow N \tag{2.7}$$

At a higher temperature reaction 2.8 also contributes to the breaking of the N_2 bond.

$$C + N_2 \longleftrightarrow CN + N \tag{2.8}$$

The nitrogen atoms from the three equations above are then oxidised to form NO. The prompt NO_x formation usually occurs at relatively low temperatures in the beginning of the combustion process and only occurs during very fuel-rich combustion[52, 58].

2.3. NO_x reaction kinetics and equilibrium

Now that it is known which chemical equations govern the formation of NO_x in diesel engines, it is time to have a look at the reaction kinetics and the reaction equilibrium. The formation of NO can be categorised in three different categories according to Turns[58]:

1. The extended Zeldovich (or thermal) mechanism in which O, OH and N_2 species are at their equilibrium values and N atoms are in steady state.

2. Mechanisms whereby NO is formed more rapidly than predicted by the thermal mechanism, either by the Fenimore mechanism, the N_2O-intermediate route or as a result of super-equilibrium concentrations of O and OH radicals in conjunction with the extended Zeldovich scheme.

3. Fuel nitrogen mechanism, in which fuel bound nitrogen is converted to NO

The primary variables affecting the formation of NO_x are temperature and oxygen availability. This can also be seen in the equilibrium equation of NO which can be seen below in equation 2.9, where [NO],[O_2] and [N_2] are the concentrations of nitrogen oxides, oxygen and nitrogen respectively. The equation(as given by Stapersma[56]) shows the dependency of the equilibrium of NO on the concentrations of oxygen, nitrogen and of the temperature T:

$$[NO] = 20.3 \cdot e^{-21650/T} [O_2][N_2]^{0.5} mol/cm^3 \tag{2.9}$$

The formation of NO is kinetically controlled and takes place at higher temperatures. Especially the thermal NO formation needs a high activation energy and thus high temperatures. The formation rate of NO is described by Heywood[24] as follows:

$$\frac{d[NO]}{dt} = 1.5 \cdot 10^{13} \cdot e^{-38000/T}[O][N_2] \cdot \frac{1 - [NO]^2/(20.3 \cdot e^{-21650/T}[O_2][N_2])}{1 + 1.6 \cdot 10^{13}[NO]/(6.4 \cdot 10^{19} T \cdot e^{-3150/T}[O_2] + 4.1 \cdot 10^{13}[OH]} \quad (2.10)$$

This equation shows again that the formation of NO is dependent on both the temperature and the concentrations of oxygen and nitrogen. The amount of nitrogen available for combustion is less important than the amount of oxygen available. Air consists of 79% nitrogen and is always present in abundance. Fuel may also contain some nitrogen, but thermal NO_x is the main contributor to the total NO_x formation.

The effects of temperature and oxygen on the formation of NO_x have already been showed in figure 2.1. This figure shows combustion temperatures and typical concentrations of oxygen(10% and 15%). It is known that the rate coefficient for equation 2.1 has a very large activation temperature and thus rapidly increases above 1800K. This means that reducing the peak temperatures of a diesel engine and reducing the oxygen concentration can significantly reduce the NO_x emissions.

Besides reducing the peak temperature and the oxygen content another factor of influence is the residence time in the engine. This means that slow-speed engines emit more NO_x than medium- or high-speed engines. Slow-speed engines might have a higher efficiency, but their NO_x emissions are higher on g/kWh basis. For this research, the residence time will not be an issue, because the used engine is operated in generator law. This means that the engine rotates at a constant speed and the speed is controlled by controlling the pitch of the propellers.

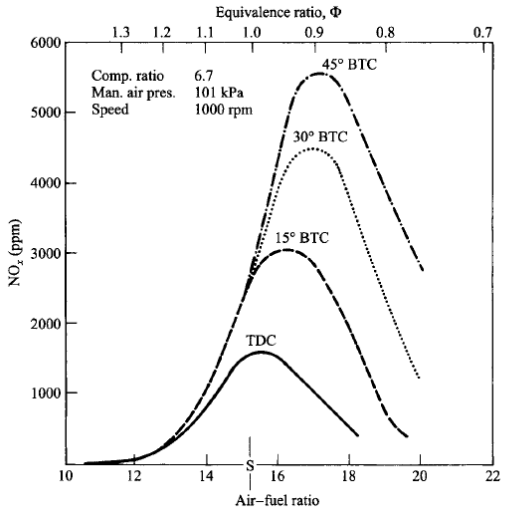

Figure 2.2: NO_x concentrations as functions of air-fuel and equivalence ratios for various ignition timings[58]

According to Turns[58] it is known that for adiabatic, constant-pressure combustions, the maximum equilibrium O-atom mole fraction lies near an equivalence ratio of 0.9. This is also the point where the maximum kinetically formed NO is found for ignition engines. This can be seen in figure 2.2. This unfortunately is also the point where maximum efficiency is achieved for many practical devices. This means that rate shaping of the injection might help with reducing the emissions. Continuous injection rate shaping introduces diesel fuel into the combustion chamber at the rate required by the combustion process. It avoids premature heat release before TDC and this way optimizes the thermal efficiency.

2.4. Factors that influence the formation of NO_x

Despite the fact that the formation of NO_x in diesel engines is an extremely complex phenomenon, the previous two sections described the basics of the formation of NO_x and the reaction kinetics of NO_x.

The problem with accurately describing the formation of NO_x is the non-uniform fuel(and temperature) distribution during combustion, the complexity of the fuel-air mixing and the combustion processes. An example of a combustion plume can be seen in figure 2.3.

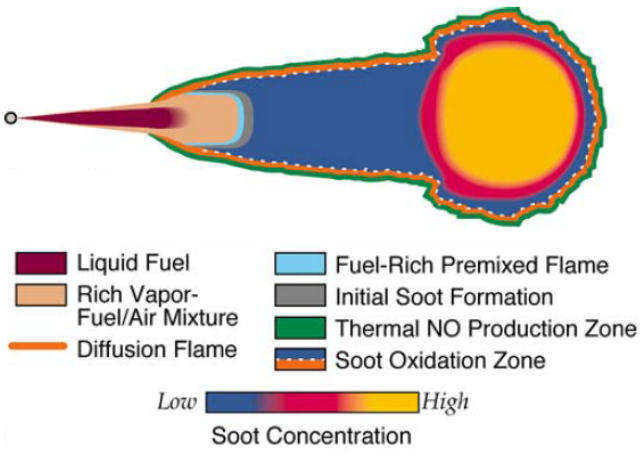

Figure 2.3: Diesel combustion plume[4]

What can be seen is that the highest temperatures occur at the flame front of the fuel injection spray. Due to the concentration of fuel and the moving flame front, this is where the so-called hot spots are more likely to occur. That is why new types of combustion processes are being developed, like homogeneous charge compression ignition. This is to avoid a the flame propagation through the combustion chamber and a lean premixed mixture of air and fuel. Another option is to use other injection nozzles where the fuel is more evenly distributed throughout the combustion chamber.

During the uncontrolled diesel combustion phase, the fuel-air mixture burns due to spontaneous ignition and flame propagation. During the combustion process, mixing occurs between already burned gases, air, and lean and rich unburned fuel-air mixture, continuously changing the composition of the gas elements. Due to this mixing, composition and thus temperature changes occur.

Another cause of temperature changes are due to compression and expansion as the cylinder pressure rises and falls. When the burned gas temperatures are at a maximum the critical time period for NO_x formation starts. This is between the start of combustion and shortly after the occurrence of the peak cylinder pressure. This means that the fuel-air mixture that burns early in the combustion process is compressed to a higher temperature, increasing the NO formation rate, while the combustion proceeds and the overall cylinder pressure increases.

After the time of the peak pressure, the cylinder gases expand and the temperature of the burned gases decreases. The decreasing temperature due to expansion and also due to mixing of the high-temperature gas with air or cooler burned gas freezes the NO chemistry. This freezing occurs more rapidly in diesel engines than in spark-ignition engines and it results in much less decomposition of the NO. This description is supported by NO concentration data obtained from experiments by Heywood[24].

The formation of NO_x is a very strange and difficult process. It is already known that it requires very high temperatures and the formation is exponentially dependent on the temperature, but only after a certain threshold. Because the process is very nonlinear, so-called hot spots, local areas with higher temperature than the average temperature, can have a very large effect on the amount of NO_x that is produced[52]. Therefore it is important to not only look at the average temperature, but also the maximum temperature.

What we have learned is that the NO_x formation mainly depends on the temperature and pressure of the burnt gas, the residence time of that burnt gas at a high temperature and the amount of excess oxygen in the combustion chamber. Because the engine in question runs in generator mode(with a controllable pitch

propeller), the residence time is the same for each engine load, meaning that it does not have to be taken into account for this research. A factor that also might be of importance is turbulence(mixing of the burned gases, air, and lean and rich unburned fuel-air mixture). Because a MVFP model is used, it will not be possible to analyse the turbulence during combustion. This will require more advanced models or CFD. This means that the main factors that influence the formation of NO_x are:

- Temperature (and hot spots)
- Amount of oxygen(excess air)

Now that it is known what factors are of most influence on the formation of NO_x, it is possible to find solutions to reduce those factors. The following section will elaborate on that.

2.5. NO_x abatement methods

Chapter 1 already explained that multiple options are available to reduce the formation and emissions of NO_x. A distinction can be made between two types of measures, namely primary and secondary measures. The primary measures focus on reducing the amount of NO_xformed during combustion by optimizing certain engine parameters. Because the most important factors that influence the formation of NO_x are the combustion temperature and the availability of oxygen, the primary measures try to reduce those factors. The secondary measures on the other hand aim to remove the already formed NO_x from the exhaust gas by a number of different methods. Besides that another combustion type will also discussed: homogeneous charge compression ignition(HCCI). This section will discuss both types of measures shortly and will elaborate on the choice for one specific measure: exhaust gas recirculation.

2.5.1. Primary abatement methods

Diesel engine manufacturers have already explored many different methods for reducing NO_x by primary control methods. Lloyd's Register[36] and Lamas and Rodríguez[32] made lists of the most publicised NO_x reduction methods:

Delaying fuel injection and injection timing

The first method is delaying the fuel injection. Retarding the fuel injection also delays the combustion process, which means that the formation of nitric oxides occurs later and with lower concentration. It also leads to lower peak pressures and therefore lower peak temperatures. This is also in favour of a smaller formation of NO_x.

Water injection

Another method is injecting water into the cylinder. There are three different possibilities: fuel-water emulsion, direct water injection and humidification. A collaboration between MAN Diesel & Turbo and Danisco[3] already did an extensive research to fuel-water emulsions. It was concluded that adding water to fuel is an effective way of reducing the flame temperature. In order to use an emulsion, a suitable emulsifier is required. Research on this subject is still ongoing. Another method tested by MAN is humidification with the so-called Humid Air Motor or HAM[38], where hot compressed air from the turbocharger is led to a humidification tower where it is flushed with hot water. The working principle is reducing the peak temperatures in the combustion chamber and a NO_x reduction of 40% is achievable without extra heating. If extra heat is added, for example from the enginen coolant or exhaust gases, a reduction up to 65% is possible. Patal Sagar et al.[46] explain the use of a separate injector to directly inject water into the intake manifold. NO_x emission reduction can be reduced up to 42%. The drawback of the system is the amount of complexity involved in integrating all the additional components and redesigning of the fuel system. The influence of water differs per engine, but in general 1% of water reduces the formation of NO_x by 1%, according to Woodyard[64].

Miller cycle

Due to the development of advanced turbocharging systems and variable valve actuation(VVA) it is alo possible to reduce the amount of NO_x with the Miller cycle or Miller timing. The Miller cycle needs a higher than normal pressure and the working principle is based on changing the inlet valve timing. If the inlet valve is closed before bottom dead center on the intake stroke, the charge air can then expend inside the cylinder as the piston still moves towards bottom dead centre. This result is a lower temperature in the combustion

chamber. Experiments for the application of Miller timing were done by Codan and Vlaskos[13] and Yfantis et al.[65]. Multiple test were done, also in collaboration with ABB, and it was shown that NO_x reductions up to 50% are possible. A disadvantage is the increase in smoke.

Exhaust Gas Recirculation

Exhaust gas recirculation already is a mature technology that has been used in the automotive industry for several decades. By recirculating part of the exhaust gas it replaces a part of the fresh air entering the combustion chamber and thereby dilutes the mixture. This is due to the fact that exhaust gas mainly consists of carbon dioxide, water and nitrogen, but also some oxygen which did not take part in combustion. The compositions of the intake mixture and exhaust gas of a typical low speed diesel engine are shown in figure 2.4:

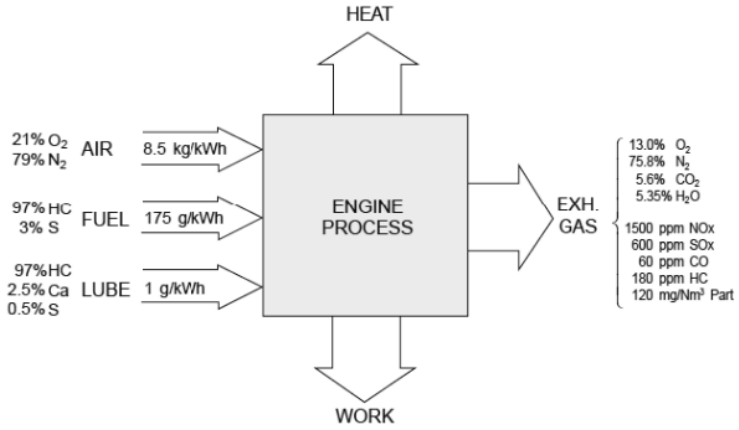

Figure 2.4: Typical exhaust gas emissions from a low speed diesel engine[64]

Due to the different composition the specific heat of the exhaust gas is higher in comparison with the fresh air. The higher specific heat of the mixture of fresh air and exhaust gas is therefore slightly higher than the specific heat of just the fresh air. This slows the combustion a bit and reduces the combustion temperature, which on its turn reduces the formation of NO_x.

Different types of EGR configurations are available for marine diesel engines. The most important distinction is made between low and high-pressure EGR. The difference between the two types of recirculation is the point of exhaust gas extraction. In the LP-EGR system, the exhaust gas is extracted after the turbocharger turbine and returned to the compressor intake. In the HP-EGR system on the other hand, the exhaust gas is extracted before the turbocharger turbine and mixed with the scavenge air, after the turbocharger compressor. Both configurations can be seen in figure 2.5. They will be discussed in more detail in chapter 5.

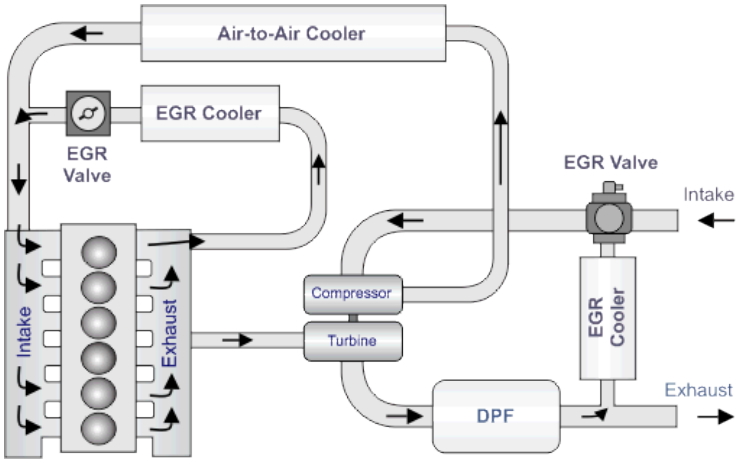

Figure 2.5: Low-pressure and high-pressure EGR systems[27]

It is reported that up to 60% NO_x can be removed with EGR. The downside of using EGR is that it cannot be used for all fuel types. Engines operating on high sulphur fuels could suffer from corrosion of the turbochargers, intercoolers and scavenging pipes. An extra scrubbing unit is then necessary to remove sulphur oxides from the recirculation loop.

2.5.2. Secondary abatement methods

The secondary abatement methods, also called end-of-pipe-technologies, are not as extensive as the primary reduction methods. This section will explain the use of non-thermal plasma and selective catalytic reduction(SCR).

Non-thermal plasma

The use of non-thermal plasma is a relatively new technology and is still the subject of extensive research. A research by Balachandran[6] explains the working principle of non-thermal plasma. The idea is that the electron temperature is much higher than the gas temperature, also due to the vibration and rotational temperature of the molecules. With molecular excitation the molecular bond between the nitrogen and oxygen molecules is broken. It is reported that a non-thermal plasma system can remove more than 90% of the formed NO_x Besides that a big advantage of non-thermal plasma is that is it not restricted to just NO_x, but has the potential to treat multiple pollutants. A downside is the need to achieve molecular excitation, which can involve expensive machinery.

Selective Catalytic Reduction

Another method to reduce the emissions of NO_x is the use of selective catalytic reduction, or SCR. SCR already is a proven technology and is widely used in land-based industry and land-based transportation. However, because the exhaust gases of marine diesel engines have a substantial oxygen content and a relatively low gas temperature, conventional catalysts cannot be used for the removal of NO_x. SCR is a technique that involves the conversion of NO_x into the non-critical products nitrogen and water vapour with the help of a urea solution. The urea solution is a selective, non-toxic reducing agent that is injected into the exhaust piping upstream of a catalytic reactor. According to Eyring et al.[19] a NO_x reduction of over 90% is possible. Downsides of SCR are the investment and operating costs(per unit weight urea is higher in price than heavy fuel oil) and costs for important items like storage tanks and replacement parts. An example of a marine SCR arrangement can be seen in figure 2.6:

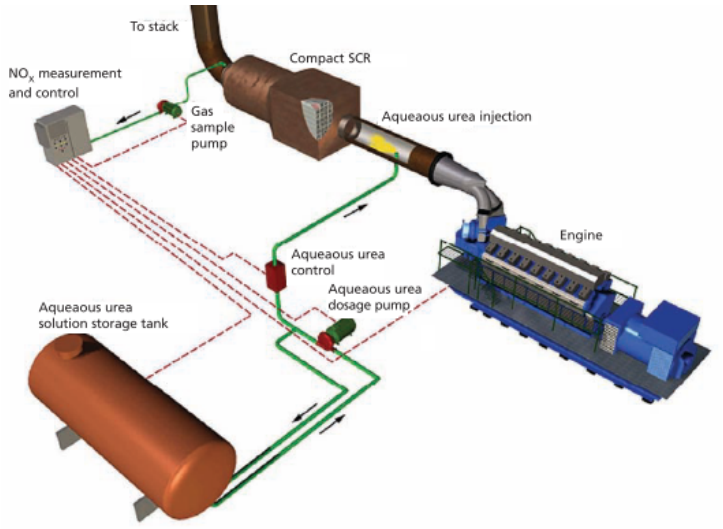

Figure 2.6: A marine SCR arrangement[35]

2.5.3. Homogeneous charge compression ignition

It is well known that the formation of NO_x generally occurs at temperatures above 2000 K. A lot of primary abatement measures aim to reduce the combustion temperature. Another way to reduce the formation of NO_x is to change the combustion process. A good example, which is still being developed, is so-called

homogeneous charge compression ignition or HCCI. HCCI aims to avoid the areas where soot and NO_x formation occurs, as is shown in figure 2.7.

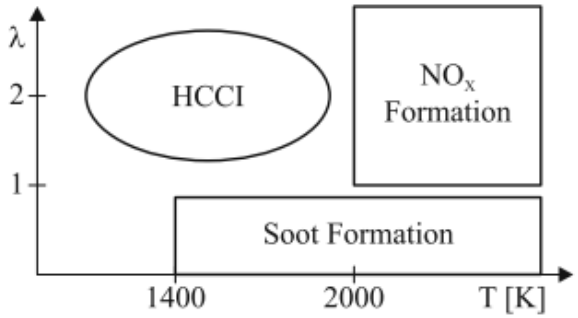

Figure 2.7: Range of the HCCI method[43]

HCCI engines have been studied vigorously due to their high thermal efficiency and ultra low NO_x and particulate matter emissions when compared to both spark ignition and compression ignition engines. The working principle of HCCI is to use a sufficiently lean premixed air-fuel mixture to keep the flame temperatures well below 1900 K. A comparison between a gasoline engine, diesel engine and HCCI engine is shown in figure 2.8.

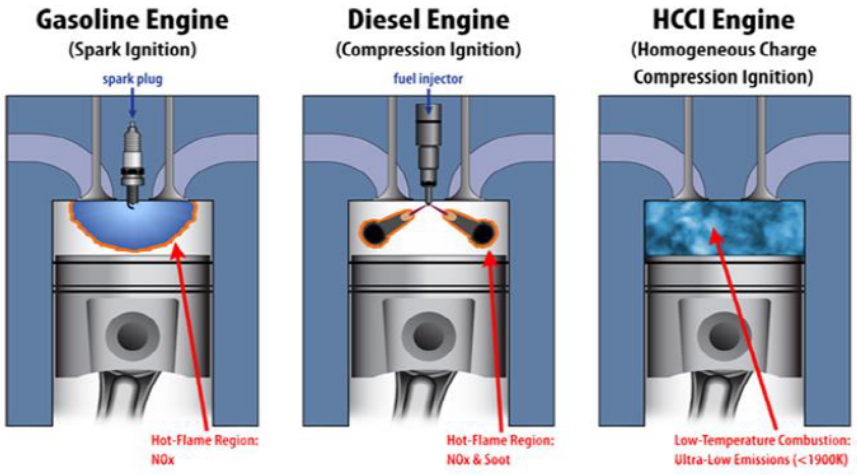

Figure 2.8: The differences among SI, CI and HCCI engines[22]

The quality of the mixture of air and fuel is lean, in order for it to auto ignite in multiple locations at the same time without discernible flame propagation. According to Hairuddin et al.[22] the combustion takes place when the homogeneous mixture has reached the chemical activation energy and is fully controlled by chemical kinetics rather than spark or injection timing. Of course, when developing a new method new challenges arise. For HCCI it is difficult to control the auto-ignition of the mixture and the heat release rate at high load operation. Another disadvantage is that knocking occurs at certain operating conditions. On the other hand, advantages are the high efficiency(close to CI engines), the ability to operate on a wide range of fuels and the ability to be used in all kinds of engine configurations.

2.5.4. Exhaust gas recirculation

A choice has been made on which abatement method was going to be used. After an extensive literature study[60], the choice was made to further elaborate on the use of exhaust gas recirculation. Exhaust gas recirculation is already a mature technology in other industries, but has not yet made its impact on the marine sector. Lots of studies have already been conducted in the automotive field, but due to the use of a different type of fuels, implementing EGR in a marine diesel engine is quite the challenge.

Besides that, EGR tackles the problem right at the source instead of an end-of-pipe solution like SCR. The combination increasing the specific heat of the combustion mixture and the reduction in availability of oxygen should ensure a decrease in the formation of NO_x. Chapter 5 will elaborate further on the working principle of EGR and will explain the implementation of the possible configurations into the simulation model.

2.6. Conclusion

This chapter began with an elaboration on the formation of NO_x in diesel engines. It was concluded that the main causes for the NO_x formation are high combustion temperatures, hot spots during combustion and the large amount of oxygen available for combustion. This was confirmed by the equations that showed the equilibrium of NO and the formation rate of NO.

Now that is is known what are the factors that influence the formation of NO_x a number of abatement methods were presented. A distinction is made between primary and secondary measures and a complete change of combustion by using HCCI. The most important primary measures are adapting the fuel injection, water injection, applying the Miller cycle and exhaust gas recirculation. The most promising secondary method or end-of-pipe solution is the use selective catalytic reduction.

The decision was made to further elaborate on the use of exhaust gas recirculation. The following chapter will first introduce the engine that forms the base for this research. After that it will focus on the models that could be used to simulate the engine and implement the EGR configurations.

3

Simulation

3.1. Introduction

Before discussing the different diesel engine modelling concepts it necessary to discuss the diesel engine that will be used for this research. The first section will elaborate a bit further on the diesel engine in question, the 9M 32C from MaK. After that a short introduction to diesel engine modelling will be given followed by a more detailed description of the model that was used for this research. Several important features of the model will be highlighted and then the chapter will be concluded with the calibration of the model with observational data from the actual engine.

3.2. Engine description

As already mentioned in chapter 1, Jumbo Maritime has a very versatile fleet. Jumbo has a fleet of ten ships with lifting capacities ranging from 500 to 3000 tonnes. The two newest vessels are of the K-class type, the Jumbo Kinetic and the Fairmaster both equipped with two cranes which combined are able to lift 3000 tonnes. Those ships were built in 2014 and 2015. The two ships before that, built in 2008 and 2009, are the J-class vessels, the Fairplayer and the Jumbo Jubilee, equipped with two cranes with a combined lifting capacity of 1800 tonnes. These four ships are all equipped with two MaK 9M 32C Caterpillar marine diesel engines with a combined output of 9000 kW. With this output a speed of over 17 knots is possible.

The engine manufacturer recommends to operate the engine within certain limits. Caterpillar recommends to operate the engine between 70% and 100% load. At low loads, the engine is less efficient, consumes more fuel and emits more pollutant emissions. The commercial department within Jumbo also takes this into account when making offers to customers. For the majority of the time Jumbo's vessels operate between 75% and 95% engine load.

The 9M 32C is a four stroke turbocharged and inter-cooled diesel engine with direct fuel injection. The main specifications of the 9M 32C engine used aboard Jumbo's vessels are given in table 3.1. A more detailed overview of the engine data can be found in Appendix A and table 3.2 later on in this chapter.

Diesel engine parameter	Value
Cylinder configuration	9 in-line
Bore:	320 mm
Stroke:	480 mm
Stroke/Bore-Ratio	1.5
Output/cylinder:	500 kW
Revolutions:	600 rpm
Mean piston speed:	9.6 m/s
BMEP:	25.9 bar
Cylinder pressure:	203 bar

Table 3.1: Specifications MaK 9M 32C[9]

The M 32C has continued the market success of its predecessor in this bore size: the M 453C and has already been on on the market since 1994. It has been such a success due its great reliability and durability in combination with stability at high power output[64]. This model was developed to cope with the new emission legislation. In the year 2000, Caterpillar identified three emissions levels for all MaK marine products in order to cope with the short to those emission regulations. This means that the base engine must comply with the IMO Tier II emission regulations.

For Caterpillar, the key to achieving these regulations was to increase the compresion ratio of the base engine. Where first a compression ratio of 11-12 was standard, for IMO I the ratio was raised to 14-15 and for IMO II ratios of almost 17 are needed. Besides that the valve timing is modified according to the Miller Cycle to achieve cooler combustion. For IMO Tier I only 5% Miller effect was utilised, but for IMO Tier II a Miller effect of 20% was required. This means higher boost ratios are necessary in order to maintain the mean effective pressue (BMEP) values.[8]

Opposed to naturally aspirated engines, turbocharged engines have a system that compresses the combustion air before it enters the cylinder. The working principle of a turbocharger is that when the combustion air is compressed, more oxygen can enter the cylinder and the amount of fuel that can be combusted increases. So if an engine is turbocharged, it delivers more power out of the same volume, and thus it increases the power density.[55]. A schematic of a typical turbocharged and inter-cooled engine can be seen in figure 3.1.

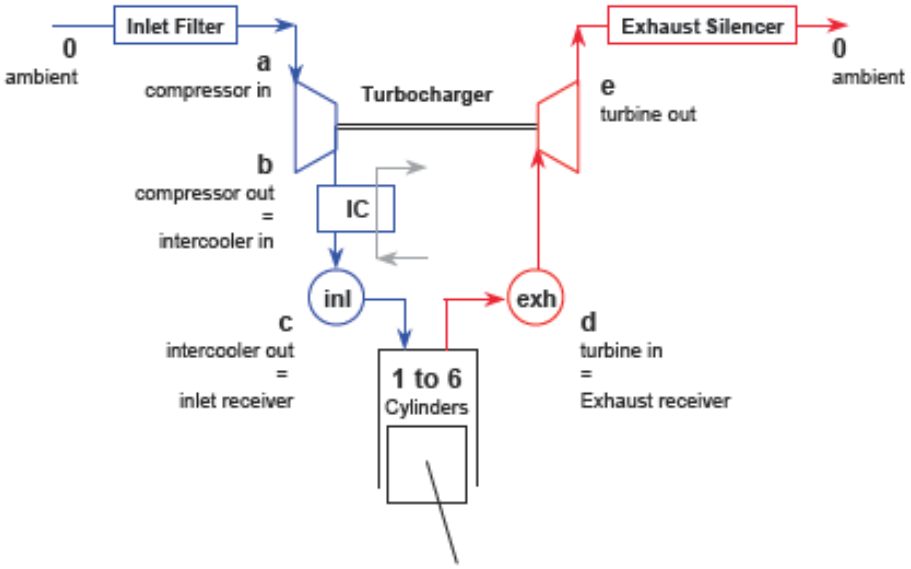

Figure 3.1: Layout of a turbocharged and inter-cooled engine with station numbering[55]

The figure also shows the station numbering (as given by Stapersma[55]) that will be used throughout this thesis :

- 0 - a air intake
- a -b compression of charge air in compressor
- b - c cooling of charge air
- c - 1 cylinder intake process closes
- 1 - 6 "Hexagon" (Seiliger) cylinder process
- 6 - d cylinder exhaust process
- d - e expansion of the exhaust gases in turbine

- e - 0 gas exhaust

The Seiliger in-cylinder process will be explained in more detail later on in this chapter when it is known which diesel engine model will be used.

3.3. Diesel engine modelling concepts

Despite the fact that diesel engines are used for a broad range of operations, only a limited number of diesel engine modelling concepts are recognised according to Schulten[50]. The first distinction can be made between analytical and empirical models. Analytical models consist of a set of algebraic and differential equations. The variation in analytical models in mainly dependent on the volume size and the time step for which all the equations are solved. A trade-off has to be made between the amount of information a model contains and the accuracy and simulation speed.

Empirical models on the other hand are usually fast and, depending on the availability of measurements, accurate. Data is acquired from lookup-tables or polynomial fits in which the needed data is stored. Disadvantages of empirical models is that they are not generic. This means that they are used to analyse the behaviour of a specific engine and, depending on the similarities between engines, it is difficult to use the model for another engine. It is not really clear how the data should be treated when engine parameters change, for example when scaling them up or down. Besides that, it is not possible to generate engine data other than the measured data that is used as input.

Analytical models can be subdivided in five main areas, varying in difficulty. These are CFD models, multi-zone models, crank angle models, mean value models and transfer function models. CFD models, or computational fluid dynamics models, are intended to model the in-cylinder process of an engine. The combustion chamber is divided in a large but finite number of elements or volumes and the basic equations between the elements are then solved. For an accurate prediction of the processes in the combustion chamber a really large number of elements is needed and this requires powerful computers and results in long computing times.

The multi-zone models are quite similar to the CFD models, but the number of control volumes, or zones in this case, are in the order of two to ten. This way the computing time can be reduced significantly. Besides basic equations, also phenomenological equations are used, which include reaction rates and heat transfer coefficients. Both the CFD models and multi-zone models provide detailed information of the cylinder process and sometimes part of the in- and outlet ducts.

For filling and emptying models, or crank angle models, the control volumes in question are the various components of a diesel engine, for example the cylinder, the turbine or the charge air cooler. The step size is defined in order of magnitude of the crank angle, and the equations governing the processes between the elements are solved. The complexity of these models is dependent on what is and what is not included in the model. If a model includes extensive inertia and friction models, this will result in more detailed cycle information.

A diesel engine is often included in a larger system, for example in a drive train or propulsion system. This means that loads are applied to the engine and the in-cycle variations are often not of prime interest. With mean value models, the focus lies on the overall engine parameters such as temperatures, pressures and mass flows. The basics of these models are similar to the crank angle models, but the time steps are in order of revolutions or time.

The simplest diesel engine models are the transfer function models. With these models, the internal processes of an engine do not matter and the only interest is the engine output. The engine is modelled as a simple system with only some basic dynamical aspects.

This research focusses on the formation of NO_x in diesel engines and therefore a detailed model of the combustion process seems necessary to accurately describe the formation of NO_x. A couple of researchers already tried to predict the combustion using multi-zone combustion models. Linden[33] and Galindo Lopez[20] used two and three-zone models respectively. Lopez concluded that the complexities of the

mixing process inside the cylinder make it difficult to make a reasonable prediction. The capacity of the model is limited because for different selection of factors, a very different conditions of the flame zone can be achieved, resulting in different emissions values.

More physics need to be incorporated into the model, particularly in the mixing process, to improve the description of the process and in the end make better predictions. The two-zone model developed by Linden also resulted in differences that were considered too large. There were some difficulties matching the model with the test engine which resulted in a limited number of data points. And at the best matching point for the fuel consumption resulted in the largest deviation between the measured and simulated NO-emissions.

Because the multi-zone models seem unable to accurately predict the emissions, a different approach shall be used in this research. The transfer function model is too basic for this research, because the internal mechanisms of the engine are all discarded. The mean value model focusses on the overall engine parameters and also has the option to implement the engine in a bigger system, or to put it otherwise, change the engine system. In this case the implemenation of EGR would be an option. Llamas and Eriksson[34] already successfully implemented EGR in a mean value engine model. The conclusion to their research was that mean value simulation model showed a good agreement with the measurements.

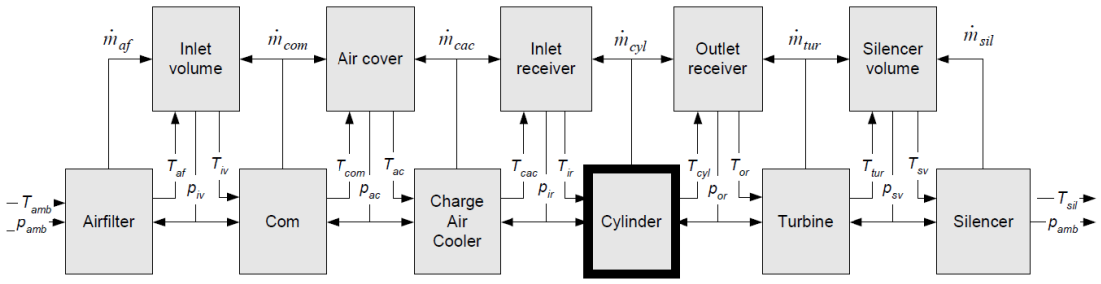

Figure 3.2: The concept of a mean value model[51]

The concept of the mean value diesel engine model is shown in figure 3.2. What can be seen in the figure is that the diesel engine model is made up of different blocks which are linked. The inlet volume, air cover, inlet receiver, outlet receiver and silencer volume are modelled as a series of control volumes. In those control volumes, the mass can be calculated by integrating the net mass flow(conservation of mass).

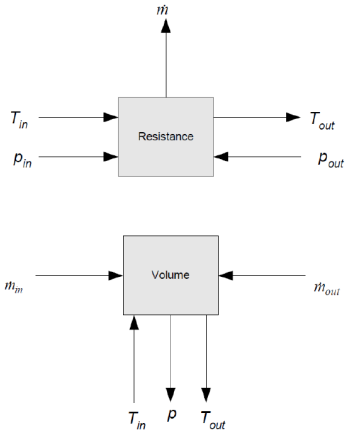

Figure 3.3: Resistance and volume element[51]

Integrating the net energy flow associated with the mass flows results in the instantaneous temperature(conservation of energy). All incoming mass flows have their own temperature and the

outgoing mass flows have a temperature equal to the instantaneous temperature off the element. Via the ideal gas law, the pressure of the elements can be calculated. The control volumes are all connected via so-called resistances. By using the momentum equation, the mass flow $\dot{m}$ in a resistance element can be calculated as of function of the pressure difference.
Figure 3.3 shows a resistance and volume element and all the in- and outputs as mentioned above. The resistance element calculates the mass flow through the element as a function of the pressure difference over the element. The volume element calculates the internal state properties of the the element as a function of the mass and energy leaving and entering the element. These resistance and volume elements form the building blocks for the mean value diesel model.

3.4. The Diesel A-Modular Model

It has already been 30 years since the Delft University of Technology started developing a diesel engine model based on the so called Mean Value First Principle (MVFP). This means that is uses cycle time instead of crank angle, which means that it can simulate a complete diesel engine system rapidly and efficiently. The diesel engine performance can be acquired under various operational conditions at a certain level of detail, but at the same time it can also be used as a sub-model in a total propulsion or power generation system simulation. A model using the MVFP approach is not primarily intended for diesel engine development, but is rather used for system studies of engine users of complex propulsion systems or where power is required for other purposes such as dredging.

The diesel engine model is developed in the MATLAB/Simulink environment, because that is very suitable to investigate large dynamic systems in the time domain. Besides that, the graphical user interface of Simulink provides the added benefits of recreating physical components as separate blocks. This way it provides a clear overview of the component relations within the entire system.

Two models have been developed at the Delft University of Technology in the department of Ship Design, Production and Operation (SDPO), namely the Diesel A and Diesel B model. They are both based on the mean value first principle, but they differ in complexity and integration. The Diesel A model is a lower entry level model that only requires basic project guide parameters, where the Diesel B model requires detailed data of the turbochargers, like operating maps of the turbine and compressor. These maps are confidential for most engines. The Diesel A model does not require operating maps, but uses a model to compute the available compressor power from which the charge pressure can be derived through a first order time delay. The diesel engine model that is used for this research was first proposed by Geertsma[21] and has recently been improved by Loonstijn[37].

For the Diesel A model it was important to look at the overall engine cycle performance as a whole. This means that the model must provide an accurate prediction of the model without sacrificing the computational performance of the model. The previous versions of the Diesel A model only have a single integrator that is used to estimate the charge pressure based on the available heat at the end of the closed cylinder process. In the Diesel A-Modular model or Diesel A-M model, this method has been improved by adding a more realistic estimation for the charge pressure through the Buchi equation. The estimation improved, but a second integrator is necessary to close the algebraic loop in the model. This integrator represents the time delay of the outlet receiver building up pressure, but is has no direct physical derivation. The biggest difference with the older A models is that the model has been cleaned and its structure is different compared to the other models. The idea of the A-modular model is, as the name already says, its modularity. This should make it easier to implement other sub models.

Thus, in comparison with previous versions of the Diesel A model, the AM model's aim was to solve the following issues:

- Provide a physical basis for the pressure build-up in the outlet receiver
- The possibility to implement advanced turbocharging strategies
- Cleaning of the model and removing redundancies

To provide a physical basis for the pressure build-up in the outlet receiver a volume element is implemented. This volume element is a thermodynamic model for an open control volume which can have multiple fluid

flows entering and exiting the volume. In this case the fluid consists of a mixture of air and stoichiometric gas. The control volume is described by the three conservation balances, namely the conservation of mass, the conservation of mass of gas and the conservation of energy.

This way the pressure, temperature and mass fraction of the control volume in the outlet receiver can be calculated. The inputs for the control volume are the mass flows that enter and exit the volume. The exit mass flow is determined by the turbine mass flow equation and is based on the flow through a nozzle. The entering mass flow is determined by the cylinder air swallow and gas disposal characteristics.

Besides that, implementing advanced turbocharging strategies also is a possibility. Because of the modular structure of this model, this should be possible in the future, but for this version of the model it is still too convoluted to split the sub model in multiple compressors and turbines for the advanced turbocharging strategies.

3.4.1. Diesel engine core

Just as the previous versions of the A model, the Diesel A-M model consists of two sub models, namely the Fuel Pump and the Diesel Engine Core. A schematic representation of the Diesel Engine Core sub model can be seen in figure 3.4. This representation slightly differs from the real model, but this figure is just to show the schematics. The figure has been adopted from Loonstijn's work[37], but has already been altered as a preparation for the implementation of exhaust gas recirculation.

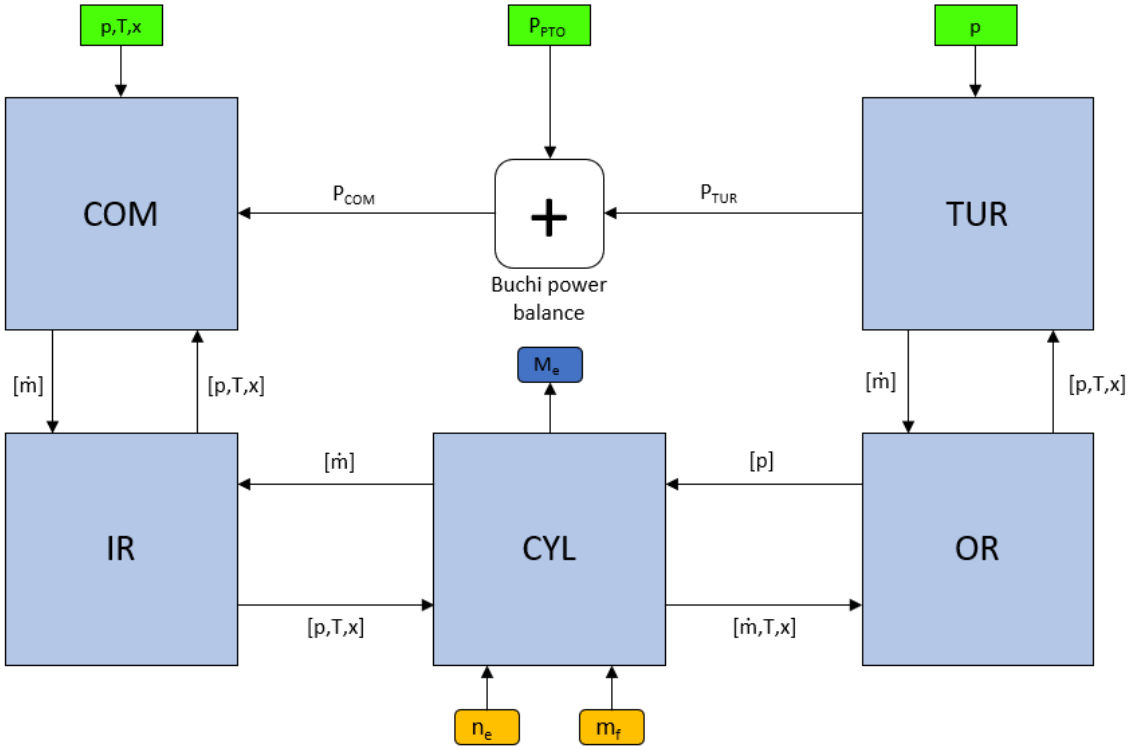

Figure 3.4: A schematic representation of the Diesel Engine Core sub model

What can be seen in the figure are the main components that form a physical engine. Five sub models can be distinguished, shown as the blue blocks, namely the compressor(COM), the inlet receiver(IR), the cylinder(CYL), the outlet receiver(OR) and the turbine(TUR). In the original representation the compressor block and inlet receiver block were combined, but for the implementation of EGR it makes more sense to split that block into two separate blocks. The five sub models are connected as shown in the figure. The orange rectangles are the inputs and the blue rectangle is the output of the system. The green rectangles are constants that are implemented as signals. In the future these constant might be replaced with variables to improve the model.

The cylinder sub model contains a mass flow model that calculates the air swallow and gas disposal, based on the speed of the engine, and the charge and scavenge conditions. The result is the total amount of mass that enters the cylinder from the compressor. The other outcome is the mass flow that leaves the cylinder and flows into the outlet receiver. This flow consists of two separate flows, namely the mass flow out of the cylinder and the slip flow. Both these flows have their own temperature and composition. These properties can be used in the outlet receiver sub model.

As already mentioned in the previous section, the outlet receiver is a volume element that is based on the conservations laws of the thermodynamic model of an open control volume. The two incoming streams are combined to one stream according to the conservation laws and a single stream flows into the turbine. This makes it possible to calculate the pressure, temperature and composition of the gas inside the outlet receiver as a result of the mass and enthalpy entering and exiting the volume.

The next sub model is the turbine. In the turbine, two sub models can be distinguished, namely the mass flow model and the specific power model. The mass flow model is based on the equation of flow through a nozzle. For this this equation, the so-called "elliptical law" and the Buchi equation are used. This model describes the mass flow through the turbine based on the pressure ratio over the turbine and the density of the mass flow at the inlet of the outlet receiver. The mass flow is used as an input for the outlet receiver and can be used to calculate the turbine power once the specific power is known.

The compressor and inlet receiver combined form the fourth sub model and it ensures that the model can operate without using compressor and turbine maps. It uses the same power calculations as the the turbine but the other way around. This can also be seen if we take a look at the inputs of the compressor block, these are reversed compared to that of the turbine block. The compressor takes the available power and imposed mass flow and determines what the pressure ratio should be in case the power and flow balances are in equilibrium.

Between the compressor and turbine blocks, it can be seen that the available power from the turbine passes through the Buchi power balance. This is the power balance from which the Buchi equation is derived. The main advantage of using the Buchi power balance is that in this form the power can be taken or supplied to the turbocharger shaft through an external source or load. This makes it possible to implement for example hybrid turbocharging.

3.4.2. Cylinder

Just as the Engine Core Sub model, the cylinder sub model also consists of four main components. These are the air swallow model, the Seiliger model, the gas disposal model and the Zinner blowdown model. A schematic representation of the cylinder sub model and the interactions between the components can be seen in figure 3.5.

This sub model starts with the air swallow model, which uses the inlet conditions p_c and T_c, the exhaust condition p_d and engine speed n_e. With these inputs, the air swallow model can determine the induction mass, which is dependent on the inlet conditions and the engine speed and the scavenge mass flow, which is dependent on the inlet and outlet conditions. These two mass flows combined make up the total mass flow into the engine($\dot{m}_{in}$). Then the trapped mass and slip flow can be calculated, by using two simplifications. $T_1 = T_{ind} = constant$ and $\eta_{sc} = constant$ are used. Further more, it is assumed that there is no further heat pick up of the slip flow beyond the induction, which means $T_{slip} = T_{ind}$.

Because a lot of the calculations are already done in the air swallow model, the gas disposal model is a lot simpler. Only a couple of summations are used to determine the total mass out from the mass in plus the added mass of the burnt fuel. The slip mass was already calculated in the air swallow model and is added to complement the mass leaving the cylinder. The final step is to determine the composition of the gas, which is dependent on the the air excess ratio which follows from the amount of fuel injected.

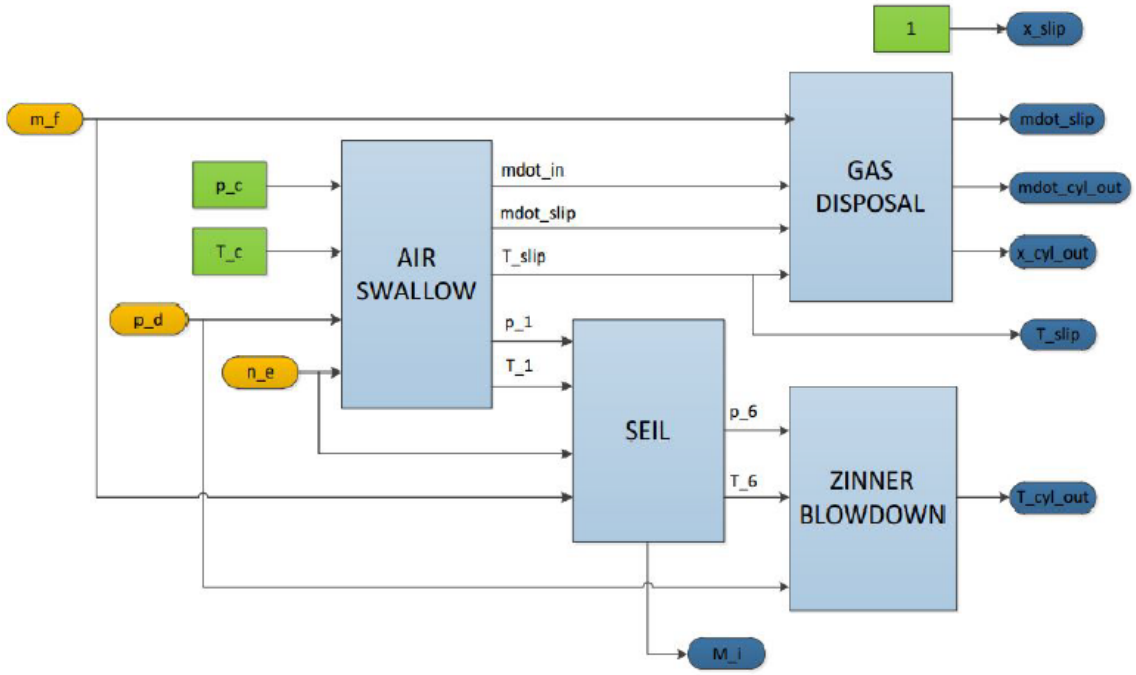

Figure 3.5: A schematic representation of the Cylinder sub model[37]

Then follows the Seiliger sub model, which consists of the closed cylinder process including the heat release model. The six point Seiliger process is used to calculate the work produced during the compression and expansion stroke of the diesel engine. The station points between the six stages are designated from 1 to 6 and are described as follows[56]:

- 1 - 2 polytropic compression
- 2 - 3 iso-volumetric combustion (at constant volume)
- 3 -4 isobaric combustion and expansion (at constant pressure)
- 4 -5 isothermal combustion and expansion (at constant temperature)
- 5 - 6 polytropic expansion
- 6 - 1 iso-volumetric heat rejection to the environment (at constant volume)

The heat release during the constant volume and constant pressure segment of the Seiliger process are inputs from the heat release calculation. The cylinder inlet pressure and temperature(constant), are the inputs of the start of the five point Seiliger process. The heat release is calculated using the cylinder inlet pressure, the amount of injected fuel and the engine speed.[21]

3.5. Air mass fraction

The previous sections have already explained the basic principles of the diesel engine model that is used for this research. This section will elaborate a bit further on some specifics of the model that are important for the implementation of EGR. Chapter 2 explained the main factors that influence the formation of NO_x in diesel engines. It was concluded that the two most important factors are the temperature during combustion and the amount of oxygen available in the combustion chamber. This section will elaborate on the air mass fraction in general and the computation of the air mass fraction in the model, according to the description given by Stapersma[55]. After that the influence of the air mass fraction on the air excess ratio and the specific heat will be explained.

3.5.1. Computation of the air mass fraction

The air mass fraction is declared as the fraction of air mass in certain mass flows and is given in kg/kg. Because the amount of oxygen available is an important parameter for determining the amount of NO_x produced, it is important to know how the air mass fraction will be used in the model. This means that the gas properties used in the model are dependant on their species and not on temperature. The definition of the air mass fraction is given in equation 3.1:

$$x = \frac{m_{air}}{m_{air} + m_{gas}} = \frac{m_{air}}{m_{total}} \tag{3.1}$$

The air mass fraction can take any value between 0 and 1, where 0 means that the mass flow contains no air and 1 means that the entire mass flow consists of air. For example, the air mass fraction of the ambient air at the compressor inlet is $x_a = 1$. After that the air is mixed with fuel and combusted and this will of course change the air mass fraction in the different stages of the model. How exactly the air mass fraction will be determined will be explained below.

In order to compute the air mass fraction during the different stages of combustion, first the complete combustion of air and fuel, resulting in stoichiometric gas, must be described. The general reaction equation of the complete combustion is given the following:

$$m_a + m_f \rightarrow m_{sg} \tag{3.2}$$

Where m_a, m_f and m_{sg} are the masses of air, fuel and stoichiometric gas respectively. The stoichiometric ratio is defined as:

$$\sigma = \frac{m_{a,min}}{m_f} \tag{3.3}$$

The reaction equation can then be described as:

$$\sigma \cdot m_f + m_f \rightarrow (\sigma + 1) \cdot m_f \tag{3.4}$$

In most cases the amount of incoming air is larger than required, meaning that there is excess air. This will result in a certain amount of air leaving the reaction without even taking part in the combustion process. For a complete combustion, and thus a combustion efficiency of $\eta_{comb} = 100\%$, the reaction equation becomes:

$$m_{a-in} + m_f \rightarrow m_{a-out} + m_{sg} \tag{3.5}$$

And the air excess ratio is defined as follows:

$$\lambda = \frac{m_a}{m_{a,min}} \tag{3.6}$$

Where m_a is the amount of combustion air available and $m_{a,min}$ is the minimum amount of required combustion air. Another way to describe the combustion reaction equation then becomes:

$$\lambda \cdot \sigma \cdot m_f + m_f \rightarrow (\lambda - 1) \cdot \sigma \cdot m_f + (\sigma + 1) \cdot m_f \tag{3.7}$$

From this equation the amount of air in the exhaust gas of the engine can be determined by simply rewriting the equation above:

$$\underbrace{(\lambda \cdot \sigma + 1) \cdot m_f}_{\text{in}} - \underbrace{(\sigma + 1) \cdot m_f}_{\text{gas out}} = \underbrace{(\lambda - 1) \cdot \sigma \cdot m_f}_{\text{air out}} \tag{3.8}$$

As can be seen in equation 3.8 the amount of air is given by $(\lambda - 1) \cdot \sigma \cdot m_f$. The diesel A-M model uses a slightly different approach to determine the air mass fraction. The 'gas out' part from equation 3.8 is used to compute the mass of the stoichiometric combustion gas in the cylinder. Then, not the air mass fraction, but the stoichiometric gas fraction is calculated. This fraction can be then used to determine the air mass fraction.

The overall process of the calculation in the diesel A-M model can be seen in figure 3.6. For the computation of the fractions, the trapped mass m_1, the stoichiometric ratio σ, the air mass fraction x_1(=1 without EGR), the fuel mass m_f, the combustion efficiency eta_{comb}(=1, meaning that it is assumed that all fuel is burned),

and the amounts of heat released at constant volume and constant temperature, X_{cv} and X_{ct}, are required. The amount of heat released at constant pressure can be computed from X_{cv} and X_{ct}.

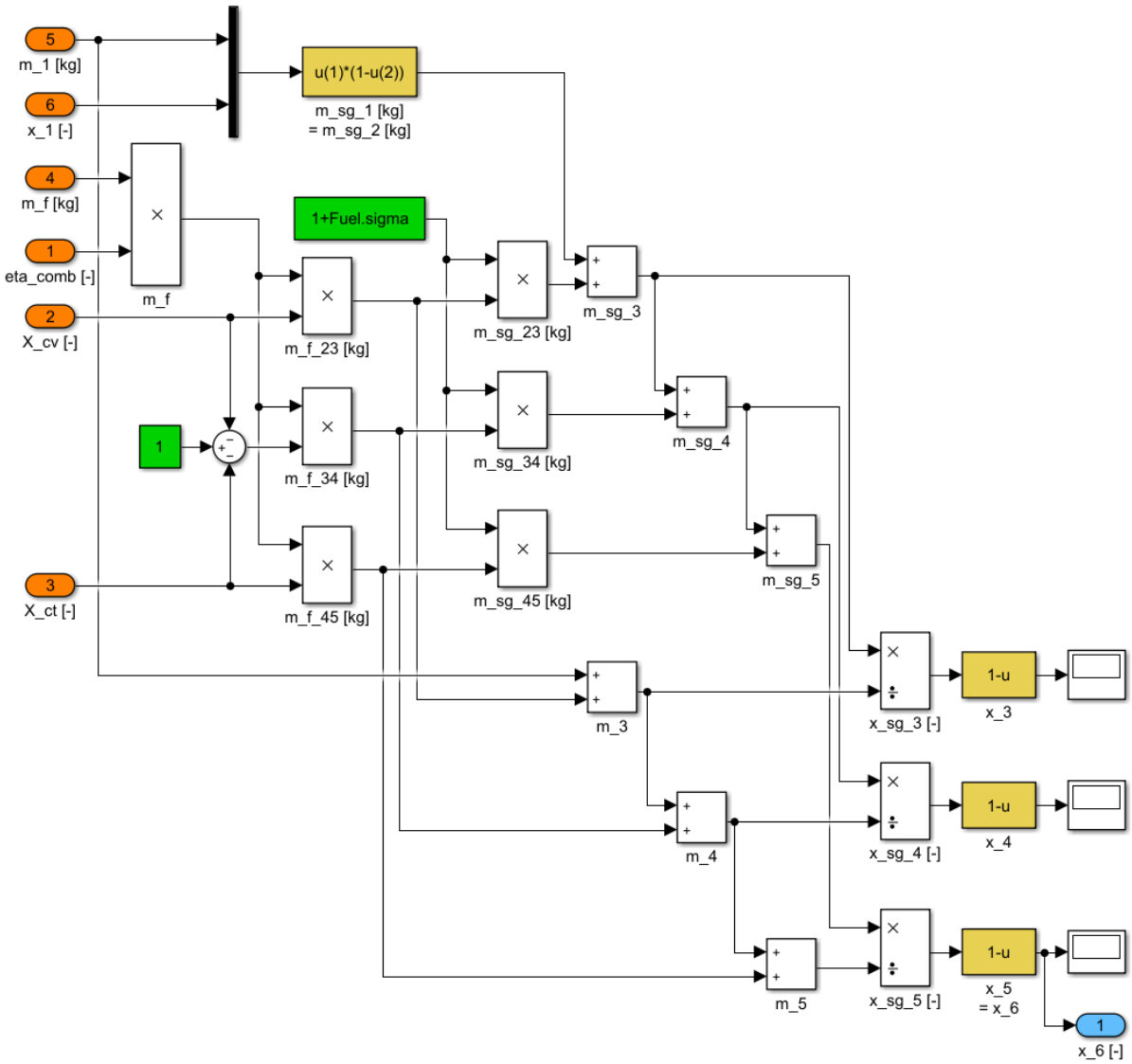

Figure 3.6: Calculation of the air mass fraction during the six-point Seiliger cycle

Because the air mass fraction is such an important part of this research, the following paragraphs will explain the computation of one of the air mass fraction, x_3 in this case, in a bit more detail. Before combustion starts, the air mass fraction at point 1 of the Seiliger cycle is always known. The mass of the stoichiometric gas at point 1 can easily be derived and because that mass does not change at point 2, the full equation becomes:

$$m_{sg,1} = m_{sg,2} = m_1 \cdot (1 - x_1) \tag{3.9}$$

Now that $m_{sg,2}$ is known, the mass of the stoichiometric gas originating from the isochoric combustion must be calculated. This is done by using the amount of heat released at constant volume and the amount of fuel used for combustion. Those variables compute the mass of the fuel used during isochoric combustion. After that the 'gas out' part of equation 3.8 can be used to calculate the mass of the stoichiometric combustion gas from the isochoric combustion. The following equations show these calculations:

$$m_{f,23} = \eta_{comb} \cdot m_f \cdot X_{cv} \tag{3.10}$$

$$m_{sg,23} = (\sigma + 1) \cdot m_{f,23} \tag{3.11}$$

The total mass of the stoichiometric combustion gas after the isochoric combustion stage is calculated by adding the mass of the stoichiometric gas after stage 2 and mass of the stoichiometric combustion gas from stage 2-3:

$$m_{sg,3} = m_{sg,2} + m_{sg,23} \tag{3.12}$$

The total mass in the cylinder at the end of stage 3 is computed in the same way as the total stoichiometric mass after stage 3:

$$m_3 = m_2 + m_{f,23} \tag{3.13}$$

The final step in the calculation of air mass fraction is determining the stoichiometric combustion gas mass fraction and finally subtracting it from 1 to get the air mass fraction at the end of the isochoric combustion stage:

$$x_{sg,3} = \frac{m_{sg,3}}{m_3} \tag{3.14}$$

$$x_3 = 1 - x_{sg,3} \tag{3.15}$$

The same method applies for the isobaric combustion stage and the isothermal combustion stage, but for these stages instead of the amount of heat at constant volume, the amounts of heat at constant pressure and temperature, X_{cp} and X_{ct} are used respectively. During the final stage of the Seiliger process, the expansion stage, no change in air mass fraction occurs, and thus $x_6 = x_5$. The air fraction of the gases leaving the cylinder will then be equal to x_6.

The next step in the diesel engine cycle is the outlet receiver and here the air mass fraction can slightly change. This is due to the so-called slip flow. The slip flow can be defined as the part of the flow that slips through the cylinder, without being trapped there. This means that the air flow that passes the inlet of a marine diesel engine is larger than the flow corresponding to the fresh mass kept in the cylinder during the closed cycle process. The total flow into the engine can be described as the fresh air flow plus the slip flow:

$$\dot{m}_{in} = \dot{m}_{fresh} + \dot{m}_{slip} \tag{3.16}$$

Then the so-called slip-factor can be defined:

$$s = \frac{\dot{m}_{slip}}{\dot{m}_{fresh}} \tag{3.17}$$

If slip occurs, this means that the slip flow will be mixed with the disposed gas from the cylinder in the outlet receiver. The slip flow will have another air mass fraction than the gases that leave the cylinder after combustion. This will result in a slight change in the air mass fraction, dependent on the ratio between the slip flow and the mass flow out of the cylinder. Besides that the mass flow out of the outlet receiver also contributes to the air fraction. The air mass fraction is first rewritten as the stoichiometric gas mass fraction. The fractions are multiplied by their respective mass flows and then added to get the total stoichiometric gas mass flow in the outlet receiver, or point d in the diesel engine cycle. The total stoichiometric combustion gas mass flow is then integrated to get the total mass:

$$m_{sg,d} = \int [\dot{m}_{slip} \cdot (1 - x_{slip}) + (\dot{m}_{cyl-out} \cdot (1 - x_{cyl-out}) - (\dot{m}_{OR-out} \cdot x_{sg,d})] ds \tag{3.18}$$

Now that the total total stoichiometric combustion gas mass in the outlet receiver is known, it can quite easily be converted to the air mass fraction of the outlet receiver:

$$x_{OR} = x_d = 1 - \frac{m_{sg,d}}{m_d} \tag{3.19}$$

Where m_d is the combined mass of flow out of the cylinder and the slip flow minus the mass of the flow out of the outlet receiver. The air mass fractions of the complete diesel engine cycle have now been discussed,

except for the final stage of the cycle, namely the turbine. The turbine does not change the composition of the gases and the air mass fraction of the exhaust gas will be the same as the air mass fraction of the outlet receiver. Because this research is looking into the effect of EGR on the diesel engine, it is important to correctly compute the air mass fractions of both the outlet receiver and the point after the turbine, because that are two possible starting points for an EGR route.

3.5.2. Air excess ratio

One of the variables influenced by the air mass fraction is the air excess ratio. The air excess ratio is important to predict the NO_x emissions, because it describes the amount of excess air in the cylinder during combustion. The air excess ratio in general is ratio of the total amount of fresh air in the cylinder to the minimum amount of fresh air required for combustion. The minimum amount of required combustion air is given by:

$$m_{a,min} = \sigma \cdot m_f \tag{3.20}$$

Where the m_f is the amount of fuel and σ is the stoichiometric air to fuel ratio. The air excess ratio is already given in equation 3.6 in the previous section. The amount of combustion air is of course determined by the air swallow characteristics of the engine. The effect of turbocharging is that it often creates a positive pressure difference between the in- and outlet receiver. If combined with a good valve overlap, this will create an ample scavenge flow. This will result in a really low amount of combustion gases remaining in the combustion chamber after burning and therefore the scavenge efficiency will be very good. That is why for this research a scavenge efficiency of $\eta_{scav} = 1$ will be assumed[55]. If the scavenge efficiency is assumed unity the air excess ratio is equal to the pseudo air excess ratio an can be defined as given in equation 3.21:

$$\lambda = \frac{m_1}{m_f \cdot \sigma} \tag{3.21}$$

Again, m_f is the mass of the fuel [kg] and σ is the stoichiometric air to fuel ratio. The variable m_1 is the mass of the trapped air at the start of the compression, also given in kg. The trapped mass at the start of compression is dependent on the charge air pressure and charge air temperature:

$$m_1 = \frac{p_1 \cdot V_1}{R \cdot T_1} \tag{3.22}$$

Where $p_1 = p_c$ is the pressure at start of the compression which is assumed equal to the charge air pressure. V_1 is the trapped volume, R the gas constant of air and T_1 is the temperature at the start of compression and is assumed equal to the charge air temperature T_c.

In a later stage of this research exhaust gas recirculation will be implemented in the model and this changes the air mass fraction and thus also the air excess ratio. The fraction of air in exhaust gases is lower than the air mass fraction of ambient air. This means that the air mass fraction needs to be incorporated into the definition of the air excess ratio. In this case, the implementation is pretty straightforward. The definition of the air excess ratio at the start of compression in the diesel A-M model is given by equation 3.23:

$$\lambda = \frac{m_1 \cdot x_1}{m_f \cdot \sigma} \tag{3.23}$$

Where x_1 is the air mass fraction of the gas at the start of compression. This equation can be used with and without EGR enabled. If EGR is disabled in the model, the air mass fraction $x_1 = 1$, resulting in equation 3.21. When EGR is enabled, the air mass fraction at the start of compression will decrease with increasing EGR rate.

Decreasing of the air excess ratio is tempting, because it increases the bmep. But when using the air excess ratio, there also is certain lower limit that should not be crossed. This is the smoke limit of a diesel engine and it sets a certain minimum air excess ratio below which there is insufficient air to burn the fuel completely[55]. It is called a smoke limit, because under this limit, not all fuel will be burned completely, causing smoke to come out of the exhaust. The smoke limit of a marine diesel engine lies at an air excess ratio of approximately 1.5 to 1.7. Marine diesel engines normally operate at an air excess ratio of 1.8 to 2.2. The smoke limit has to be taken into account when implementing EGR, because recirculating exhaust gas back into the combustion chamber will result in a lower air excess ratio. An increase in EGR rate will result in a decrease in the air excess ratio. So the EGR rate will be limited by the smoke limit.

3.5.3. Specific heat

Another important variable affected by the air mass fraction is the specific heat at constant volume c_v and the specific heat at constant pressure c_p. The specific heat is the amount of heat needed to raise the temperature of one kilogram of mass by $1K$ and is given in kJ/kgK.

For this research the Seiliger process is used to predict the performance of the diesel engine. For the Seiliger process it is assumed that the specific heats do not vary with temperature, but they are dependent on their species. This means that during one engine cycle $c_v, c_p = constant$ and for mixtures other than air the mean gas properties are assumed. And thus, due to the difference in the composition of the inlet air and the stoichiometric combustion gases different specific heats are specified. For the specific heats of dry air (at 300 K), the following values are assumed

- At constant volume: $c_{v,a} = 717.5 J/kgK$
- At constant pressure: $c_{p,a} = 1005 J/kgK$

Because for dry air the specific heats at 300 K are used, one must check in which range the specific heats of the stoichiometric combustion gases are at that temperature. The following figure shows the specific heats for dry air, stoichiometric gas and combustion gas at different temperatures.

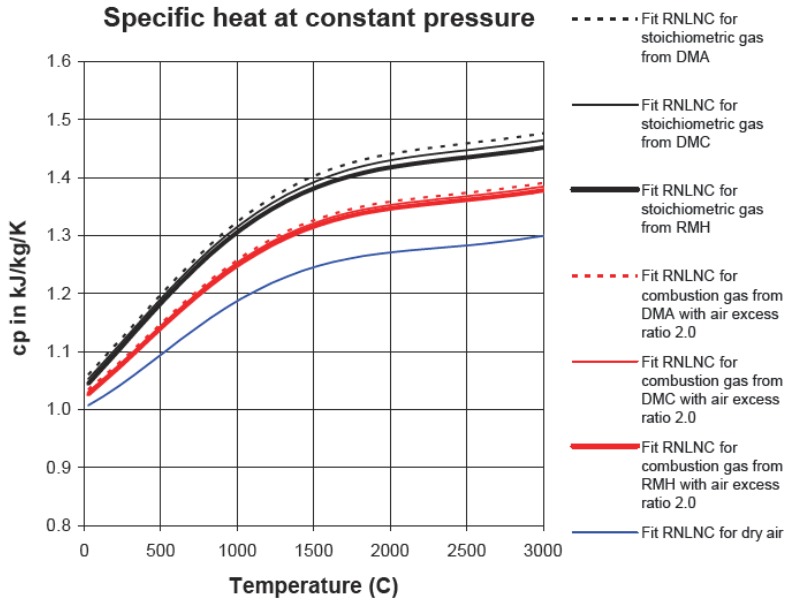

Figure 3.7: Specific heat at constant pressure as function of temperature for dry air, stoichiometric gas and combustion gas produced by three different types of fuel[57]

What can be seen in the figure is that the specific heat at constant pressure increases with increasing temperature. Besides that, the composition of the fuel is not of much influence on the specific heat. If the specific heat for the stoichiometric gas has to be defined the same as for dry air, it would be around 1050 J/kgK at 300K.

However, the ratio of specific heats between the stoichiometric gas and dry air is around 1.1 for the entire temperature range except for the the lowest temperatures up to 200°C. The used diesel engine operates at temperatures well above 1000°C and thus a choice has to be made for a good value of the specific heat for the stoichiometric gas. Looking at figure 3.7, it seems that the ratio of the specific heats between the stoichiometric gas and dry air is almost constant over the entire temperature range, especially when looking at the operating range for this specific engine. For that reason, the following specific heats are assumed for the stoichiometric combustion gas:

- At constant volume: $c_{v,sg} = 813 J/kgK$
- At constant pressure: $c_{p,sg} = 1100 J/kgK$

These specific heats are assumed constant for both with and without EGR enabled. But as already mentioned, the specific heats are dependent on the composition of the species. If EGR is enabled, part of the exhaust gases will be recirculated back into the engine and this will of course affect the specific heat of the mixture in the combustion chamber. This is also the case for the air and stoichiometric combustion gas mixture in the outlet receiver. Not all air is used during combustion and thus the outlet receiver contains a mixture of unburned combustion air and combustion products.

The specific heats are known for both the stoichiometric combustion gas and the dry (intake) air itself, and thus the specific heat of the mixture of those two species needs to be calculated. This is done by using the air mass fraction. Section 3.5.1 already elaborated on how the mass of the stoichiometric combustion gas was calculated and subsequently how the air mass fraction was defined. The combustion process in the cylinder can be described by:

$$m_{a-in} + m_f \rightarrow m_{a-out} + m_{sg} \tag{3.24}$$

The combustion process can also be described by the amount of fuel:

$$\lambda \cdot \sigma \cdot m_f + m_f \rightarrow (\lambda - 1) \cdot \sigma \cdot m_f + (\sigma + 1) \cdot m_f \tag{3.25}$$

Via the equation above, the mass fraction of the stoichiometric combustion gas and the mass fraction of the dry air can be described as follows:

$$x_{sg} = \frac{\sigma + 1}{\lambda \cdot \sigma + 1} \tag{3.26}$$

$$x_{da} = \frac{(\lambda - 1) \cdot \sigma}{\lambda \cdot \sigma + 1} \tag{3.27}$$

The (dry) air mass fraction gives the fraction of air in the respective species and is used throughout the diesel engine cycle. The specific heats of the mixture of dry air and stoichiometric gas at constant volume and constant pressure are given by the following equations. In this case these are the specific heats in the outlet receiver, at point d in the diesel engine cycle:

$$c_{v,d} = c_{v,air} \cdot x_d + c_{v,sg} \cdot (1 - x_d) \tag{3.28}$$

$$c_{p,d} = c_{p,air} \cdot x_d + c_{p,sg} \cdot (1 - x_d) \tag{3.29}$$

What can be seen in the equations is that a relatively simple method is used to specify the new specific heats, namely using the ratio of air and stoichiometric gases. How the air mass fraction will affect the air excess ratio and the specific heats when exhaust gas recirculation is implemented will be discussed in chapter 5.

3.6. Calibration of the diesel engine model

Now that it is known which engine will be used for this research and how it is going to be modelled, this section will bring those two together. The engine data extracted from the factory acceptance test and the EIAPP report will be used to calibrate the diesel engine model to match the actual engine. A validation will be performed by comparing the results of the model with test results from the acceptance test and EIAPP report.

The parameters that are required to calibrate the diesel A-M model are found in the project guide of the engine[9], the factory acceptance test(FAT)[10] of the engine and the EIAPP report[10]. Missing parameters will be substantiated by physics or estimated. Besides the large number of engine parameters, the model also contains the fuel, gas, water and general properties. The most important properties and constants can be found in table 3.2.

Diesel engine parameter	Variable	Value
Nominal engine power	$P_{e_{nom}}$	4500 kW
Nominal engine speed	$n_{e_{nom}}$	10 rev/s
Minimal engine speed	$n_{e_{min}}$	6 rev/s
Cylinder configuration	-	in-line
Number of cylinders	i	9
Number of revolutions per cycle	k	2
Bore	D_B	320 mm
Stroke	L_S	480 mm
Stroke/Bore-Ratio	-	1.5
Geometric compression ratio	ϵ	16.8
Effective compression ratio	r_c	14.2
Specific fuel consumption at nominal load	sfc_{nom}	185.8 g/kWh
Firing pressure	p	200 bar
Temperature after intercooler	T_c	315 K
Temperature at engine inlet	T_{inl}	335 K
Intercooler pressure loss ratio		0.01
Gas constant of air	R_a	287 J/kgK
Specific heat at constant volume of air	$c_{v,a}$	717.5 J/kgK
Specific heat at constant pressure of air	$c_{p,a}$	1005 J/kgK
Specific heat at constant volume of exhaust gas	$c_{v,g}$	813 J/kgK
Specific heat at constant pressure of exhaust gas	$c_{p,g}$	1100 J/kgK
Isentropic index of air	κ_a	1.4
Isentropic index of stoichiometric gas	κ_g	1.353
Lower heating value of fuel	h^L	42700 J/kg
Stoichiometric air to fuel ratio	σ	14.5
Nominal mechanical efficiency	$\eta_{m_{nom}}$	0.90
Ambient pressure	p_{amb}	$1e^5$ Pa
Ambient temperature	T_{amb}	293 K

Table 3.2: MaK 9M 32C diesel engine parameters for diesel A-M model

Now that the most important engine parameters and properties are known it is time to see how well the model represents the actual 9M 32C engine. This can be checked with data from the factory acceptance test(FAT) and the EIAPP emissions test report. One of the most important parameters of a diesel engine is the fuel efficiency. Multiple data points for the fuel consumption of the engine are known from both the acceptance test and the EIAPP report. Figures 3.8 and 3.9 show the fuel consumption data for the 9M 32C diesel engine.

Fuel consumption

The measurements were done at different load points as will be further explained in chapter 4. The data from both the FAT and EIAPP test report are shown as individual data points. The data extracted from the model is shown as the continuous line. The dotted lines are the + and − 5% error margins of the model. What can be seen in the both figures is that the model represents the fuel consumption of the 9M 32C engine very well, because all points are within those 5% margins.

Figure 3.8 shows the specific fuel consumption of the 9M 32C diesel engine. The horizontal axis shows the delivered engine power. Because Jumbo's vessels are propelled by controllable pitch propellers, the engine rpm is kept constant at 600 rpm and the delivered engine power depends on the load. The vertical axis shows the brake specific fuel consumption in g/kWh. The higher specific fuel consumption at lower loads is due to lower temperatures and lower pressures, which result in lower engine efficiency.

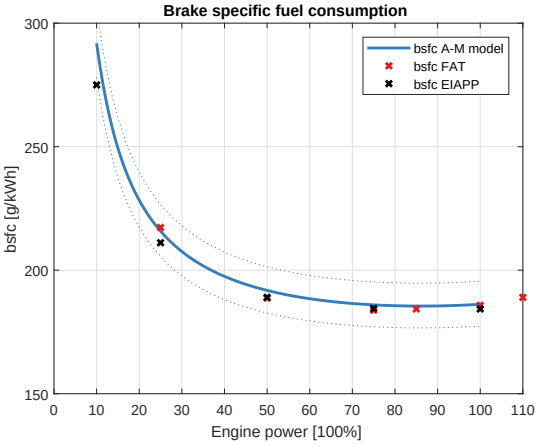

Figure 3.8: Brake specific fuel consumption against engine power [g/kWh]

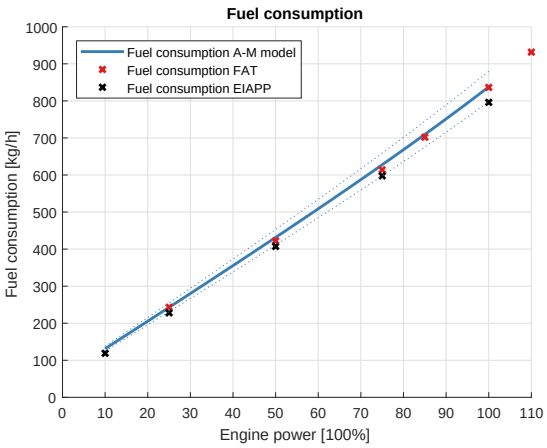

Figure 3.9: Fuel consumption against engine power [kg/h]

The figure on the right also shows the fuel consumption, but in other units, namely kg/h. The horizontal axis shows the delivered engine power and the vertical axis shows the fuel consumption in kg/h. What can be seen is that the fuel consumption increases linearly with increasing engine power.

Charge air pressure and mean effective pressure

Two other parameters that are available in both the FAT and the EIAPP report are the charge air pressure p_c and the mean effective pressure p_{me}. The charge air pressure is the pressure after the compressor, before it the charge air enters the combustion chamber. The charged air is cooled to a certain temperature with the intercooler after the compressor, which causes a small pressure loss. The FAT records show that the pressure loss ratio over the intercooler is only 0.01, which is almost negligible.

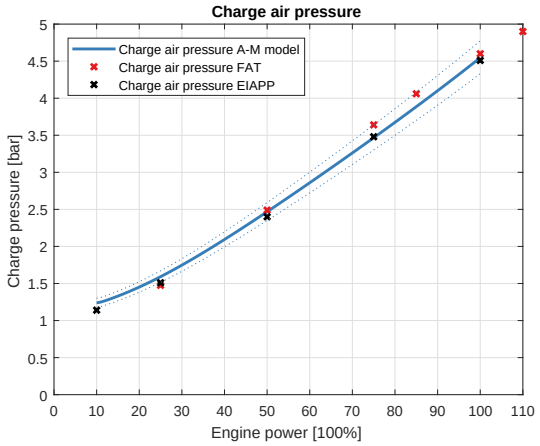

Figure 3.10: Charge air pressure against engine power [bar]

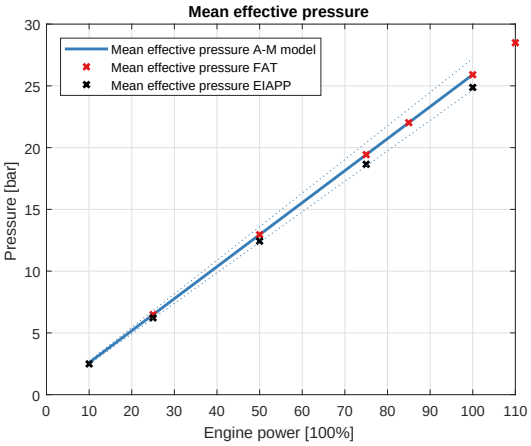

Figure 3.11: Mean effective pressure against engine power [bar]

Figure 3.10 shows the charge air pressure after the intercooler against the delivered engine power. What can be seen in the figure is that the charge air pressure increases linearly with the engine power. The vertical axis shows the charge air pressure in bar and it can be seen that the pressure rises up to the nominal charge air pressure of 4.6 bar for the rated output power of the engine. The figure also shows that the model represents the observational data from the EIAPP report and FAT records really well.

The mean effective pressure, or in this case the brake mean effective pressure is shown in figure 3.11. It can be regarded as the average pressure in the cylinder for a complete engine cycle and is defined as the ratio between the effective work and engine displacement. For this mean value simulation model it is calculated via the effective torque delivered by the engine:

$$p_{me} = 2\pi \cdot k \cdot \frac{M_e}{i \cdot V_S} \tag{3.30}$$

It can be seen that for any given engine, the brake mean effective pressure is directly proportional to the effective torque of the engine. Again, the model is able to simulate the actual engine really good and all data points are will within the 5% margins.

Temperatures

The data available in the EIAPP report and the FAT records is not really extensive, but some temperature measurements are also available and can be used to calibrate the engine. These temperatures are the temperatures before the turbine, after the turbine, and the temperature after the compressor, which are T_d, T_e and T_c respectively. The results of how well these temperatures are represented by the model, again with the 5% error margins, can be seen in figure 3.12.

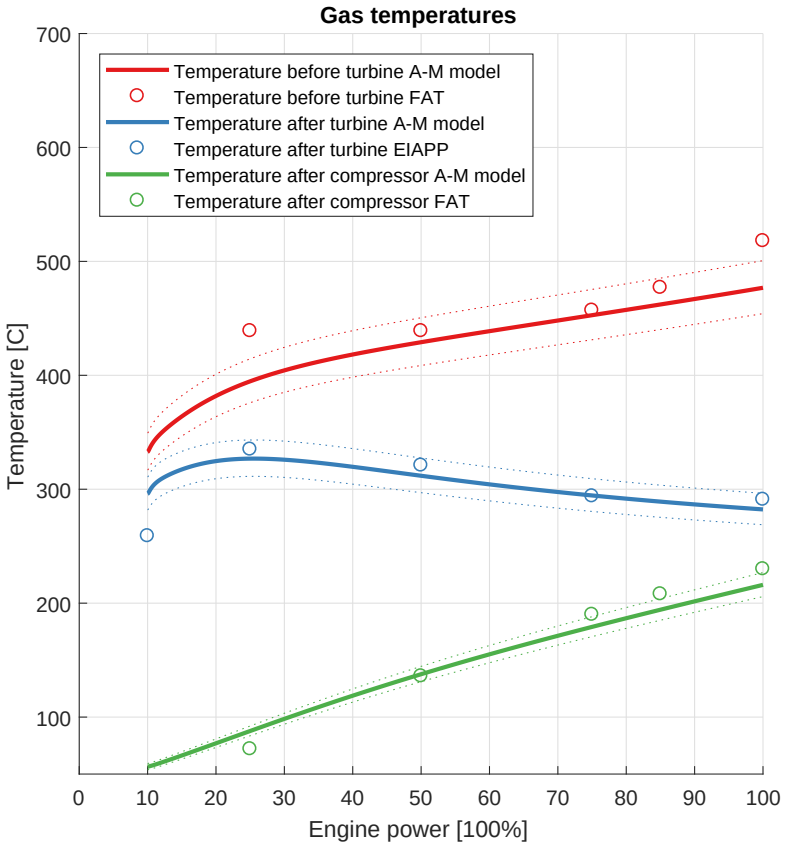

Figure 3.12: Gas temperatures against engine power [bar]

The overall trend of the temperatures is good, but there are some small outliers. The temperature before the turbine, T_d, shows two small outliers up at 25% load and 100% load. Those points are somewhat out of the 5% margin, but those temperatures are of less importance for this research and thus still acceptable. The temperature after the turbine, T_e, shows a small outlier at 10% load. This outlier is somewhat lower then the 5% margin, but still seems to follow the trend of that temperature profile. Altogether, it can be concluded that the model represents the observational data from the EIAPP report and FAT records quite well.

Partial efficiencies and effective efficiency

Another important factor is of course the engine efficiency. No observational data is available in the FAT or EIAPP reports, but it can be checked in what range the partial efficiencies of the engine model are. Because

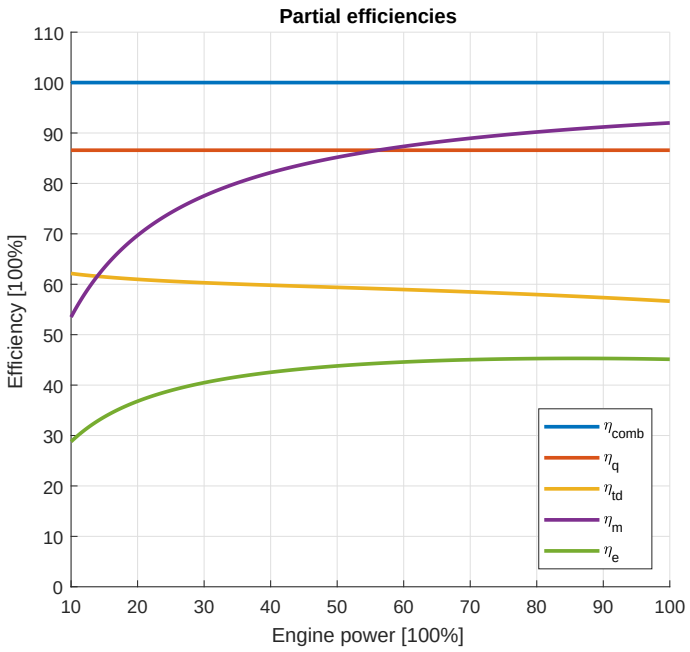

Figure 3.13: Efficiencies extracted from the mean value simulation model [%]

the used model is quite extensive, the following partial efficiencies are available to evaluate: combustion efficiency, heat input efficiency, thermodynamic efficiency, mechanical efficiency and the overall or effective engine efficiency. These five efficiencies can all be seen in figure 3.13:

Starting with the combustion efficiency η_{comb}. According to Betz and Woschni[7] the combustion efficiency is dependent on the pseudo air excess ratio and the smoke limit of the engine. As long as the pseudo air excess ratio is above the smoke limit of the engine, the combustion efficiency is assumed to be 100%. The combustion efficiency can be defined as the ratio of the combustion heat over the heat input. A combustion efficiency of 100% means that all heat is used for combustion.

The second type of efficiency is the heat input efficiency η_q. Despite the fact that all available heat is used for the combustion, a significant amount of the combustion heat lost: some of the heat is carried away through the cylinder liner and the cylinder head into the jacket cooling water and through the piston crown to the cooling oil[31]. And thus, the heat input efficiency indicates the percentage of toe combustion heat that is actually put into the cycle process. The total heat put in the cycle process can then be defined as:

$$Q_{in} = \eta_{comb} \cdot \eta_q \cdot Q_f \tag{3.31}$$

Where Q_f is the total heat input which is equal to the injected fuel per cycle times the lower heating value of the used fuel. According to Klein Woud and Stapersma[31] in this equation, the combustion efficiency is almost 100% or equal to 100%, and the heat input efficiency is somewhere between 80% and 90%. Figure 3.13 shows a combustion efficiency of 100% and a heat input efficiency of 88%. This means that those percentages are in the right range.

The percentage of heat lost is dependent on the engine speed n_e and the nominal heat input efficiency, meaning that for this engine, the heat input efficiency is constant, because the engine speed is constant. The nominal heat release efficiency is determined by using a iterative loop which decreases the heat input efficiency until the nominal cycle work of the model is correct for the nominal operating point, as described by Klein Woud and Stapersma[31].

The yellow line shows the thermodynamic efficiency η_{td}. This efficiency describes the heat losses during compression and the last part of expansion, because they are not included in the definition of η_q. The

thermodynamic efficiency is completely determined by the shape of the p-V and T-S diagrams.

The final type of efficiency is the mechanical efficiency of the engine. This efficiency includes mechanical losses such as the friction between the piston and the wall, friction in the bearings and pump losses. The power take off for the lubrication oil pump, cooling water pumps and fuel pumps are also incorporated in the mechanical efficiency. Altogether it can be defined as the ratio of the effective work over the indicated work and according to Kleinwoud and Stapersma[31] it is approximately 90% in full load condition. This means that figure 3.13 shows a realistic mechanical efficiency.

Finally, now that all the partial efficiencies, namely the mechanical, heat loss, combustion and thermodynamic efficiency, have been defined, the effective (or overall) efficiency of the engine can be written as:

$$\eta_e = \eta_m \cdot \eta_{comb} \cdot \eta_q \cdot \eta_{td} \tag{3.32}$$

Or also as the work output divided by the heat input. It can be seen that the overall efficiency of the 9M 32C engine increases from around 30% and flattens out to around 46%. Altogether, the shown efficiencies are all in the right range and the overall efficiency is also shows a realistic value.

3.7. Conclusion

This chapter started with a short description of the engine in question, the 9M 32C MaK marine diesel engine. After that a small introduction to turbocharged engines was given together with the engine station numbering that will be used throughout this research.

After that a short introduction into different diesel engine modelling concepts was given and one final modelling concept was chosen and the choice was substantiated. For this research a mean value simulation model is used. The model structure and different Simulink blocks were explained in more detail. A couple of important factors, like the air mass fraction, the air excess ratio and the specific heat were also thoroughly discussed, because they are important for the implementation of exhaust gas recirculation later on in this research.

But before implementing exhaust gas recirculation the model had to be tuned to match the available observational data from the 9M 32C engine. This data was extracted from an EIAPP report and the FAT records. The available data contained the fuel consumption, charge air pressure, mean effective pressure and several temperatures. After that the partial efficiencies extracted from the model were shortly discussed. It can be concluded that the model represents the actual engine very well and forms a good basis for the continuation of this research.

4

Fitting of the NO_x emission data

4.1. Introduction

The previous chapter explained how the diesel engine model was fitted with the 9M 32C diesel engine data. The next step is to evaluate the emission data found in the EIAPP report. First, the quality and origin of the data will be discussed. The next step is to evaluate the engine parameters that influence the formation of NO_x a bit further, in this case the combustion temperature and the availability of oxygen during combustion.

After that this chapter will explain the working principle of fitting data using a nonlinear regression model. This model will be used to derive fits for both the kg/h and g/kWh NO_x emission data. These fits will be used for the NO_x emission predictions later on. This chapter will be concluded with the evaluation of the fits using a set of goodness of fit statistics.

4.2. The NO_x emission data

This section will elaborate on the NO_x data found in the EIAPP report. The origin of the data will first be discussed, meaning that the used test cycles will be evaluated. The results from those tests give the NO_x emissions in ppm, kg/h and g/kWh. All those results will be discussed, inaccuracies will be highlighted and a decision will be made on which data is useful for the fits.

4.2.1. EIAPP NO_x data

All seagoing ships with diesel engines have to comply with IMO MARPOL Annex VI regulation 13 and the NO_x technical Code 2008. This means that an Engine International Air Pollution Prevention Certificate (EIAPP certificate) is required for each engine or each engine group. This EIAPP certificate is proof that the used engine system is compliant with the regulations and also contains a supplement that contains all the details and parameters that may influence the engine's NO_x emissions. A certificate can only be issued by a recognized organisation on behalf of the respective flag as stated by DNV GL[17].

For every individual engine or parent engine of an engine family or group, certain relevant test cycles are specified. For example, there are different cycles for a "Propeller law operated main and propeller law operated auxiliary engine" application, "Constant-speed auxiliary engine" application and "Variable speed, variable load auxiliary engine" application. In this case, the used test cycles are for the "Constant-speed main propulsion" application(E2) and the "constand-speed auxiliary engine" application(D2). The "constant speed main propulsion" test cycle also includes the controllable-pitch propeller installation, which is used for the 9M 32C engine of the latest Jumbo vessels. A more elaborate explanation of the possible test cycles is given by the Marine Environment Protection Committee in the amendments to the NO_x Technical Code[40].

For all marine diesel engines, the specified test cycle shall be applied to verify the compliance with the applicable NO_x emissions limits. Each test cycle uses different engine speeds, power, but most important different weighting factors for each part of the test.

The test cycle used for a controllable-pitch propeller installation(E2) can be seen in table 4.1 and the test cycle used for the constant speed auxiliary engine(D2) can be seen in table 4.2.

Test cycle type E2	**Speed**	100%	100%	100%	100%
	Power	100%	75%	50%	25%
	Weighting factor	0.2	0.5	0.15	0.15

Table 4.1: Test cycle E2 for the "Constant-speed main propulsion" application[40]

Test cycle type D2	**Speed**	100%	100%	100%	100%	100%
	Power	100%	75%	50%	25%	10%
	Weighting factor	0.05	0.25	0.3	0.3	0.1

Table 4.2: Test cycle D2 for the "Constant-speed auxiliary engine" application[40]

The results of these tests can be found in EIAPP reports which should be kept aboard the vessels at all time. Jumbo Maritime also has EIAPP certificates for their latest ships, the Jumbo Kinetic and the Fairmaster. Because both ships were manufactured at the same time and with the same specifications they share the same type of propulsion plant. They each have two 9M 32C MaK engines on board. For these four engines, an EIAPP certificate is available for the parent engine of the group. This parent engine is slightly different than the engines used aboard the vessels.

The parent engine is the MaK 6M 32C, while the engines used in the ships are of the type MaK 9M 32C. The only difference between these engines is the number of cylinders. The rest of the engine specifications is exactly the same. The engines used aboard Jumbo's vessels have 9 cylinders(9M), where the tested parent engine only has 6 cylinders(6M). This has to be taken into account when it comes to the engine emission data. The NO_x emission data for the parent engine(6M 32C) can be seen in table 4.3. More detailed information from the EIAPP report, including data of other pollutant emissions can be found in appendix A.

Power/Torque (%)	**10**	**25**	**50**	**75**	**100**
NO_x concentration wet (ppm)	822.3	681.6	913	898.7	875.9
NO_x mass flow (kg/h)	5.2	6.319	14.653	21.199	26.383
NO_x specific (g/kWh)	18.634	9.018	10.479	10.157	9.55

Table 4.3: NO_x emission data EIAPP Certificate 6M 32C[10]

Because the parent engine has a different number of in-line cylinders, the EIAPP emissions data has to be converted to match the engine specifications of the 9-cylinder engine used by Jumbo. Because that is the only difference and the rest of the engine is exactly the same, this can be done really easily. The wet concentration of NO_x stays the same, because this is measured in parts per million. This means that the concentration of the NO_x in the exhaust gas does not change when the number of cylinders changes. The same can be said about the specific NO_x emissions, because this is measured or converted to g/kWh. The NO_x mass flow however does change, because the three extra cylinders means that more fuel is burned and the mass flow will increase by a factor of $9/6 = 1.5$. The adapted values for the NO_x emissions of the 9M 32C engine can be seen in table 4.4.

Power/Torque (%)	**10**	**25**	**50**	**75**	**100**
NO_x concentration wet (ppm)	822.3	681.6	913	898.7	875.9
NO_x mass flow (kg/h)	7.8	9.4785	21.98	31.799	39.575
NO_x specific (g/kWh)	18.634	9.018	10.479	10.157	9.55

Table 4.4: NO_x emission data converted to 9M 32C

The data shown in tables 4.3 and 4.4 has also been implemented in graphs. The first graph, which can be seen in figure 4.1, shows the NO_x emissions data of the engine given in the unit parts per million(ppm).

The NO_x emissions are analysed using the ECO Physics CLD 82 Shr which has a measurement range of 0 - 2000 ppm and a deviation of only 0.09%.[10] It can be seen that the emissions, measured in ppm, are quite constant for the entire load case, except for the point at 25% load. There is a big outlier in the NO_x emissions at that point. Why this point deviates so much from the rest will be explained later on.

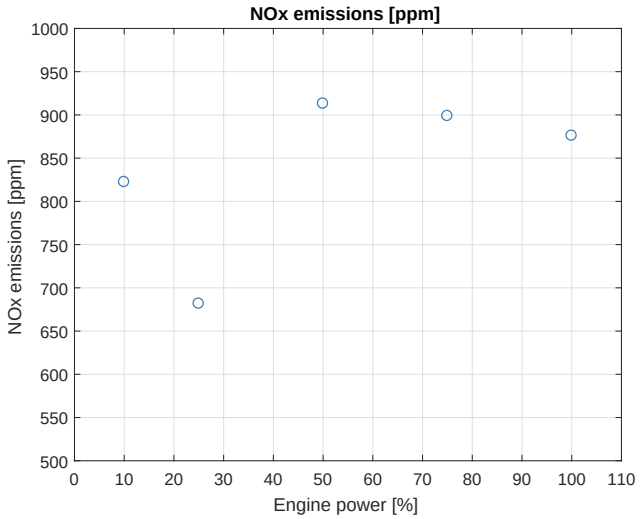

Figure 4.1: NO_x emissions against engine power [ppm]

Figure 4.2 shows the emission data for NO_x in kg/h for both the parent engine, the 6M 32C, and the 9-cylinder engine aboard Jumbo's vessels, the 9M 32C. The trend that can be seen is that the emissions increase with increased engine power. This can have multiple reasons: if we look at the variables that also increase with increased engine power, it can be seen that a couple of these variables are the mass flow of air and fuel into the engine and the pressure during combustion. This should also be taken into consideration when trying to fit the engine to the NO_x emission data. Just as with the emission in ppm, this graph also shows a deviation for the load at 25% engine load. However, the deviation is not as big as with the emissions given in ppm.

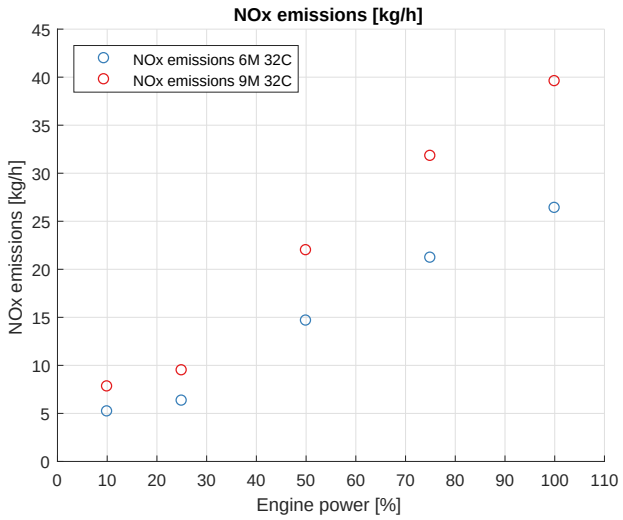

Figure 4.2: NO_x emissions against engine power [kg/h]

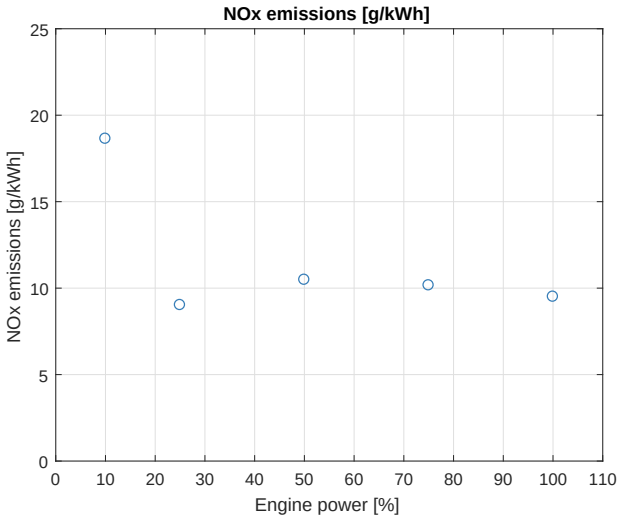

Figure 4.3: NO_x emissions against engine power [g/kWh]

The third graph, shown in figure 4.3, displays the power specific NO_x emissions. This means that the emissions are shown in g/kWh. The data can be interpreted in two ways: an outlier at 10% load or an outlier at 25% load. The outlier at 10% engine can be substantiated: at lower engine loads there is large amount of excess air and the specific fuel consumption is really high. A diesel engine is less efficiency at lower engine loads. Another way to observe the data is that the data is reciprocal, meaning that it is of the form $y = k/x$, where k is positive. If this is the case, the same observation can be made as with the ppm and kg/h data can be made, namely that the point at 25% load deviates from the rest. The deviations in all of the available data will be discussed in the following subsection.

4.2.2. Interpretation of the NO_x emission data

Because there are some deviations and outliers in the available emission data, this subsection will elaborate a bit further on these deviations and it will explain how the data will be interpreted for the rest of this research. Because the emissions have to be linked to a MATLAB/Simulink model it is important that the units are in accordance with the units of the model and vice versa. That is why the units of the available emissions data, ppm, kg/h and g/kWh, will be shortly discussed. After that the mentioned inaccuracies and outliers will be will be evaluated.

Units of the NO_x emission data

First of all, the NO_x emissions in ppm will shortly be discussed. As mentioned in the introduction, the emissions have to be linked to a MATLAB/Simulink model and the units need to be in accordance with each other. The ppm emissions cannot be directly linked to the engine parameters which are derived from the Simulink model. In order to use the emissions in ppm, they need to be converted to units that can be directly linked to the model. In order to do this the exact composition of the exhaust gas is required. Because the used model is a mean value model, the exact composition of the exhaust gas is not known. As already explained in section 3.5 the air mass fraction is an important factor in the diesel A-M model, but this factor only determines the division of exhaust gas and air. Because the exhaust composition of the exhaust gases cannot be exactly determined, it has been decided that the NO_x emissions in ppm will not be used for this research.

The next type of emissions are the NO_x emissions in kg/h. As already discussed in the previous section, the difference between the parent engine and the actual engines on board Jumbo's vessels needs to be kept in mind. The parent engine only has six cylinders, while the Jumbo's vessels all have the 9-cylinder variant on board. The emissions have already been converted to the 9-cylinder engine and because the units are in kg/h, they can easily be used with data from the Simulink model. A possible engine parameter that can be used for these emissions are the flow of fresh air into the engine.

The final type of available emission data is given as the power specific emissions in g/kWh. As can be seen in the units, this type of emission takes the delivered engine power into account and is therefore often used. With the specific emissions, engines of different sizes can easily be compared. This is also the reason why the NO_x emissions given by MARPOL are also given as specific emissions. The used diesel engine model also takes engine load into account and thus this type of emissions could be deducted from the model.

Inaccuracies in the NO_x emission data

The next step in determining the usability of the data is to look at the available datasets and look for deviations or inaccuracies. The inaccuracies have already been shortly discussed in the previous section, but it still have to be determined how they will be dealt with. The similarity between the NO_x emissions in ppm, kg/h and g/kWh is the point at 25% engine load. Because the kg/h data shows almost shows a straight line, except for the 25% load point, the fits will not be affected much by this deviation. The ppm and g/kWh data however are a different story.

Starting with the g/kWh data, the outlier at 10% engine load can be substantiated by the fact that diesel engines operate at lower temperatures and pressure and are therefore less efficient at lower loads. The overall engine efficiency of the 9M 32C diesel engine is shown in figure 4.4. The efficiency rises up to maximum of around 45% for the engine loads ranging between 70 and 100%. The 70 to 100% load segment is also the recommended operating range according to the engine manufacturer.

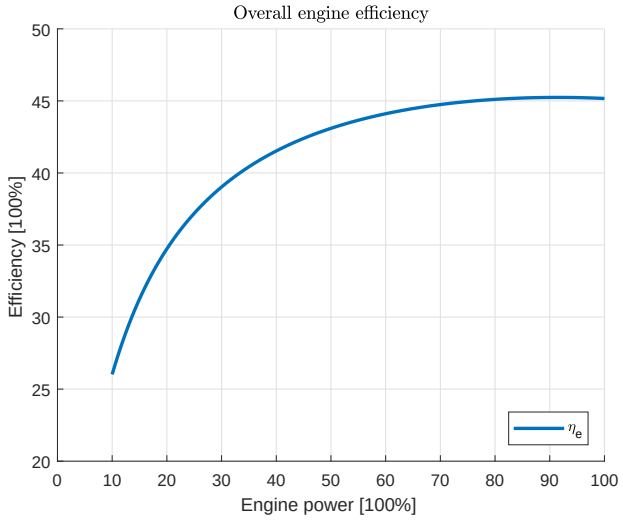

Figure 4.4: 9M 32C overall engine efficiency

Another factor that influences the formation of NO_x is the availability of oxygen. Because there is a large amount of excess air available at lower engine loads, this also means that more oxygen is available. This higher concentration of air and thus also oxygen makes the reaction to form NO_x easier. The engine efficiency and high amount of excess air substantiate the outlier for the g/kWh emissions.

The 10% emission point is assumed to be correct. This means that the g/kWh emission data shows kind of a reciprocal curve, with the 25% data point being an outlier. It would then be expected that the 25% data point would have a slightly higher value. A value of around $12 g/kWh$ would give a perfect fit, but this is not the case. However, it is not sure why this point has such a low value compared to the other values. Different engine parameters have been checked and no big outliers or deviations occur for any of the parameters.

Just as with the g/kWh emissions, the difference in value is even bigger for the ppm emission data. Despite the fact that the emissions given in ppm will not be used for this research, it is still good to know why there is an outlier at 25% load point. Especially because this deviation also occurs in the other emission data. For the ppm data set, the four other data points are all in range between 820 and 920 ppm, and the outlier is situated

around 680 ppm.

What might be an option is that variable valve timing or variable injection timing have been used during the test cycles in order to cope with the NO_x emissions. The EIAPP report has been checked for these occasions and the report confirms that there is no question of variable injection timing or variable valve timing.

Having said that, it is also important to keep the engine test cycles in mind. Appendix A shows the records of the acceptance test and the emission test report. For the acceptance test, the test run at 25% engine load lasted 30 minutes and for the emission test the run lasted 20 minutes. It is most likely that the final result of the test run is an average over the entire run and not just a snapshot at one point of the test run. This would of course imply that the available data is correct.

The best way to clarify the emission data one should of course compare the data of the 9M 32C engine with other similar marine diesel engines. However, the EIAPP certificate only applies for new build ships and has only made its introduction in 2008. This means that not that many certificates are available. Besides that, engine manufacturers are not so keen on sharing this information with everyone. The EIAPP certificate does not have to made public, it should however be available for the manufacturers' clients and it should also be available on the ship at all time. Despite the fact that comparing the emission data with other engines is not possible, a decision has to be made on the usability of the data.

Now that is has been determined that the 25% load point is questionable, a choice has to be made on how that load point is interpreted for the emissions fits. Despite the fact that accepting the 25% load point would make the fitting a more difficult process, the engine tests have been used for years and are assumed to be correct. For that reason it has been decided that the fits will be with the 25% load point included. How this influences the fits and the goodness of the fits will be discussed in the following sections.

4.3. NO_x emission influence factors

Section 3.6 discussed the calibration of the diesel A-M model with the available data from the project guide, factory acceptance test and the EIAPP report. After that, section 4.2 discussed the available NO_x data, also obtained from both the factory acceptance tests and the EIAPP report. The usability of the data has been discussed in the previous section. This section will bring those two together, and will describe how different fits are made with engine parameters from the A-M model to match the available NO_x emission data.

Chapter 2 explained the main causes for the NO_x formation in diesel engines. It was concluded that the most important factors were the oxygen available for combustion and the combustion temperature(and with that also hot spots). This section will look at engine parameters that can be linked with the amount of oxygen and the combustion temperature. These parameters will then be used to create fits in such a way that the amount of NO_x produced can be directly linked with one or multiple parameters. For example, the air excess ratio λ, the fresh air drawn into the engine $\dot{m}_{fresh}$ and the maximum combustion temperature T_4 can be used.

This means that the prediction of the NO_x emissions is based on the hypothesis that these emissions are the direct consequence of certain engine parameters, of which some are already mentioned above. The most important engine parameters that are used are those that are linked to the oxygen availability and the combustion temperature. Before explaining how the fits are prepared, these influence factors will be shortly discussed.

4.3.1. Oxygen availability

The amount of oxygen available during combustion can be described in a number of ways. This section will describe which engine parameters are used to describe the oxygen content.

What might be the most important factor is the air mass fraction, which is discussed in section 3.5. The air mass fraction defines what part of the gas mixture in any point of the engine consists of air. The other part if the mixture is assumed to be non-combusting exhaust gas. The air mass fraction changes throughout the engine cycle and influences a lot of other engine parameters. Therefore, the air mass fraction itself will not be used to make the NO_x fits.

An engine parameter which is partly dependent on the air mass fraction is the air excess ratio λ. It is defined as amount of fresh air in the cylinder divided by the minimum amount of fresh air required for combustion:

$$\lambda = \frac{m_1 \cdot x_1}{m_f \cdot \sigma} \tag{4.1}$$

The air excess ratio gives the ratio of redundant air in the cylinder and provides a good basis for the amount of fresh air in the cylinder. Other engine parameters that can be used are the mass flow of fresh air into the engine, $\dot{m}_{fresh}$, and the mass of fresh air in the cylinder cylinder chamber, m_{fresh}.

The definition of $\dot{m}_{fresh}$ in this case is a little bit different than already mentioned earlier in this thesis. Because it is known that the amount of oxygen available for combustion is an important factor, it is important to also take the air in the recirculated exhaust gas into account. The way to do this is using the trapped mass (converted to mass flow) and the air mass factor. $\dot{m}_{fresh,x}$ is then defined as follows:

$$\dot{m}_{fresh,x} = \dot{m}_1 \cdot x_c \tag{4.2}$$

The difference between $\dot{m}_{fresh}$ and $\dot{m}_{fresh,x}$ is relatively small, but because the oxygen content is such an important engine parameter, the small amount of air in the exhaust gases cannot be neglected. The difference between $\dot{m}_{fresh}$ and $\dot{m}_{fresh,x}$ can be seen in chapter 6 in figures 6.5 to 6.8.

4.3.2. Combustion temperature

It is already known that one of the main factors for the formation of NO_x is a high combustion temperature. The maximum cylinder temperature in an engine only occurs during a short time of the combustion process and it does not really influence the maximum temperature of the metal parts surrounding the combustion chamber. The maximum temperatures in the combustion chamber of a diesel engine can be as high as 1500 to 2000 °C. This is also one of the reasons that the diesel engine has such a high thermal efficiency.

A high mean temperature in the cylinder is disadvantageous for the formation of NO_x, because the higher background temperature causes hot spots to be larger or have a higher temperature or both. This is because the hot spots will lose less heat to the surrounding area. Figure 2.1 showed that the formation of NO_x rises exponentially above 2250 °C and hot spots in a diesel engine can easily achieve those values. Because a mean value first principle model is used, only the average combustion temperature in the cylinder is known. One of the most important effects of exhaust gas recirculation is that the average temperature during combustion will decrease due to an increase in specific heat and the smaller amount of oxygen available.

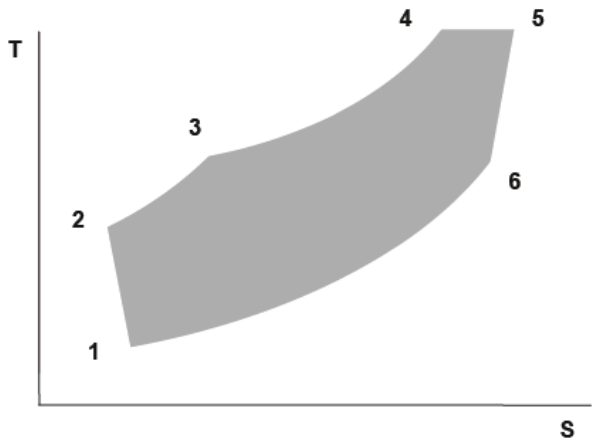

Figure 4.5: 6-stage Seiliger process T-S diagram[55]

To evaluate the temperature during combustion, it is first necessary to decide which temperature should be evaluated. As mentioned above, NO_x is formed during peak temperatures in the cylinder. Figure 4.5 shows the Temperature - Entropy diagram of a standard 6-stage Seiliger process. What can be derived from the

diagram is that the maximum cylinder temperature is reached after the isobaric combustion and expansion at constant pressure and the isothermal combustion and expansion at constant temperature between T_4 and T_5. What can be concluded is that T_4 is equal to T_5 and that at that point in the Seiliger cycle the maximum temperature is reached.

Because the average combustion temperature reaches its maximum at T_4, this is the stage that will be used to further evaluate the effect of EGR on the temperature. Because only using the temperature for the fits would result in the wrong units, it has been decided that a temperature ratio will be used. Because we do not want to change the maximum combustion temperature too much, the other temperature in the ratio must be constant or close to constant. That is why the temperature prior to the maximum combustion temperature will be used: T_3. This temperature is close to constant and will not influence the trend of the maximum combustion temperature too much. Figure 4.6 shows both temperatures, T_4 and T_3, and figure 4.7 shows the ratio between those two temperatures.

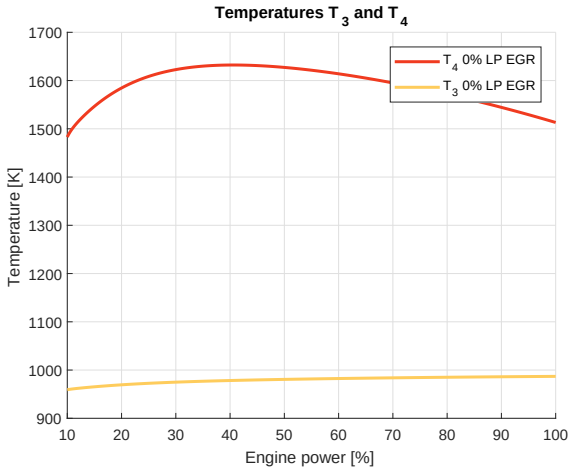

Figure 4.6: Temperatures T_4 and T_3

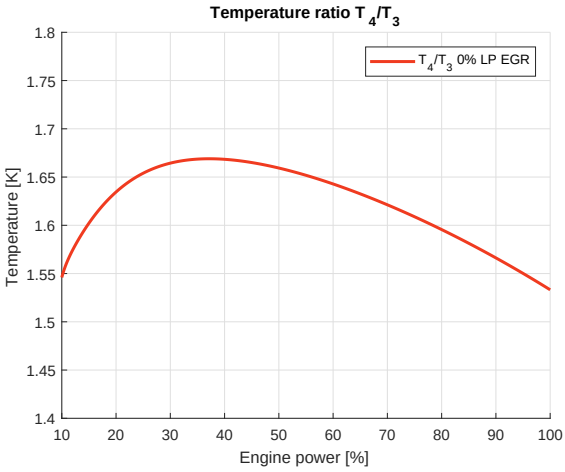

Figure 4.7: Temperature ratio T_4 over T_3

Now that the origin of the emission test cycles and the NO_x emission data have been evaluated and all the important engine parameters have been discussed, the next step in this research is to make the actual fits that can be used to predict the NO_x emissions.

4.4. Fitting of the NO_x emission data

It is important that these fits will be created according to certain systematics in order to compare all the fits on the same aspects. Besides that, the units of the fits also need to be the same as the units of the available NO_x emission data. In this case that means that the fits need to comply with the units kg/h and the specific NO_x emissions in g/kWh. It has already been decided that the emissions in ppm will not be used for this research. The entire fitting process of course needs to be, if possible, physically substantiated. The following section will elaborate on the used fitting method and after that an explanation will be given on how the fits are evaluated.

Of course, as will be explained more thoroughly in chapter 5, this thesis will conduct research on two different EGR configurations. A distinction is made between a low-pressure and high pressure EGR configuration. The EGR route of the low-pressure variant starts downstream from the turbine and re-enters the regular diesel engine cycle upstream of the compressor. The high-pressure EGR already starts after the outlet receiver upstream of the turbine and re-enters the cycle downstream of the compressor. This also explains the names of the EGR configurations. The working pressure of the low-pressure configuration is around the ambient pressure and the pressure in the high-pressure configuration is equal to the charge air pressure, which can go up to about 4.5 to 5 bars. A schematic overview of these configurations can be seen in figures 5.2 and 5.3.

Now that the two EGR configurations have been briefly discussed, the question remains whether the fits will

be influenced by the difference in these configurations. The answer to that question is that, as long as EGR is disabled, the two different models will give the exact same results. This is beneficial because the same fits can be used for both the low-pressure and high-pressure configurations. However, when EGR is enabled, the fits will of course react differently to both configurations. So, as shall be seen in chapter 6, the effect of the different EGR configurations on the fits will be discussed in more detail.

4.4.1. Fitting with a nonlinear regression model

In order to make good fits of the NO_x emission data one or more engine parameters will be used for each fit, meaning that a method has to be used were one or more variables can be used to make the fits. One way to incorporate multiple independent variables or parameters into a single fit is by using nonlinear regression. This is a form of regression analysis where the observational data is modelled by a function which is a combination of model parameters and it depends on one or more independent variables. A general nonlinear regression equation takes the following form [42]:

$$y = f(X, \beta) + \varepsilon \tag{4.3}$$

Where

- y is a vector of observations of the response variable.
- f is a regression function of X and β that evaluates how each row of X along with the vector β to compute the prediction for y.
- X is a matrix of predictors, with a row for each observation and a column for each predictor.
- β is a vector of unknown parameters to be estimated.
- ε is vector of independent, identically distributed random disturbances, also known as the error term.

MATLAB has a function to fit a nonlinear model to data and it is called `fitnlm`, which stands for fit nonlinear model. What `fitnlm` or any regression model tries to do is find values of the parameters β that minimize the mean squared differences between the observed responses y and the predictions of the model $f(X, \beta)$. The mean squared differences are combined to the sum of squares, which tracks how much the observations vary from the mean of the data set. The smaller the sum of the squared values, the better the function fits the data points in the set.

To use a nonlinear regression function, a starting value for the parameters β is necessary. The starting value, for this research `beta0`, is the starting point for the iterative process that modifies the vector β to a vector with a minimal mean squared error. A wrong starting vector `beta0` can greatly influence the quality of the resulting fitted model. A good choice of `beta0` leads to a quicker and more reliable model, whereas a poor starting value can lead to a longer computation or an inadequate model.

An example will be given for the first kg/h fit. This is a relatively easy fit, because it is dependent on only one engine parameter, namely the fresh air mass flow into the engine, $\dot{m}_{fresh,x}$. The fitting starts with loading the required datasets into MATLAB. In this case the only engine parameter that is used is $\dot{m}_{fresh,x}$. Besides that, the known NO_x data points are also required. These are loaded into a `NaN` (Not-a-Number) vector with the same size as the $\dot{m}_{fresh,x}$ dataset. The `NaN`'s are required, because the regression model does not work for empty spots in a vector.

The next step is to load the vectors into a table or matrix: table x contains the fresh air mass flow and table y only contains the NO_x data points and `NaN`'s. Of course, table x can be expanded with other engine parameters. After that the model function can be described, and the starting values for `beta0` can be estimated:

```
modelfun = @(b,x) b(1)*x(:,1).^b(2);
beta0 = [3 1];
```

In this example `x(:,1)` is $\dot{m}_{fresh,x}$ and `b(1)` and `b(2)` are the coefficients to be estimated. A first estimation is made in the second line, where the following estimates are made: `b(1)=3` and `b(2)=1`. Then certain

options can be used to adapt the model. The following lines make sure the change in the sum of squares due to error (SSE) is smaller than `1e-10` and after that `fitnlm` runs the model with the selected options:

```
opts = statset('Display','iter','TolFun',1e-10);
mdl = fitnlm(x,y,modelfun,beta0,'Options',opts);
```

Figure 4.8 shows the result of running the model. The result shows the iterations that have been made to get to the final solution. For this example five iterations have been made until the SSE was smaller than `1e-10`. After that the equation of the nonlinear regression model is shown followed by the estimated coefficients `b(1)` and `b(2)`. The results are completed with some statistics that evaluate the goodness of the fit. The following section will elaborate a bit further on these statistics.

```
                                  Norm of         Norm of
   Iteration             SSE      Gradient          Step
  ------------------------------------------------------------
           0         401.168
           1         44.1933         736.72       0.601228
           2         17.6319         39.9525       0.108084
           3         17.6062       0.0100471      0.00615438
           4         17.6062     1.33152e-05      7.85875e-05
           5         17.6062     2.42622e-07      5.92223e-06
Iterations terminated: relative change in SSE less than OPTIONS.TolFun

mdl =


Nonlinear regression model:
    y ~ b1*x1^b2

Estimated Coefficients:
          Estimate      SE       tStat      pValue
          ________    _______    ______    _________

    b1     2.402      0.70099    3.4266     0.041641
    b2    1.3327       0.1498    8.8967    0.0029948


Number of observations: 5, Error degrees of freedom: 3
Root Mean Squared Error: 2.42
R-Squared: 0.977,  Adjusted R-Squared 0.969
F-statistic vs. zero model: 272, p-value = 0.000406
```

Figure 4.8: Results of the MATLAB `fitnlm` model for $\dot{m}_{fresh,x}$

4.4.2. Evaluation of the fits

The previous section already elaborated on the used regression model in MATLAB and showed an example of the results. All the results will be evaluated on the same basis, namely by using the sum of squares due to error (SSE) the Root Mean Squared Error (RMSE), the R-square and adjusted R-square. The definitions of those goodness-of-fit statistics can be seen in the equations below:

$$SSE = \sum_{i=1}^{n} w_i (y_i - \hat{y}_i)^2 \tag{4.4}$$

$$RMSE = s = \sqrt{MSE} \tag{4.5}$$

where MSE is the mean square error or the residual mean square.

$$MSE = \frac{SSE}{v} \tag{4.6}$$

$$R-square = \frac{SSR}{SST} = 1 - \frac{SSE}{SST} \tag{4.7}$$

$$adjusted\ R-square = 1 - \frac{SSE(n-1)}{SST(v)} \tag{4.8}$$

More information on these statistics can be found in appendix B. Now that it is clear how the goodness of the fits can be calculated it is time to fit the NO_x data from the EIAPP report.

4.4.3. Fitting of the kg/h emissions

This section will elaborate on the fits that are based on the NO_x emission data in kg/h. It will give an insight in the approach that was used to make the fits. It is important that the systematic approach that is used, can be used for al the kg/h fits. It starts with selecting a basis for the fit that matches the units of the actual emissions. Besides that, the base parameter must follow the same trend as the emissions, or that it could fit the data when scaled up or down. The following section will elaborate on the fits using certain specific engine parameters and combinations of those parameters. In this case, the parameters are $\dot{m}_{fresh,x}$, T_{max}, T_3 and λ.

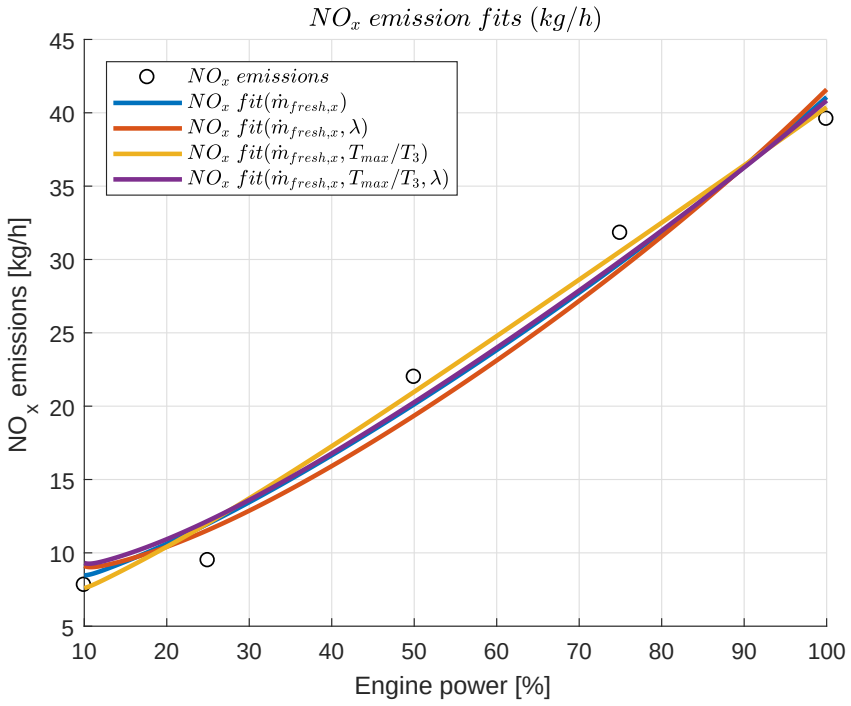

Figure 4.9: NO_x emissions fits (kg/h)

This means that different fits will be made with different combinations of those parameters. The first fit will form the basis for the following fits and is mainly dependent on $\dot{m}_{fresh,x}$. This engine parameter was chosen over the fuel mass flow into the engine, because the amount of NO_x formed directly from the fuel is negligible compared to the thermal NO_x formation. This has already been thoroughly discussed in chapter 2. The second fit will also incorporate the air excess ratio. The third will contain the temperature ratio and the last fit will be a combination of $\dot{m}_{fresh,x}$, T_{max}, T_3 and λ. Figure 4.9 shows the result of the four different fits and table 4.5 shows the goodness of fit statistics for all the fits. The different fits will all be individually discussed below.

NO_x fits using $\dot{m}_{fresh}$

Because the NO_x emissions are wanted in kg/h, a logical way to start the fits is by using an engine parameter that also uses these units. The two most important mass flows into the engine are the fuel mass flow and the total fresh air flow into the engine. The previous section and chapter 2 already explained that the fuel NO_x formation is negligible and thus the total flow of fresh air into the engine will be used. The total mass flow means that the non-combusted air in the recirculated exhaust gas is also taken into account. This is done by defining $\dot{m}_{fresh}$ a little bit different than earlier in this thesis, so for the fits $\dot{m}_{fresh,x}$ will be used. The difference between $\dot{m}_{fresh}$ and $\dot{m}_{fresh,x}$ is discussed more thoroughly in chapter 6.

The fit is optimized by multiplying $\dot{m}_{fresh,x}$ with a scalar. Because only adding a scalar was not sufficient for a good fit. A power factor was also added to $\dot{m}_{fresh,x}$. Because the trend of the graph is known, it is known how changing the power factor will influence the trend of the line. A more thorough explanation of the fitting process is given in section 4.4.1. The equation for the final optimized fit can be seen below:

$$kg/h\ NO_x\ fit(\dot{m}_{fresh}) = 2.2 \cdot \dot{m}_{fresh}^{1.32} \tag{4.9}$$

NO_x fits using $\dot{m}_{fresh}$ & λ

The basis for the kg/h fits is already described above. Another influence factor or engine parameter will now be added to the fit to see how this influences it. The first factor to be added is the air excess ratio λ. This is an important engine parameter because it describes the amount of excess air during combustion. A higher concentration of air and thus oxygen will make the formation of NO_x faster and easier. One must keep in mind that the air mass fraction will decrease for increasing EGR, and thus the choice is made to multiply $\dot{m}_{fresh}$ with the air excess ratio. This should ensure a decrease in NO_x emissions when the EGR ratio is increased. The final equation for the NO_x emissions using $\dot{m}_{fresh}$ and λ can be seen below:

$$kg/h\ NO_x\ fit(\dot{m}_{fresh}, \lambda) = 0.74 \cdot \dot{m}_{fresh}^{1.52} \cdot \lambda^{0.63} \tag{4.10}$$

NO_x fit using $\dot{m}_{fresh}$ & T_{max}/T_3

Another factor that is of big influence on the formation of NO_x is the combustion temperature. Especially the highest average value of this combustion temperature. EGR should ensure a decrease in temperature due to an increase in heat capacity. Just as with the air excess ratio, the equation should then be multiplied by the temperature. In this case a temperature ratio will be used instead of the maximum temperature itself. This is because the units need to be in kg/h and not kgK/h. The result of implementing the temperature ratio T_4/T_3 can be seen in the following equation:

$$kg/h\ NO_x\ fit(\dot{m}_{fresh}, T_{max}/T_3) = \dot{m}_{fresh}^{1.4} \cdot \left(\frac{T_{max}}{T_3}\right)^{1.32} \tag{4.11}$$

NO_x fit using $\dot{m}_{fresh}$, T_{max}/T_3 & λ

The final fit that will be made is with the air excess ratio λ as well as the temperature ratio T_4/T_3. Because the function gets more and more unknown parameters, more iterations are required before the best fit is found. Also, because the fitting process stops after 200 iterations, it was necessary to already assign values to some of the variables. This was also needed to avoid that some variables got a value of zero and would be of no influence on the fits.

$$kg/h\ NO_x\ fit(\dot{m}_{fresh}, T_{max}/T_3, \lambda) = 0.5 \cdot \dot{m}_{fresh}^{1.59} \cdot \left(\frac{T_{max}}{T_3}\right)^{0.73} \cdot \lambda^{0.7} \tag{4.12}$$

Goodness of statistics for the kg/h fits

Of course, the fits all need to be evaluated on how well they match the NO_x data found in the EIAPP report. What always is the first check with making fits is having a first glance at the fits. What figure 4.9 shows is that all four fits seem to represent the NO_x emission data quite well. But, of course, this also needs to be quantitatively substantiated. Table 4.5 shows the goodness of fit statistics for the kg/h fits:

NO_x **fit** (kg/h)	$\dot{m}_{fresh,x}$	$\dot{m}_{fresh,x},\lambda$	$\dot{m}_{fresh,x},T_{max}/T_3$	$\dot{m}_{fresh,x},T_{max}/T_3,\lambda$
SSE	16.47	23.07	9.68	18.71
RMSE	2.34	2.77	1.8	2.16
R-square	0.978	0.97	0.987	0.975
adjusted R-square	0.971	0.955	0.983	0.973

Table 4.5: Goodness of fit statistics for the kg/h NO_x emission fits

What can immediately be seen from the table is that statistics are quite good. This makes sense, because the fits have to follow a pretty straightforward line, and the basis of the fits, $\dot{m}_{fresh,x}$, also follows the same trend as the NO_x emissions. Starting with the sum of squares due to error, or SSE, it can be seen that the values are in range between 9 and 26. This is the sum of the total deviation of the response values from the fit to the actual response values. The value can range from 0 to infinity, where a value closer to 0 indicates a smaller random error component. Because the SSE can take a value up to infinity, it is difficult to say when a value indicates a good fit. But the SSE is shown because this statistic will be used to determine other goodness of fit statistics.

Following the SSE, is the RMSE, which is the Root Mean Squared Error. The RMSE is derived from the SSE and a value closer to 0 also indicates a better fit that is more useful for prediction. The values for the RMSE of the kg/h fits range from 1.7 to almost 3 and are quite close to 0, but just as with the SSE, it is difficult to say how well this is for the overall statistics.

The R-square and adjusted R-square are better statistics to evaluate the fits. R-square can take a value between 0 and 1 and the adjusted R-square can take a value less or equal to 1. The adjusted R-square also takes the number of independent pieces of information involving the number of data points into account. The table shows that the values for R-square and the adjusted R-square are all higher than 0.95, meaning that at least 95% of the total variation in the data is accounted for. A more elaborate description of the goodness of fit statistics can be found in appendix B.

Because the trend of the kg/h emission data is pretty straightforward and the fresh air mass flow follows the same trend, it can be said that the made fits are a good representation of the actual NO_x emission data. This is also confirmed by the goodness of fit statistics in table 4.5.

4.4.4. Fitting of the g/kWh emissions

Now that the all the kg/h NO_x fits have been made, it is time to start with the g/kWh fits. The kg/h fits can quite easily be converted to the g/kWh units. The only differences between the two different units are the extra factor that includes the engine power and the conversion from kg to g. However, the question remains whether or not the fits themselves will be affected by this relatively simple conversion.

The added engine parameter is the power of the engine. The power of the engine increases linearly with engine load, meaning that for 10% load the power is 450 kW and for 100%, which is the nominal engine power, the power output is 4500 kW. The conversion from kg to g is of course a multiplication with a factor 1000. The results of the conversion can be seen in the figure 4.10.

At first sight, the converted plots look quite good, but when one takes a closer look it can be seen that there is a lot of deviation around the 10% load point and the 25% load point is almost completely ignored. Both scenarios can be explained. The deviation at the 10% load point is due to the fact that the NO_x emission is 8 kg/h at 10% load and keeps increasing for increasing engine load. This is different for the g/kWh emissions which start at 18.5 for 10% engine load and immediately flattens out to a value of around 10 g/kWh. The small deviations of the kg/h fits at 10% load are increased due to the value of the first g/kWh load point at 10%. And because this value is quite high in comparison with the rest, this will result in an increase in the SSE.

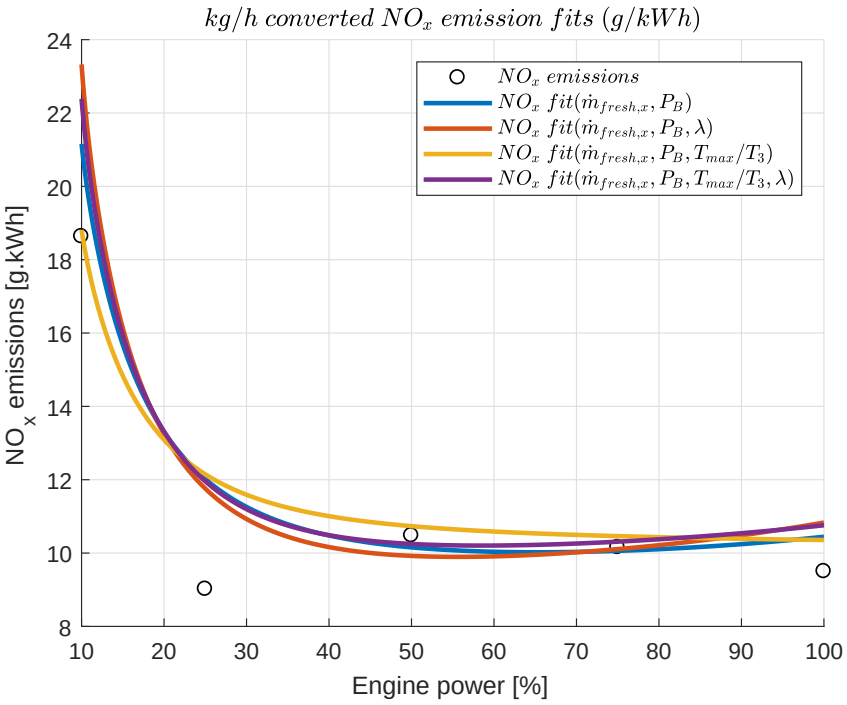

Figure 4.10: kg/h converted NO_x emissions fits (g/kWh)

What has already been showed in the kg/h fits is that the 25% load point is an odd data point and all the other data points are almost in a straight line. This results in the fact that all the kg/h fits are well above the 25% load point. This is then passed on to the g/kWh fits, which are also all above the observed data point.

NO_x **fit** (g/kWh)	$\dot{m}_{fresh,x}, P_B$	$\dot{m}_{fresh,x}, P_B, \lambda$	$\dot{m}_{fresh,x}, P_B, T/T_3$	$\dot{m}_{fresh,x}, P_B, T/T_3, \lambda$
SSE	7.43	12.29	8.51	8.34
RMSE	1.57	2.02	1.68	1.44
R-square	0.88	0.81	0.87	0.85

Table 4.6: Goodness of fit statistics for the g/kWh NO_x emission fits (converted from the kg/h fits)

Because the goodness of fit statistics for the converted kg/h fits (table 4.6) are not really good in comparison with the statistics found for the kg/h fits, it has been decided that the g/kWh fits will also be fitted with their own regression models. The data acquired from the converted kg/h fits can of course be used to make a first estimate for `beta0`, the starting value of the regression model.

Because the data is not as straightforward as the kg/h data fitting the data points will be more difficult and the goodness of fit statistics will probably not be as good as was the case for the kg/h statistics. Just as with the kg/h fits, a basis for the fits has to be provided first. This basis needs to meet the units in which the NO_x data is given, in this case in g/kWh. Just as with the kg/h fits, $\dot{m}_{fresh,x}$ is used again to meet the g/h term in g/kWh. The only way to meet the kW term is to use the brake power of the engine. Again, the fuel mass flow will not be used for the fits.

Figure 4.11 shows all the g/kWh fits. Just as with the kg/h fits, the used engine parameters are the same: $\dot{m}_{fresh,x}$, λ, T_{max} and T_3. What can immediately be seen in the figure is that the 25% load points causes a bit of doubt in the fitting of the data. Two of the four fits are closer two the second load point. A consequence of those two fits is that the value of the fits increases from around 50% engine load, where the other two fits seem to stabilize around a value of 9.5. The following paragraphs evaluate the fits a bit further.

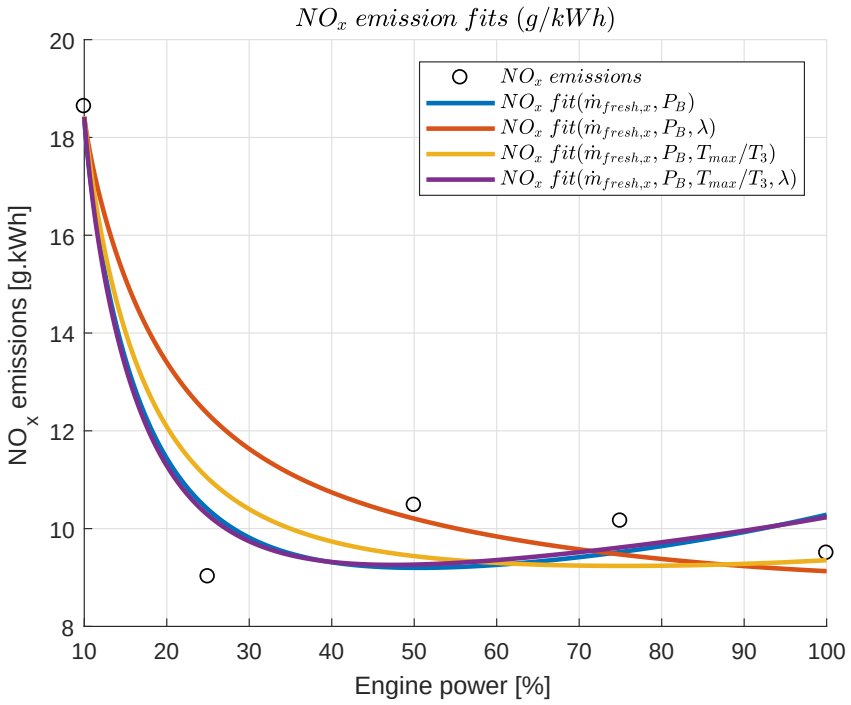

Figure 4.11: NO_x emissions fits (g/kWh)

NO_x fits using $\dot{m}_{fresh,x}$ & P_B

The first fit is the base fit and is dependent on $\dot{m}_{fresh,x}$ and P_B in order to meet the unit requirements. It is already known that P_B increases linearly with the engine load. If $\dot{m}_{fresh,x}$ is divided by P_B the fit already seemed to follow the trend of the emission data quite well. Again a scalar and a power term optimize the fit. The equation of the resulting fit is showed below:

$$g/kWh\ NO_x\ fit(\dot{m}_{fresh,x}, P_B) = 4.34 \cdot 10^6 \frac{m_{fresh}^{1.58}}{P_B^{1.08}} \tag{4.13}$$

NO_x fit using $\dot{m}_{fresh,x}$, P_B & λ

This fit caused a bit of a problem and that can be seen in the goodness of fit statistics. Because both the $\dot{m}_{fresh,x}/P_B$ and the air excess ratio term already follow the same reciprocal curve as the overall g/kWh curve, it is difficult to combine both engine parameters to a good fit.

$$g/kWh\ NO_x\ fit(\dot{m}_{fresh,x}, P_B, \lambda) = 609.7 \left(\frac{m_{fresh}}{P_B}\right)^{0.37} \cdot \lambda^{0.62} \tag{4.14}$$

NO_x fit using $\dot{m}_{fresh,x}$, P_B & T_{max}/T_3

The temperature ratio between T_{max} and T_3 will be used again to introduce a temperature term in the fitting equation. Because of the trend of the temperature ratio (seen in figure 4.7) the fit seems to deviate a bit further from the 25% load point and it ensures that the fit does not increase after around 50% load. The full equation for the T_{max}/T_3 fit is shown below:

$$g/kWh\ NO_x\ fit(\dot{m}_{fresh,x}, P_B, T_{max}/T_3) = 1.53 \cdot 10^6 \frac{m_{fresh}^{1.36}}{P_B} \cdot \left(\frac{T_{max}}{T_3}\right)^{0.65} \tag{4.15}$$

NO_x fit using $\dot{m}_{fresh,x}$, P_B, T_{max}/T_3 & λ

Again, the last fit incorporates all the above mentioned engine parameters. Some estimates were already made in order to limit the number of coefficients to be estimated and to let the model conclude its iterations. This was also needed to prevent some coefficients from getting a value that was to high or low, meaning that

they did not influence the overall equation any more. The final result of the fitting equation can be seen below:

$$g/kWh\ NO_x\ fit(\dot{m}_{fresh,x}, P_B, T_{max}/T_3, \lambda) = 2.9 \cdot 10^5 \frac{m_{fresh}^{1.73}}{P_B} \cdot \frac{T_{max}}{T_3} \cdot \lambda^{0.75} \tag{4.16}$$

Goodness of statistics for the g/kWh fits

Now that all the fits have been completed, it is time to evaluate their goodness again. It was already known that it would be more difficult to get some good fits out of the available data, because the g/kWh emission data trend was not as straightforward as the kg/h emission data. On first sight the fits look quite good, but what can be seen is that the data deviates further from the available NO_x emission points than was the case for the kg/h fits. Also, a distinction can be made between two trends in the fits. The base fit(purple) and the fit using $\dot{m}_{fresh,x}$, P_B, T_{max}/T_3 and λ(blue) show the same trend. In this trend the fits are closer to the 25% load point and increase from around the 50% load point. The two other fits deviate a bit further from the 25% load point, but seem to go to a constant value of around 9.5. What effect this has on the goodness of fit statistics can be seen in table 4.7.

NO_x **fit** (g/kWh)	$\dot{m}_{fresh,x}, P_B$	$\dot{m}_{fresh,x}, P_B, \lambda$	$\dot{m}_{fresh,x}, P_B, T/T_3$	$\dot{m}_{fresh,x}, P_B, T/T_3, \lambda$
SSE	4.63	11.05	6.04	3.94
RMSE	1.24	1.92	1.23	1.15
R-square	0.93	0.83	0.91	0.94
adjusted R-square	0.82	0.77	0.91	0.92

Table 4.7: Goodness of fit statistics for the g/kWh NO_x emission fits

In contrast with the kg/h fits the SSE values are much closer to 0. As already mentioned above, the value of the SSE is dependent on the y-values of fits. The values of the g/kWh fits all lie between 9 and 19, where the values of the kg/h fits can take a value up to 40. This explains the difference in those values. Of course, as was already mentioned with the kg/h fits, the SSE does not say a lot about the goodness of the fits, but is important for other goodness of fit statistics. The lower SSE also results in lower values of the RMSE.

The more important statistics are the R-square and adjusted R-square. What can immediately be seen is that these values are somewhat lower than the R-square values for the kg/h fits. All R-square values are in range of 0.9. Most adjusted R-square values are also in that range, with the exception of an outlier of 0.81 for the base fit. This is due to the difference in trend and of course the used engine parameters. When the engine parameters do not match the trend of the fit to well, it is difficult to achieve a good result.

Despite the difficulties with the fitting, it can be said that the fits are quite good. The R-square and adjusted R-square are al in the range of about 0.90, which suggests that a great proportion of the variances is accounted for. Besides that, the SSE and RMSE values are quite close to 0, meaning that the fits are useful for the prediction of data.

4.5. Conclusion

This chapter started with a thorough evaluation of the available NO_x emission data. The available NO_x data is the result of certain test cycles. These test cycles differ for each ship type and are dependent on how the engine of a ship is used. Because Jumbo's vessels are all equipped with controllable pitch propellers, the test cycles that have been carried out were for constant-speed main propulsion. The available NO_x emission data is quite limited, due to the fact that the engine is only tested at one engine speed and five load points, namely 10%, 25%, 50 %, 75% and 100%.

Unfortunately this means that the EIAPP report only supplied the NO_x emission data for those five load points. The data that was available was given in ppm, kg/h and g/kWh. It was decided that the ppm data was not sufficient for the wanted fits, leaving the kg/h and g/kWh emission data. The kg/h data was only available for the parent engine, which is a 6-cylinder engine. This data was converted to match the 9-cylinder engine used aboard Jumbo's ships. After that some inaccuracies in the data were discussed and it

was decided how these inaccuracies were to be interpreted.

The next step in this research was to determine which engine parameters would be used for the emissions fits. As already discussed in chapter 2 the most important factors are the combustion temperature and oxygen availability. That is why the following parameters were chosen for the fits: $\dot{m}_{fresh,x}$, P_B, T_{max}/T_3 and λ. In order to keep the units of the fits right a temperature ratio (T_{max}/T_3) instead of just a temperature was used.

After determining all the important influence factors, it was time to start the actual fitting. For this research a nonlinear regression model was used to make the fits. With a nonlinear regression model observational data can be modelled by a function which is a nonlinear combination of certain parameters and in depends on one or more independent variables. The model uses iteration to make the sum of squares due to error smaller than $1e-10$, and shows the estimated coefficient for the above mentioned engine parameters.

The results of the kg/h fits can be seen in figure 4.9 and the results for the g/kWh fits are shown in figure 4.11. The equations for all the fits are shortly discussed and than, the goodness of fit statistics are evaluated for both the kg/h and g/kWh fits. At first sight all the fits seem to match the available NO_x emission data quite will and this is also confirmed by the goodness of fit statistics shown in tables 4.5 and 4.7.

The next step in this research is to implement the two different EGR configurations into the existing diesel engine model and use the results from those models to predict the NO_x emissions for different EGR rates.

5

Exhaust Gas Recirculation

5.1. Introduction

The previous chapter explained the Diesel A-M model and how it was calibrated with the available emission data. Besides that it described how the NO_x fits were made. The next step is to implement exhaust gas recirculation into the Diesel A-M model. This chapter will first elaborate a bit more on the working principles of exhaust gas recirculation. After that, different EGR configurations will be discussed. It will then be explained how these configurations will be implemented in the model and what changes to the original model have to be made to let it function correctly.

5.2. EGR Working Principle

In order to comply with the emission legislation, a number of after treatment systems are available. But it is also possible to avoid the formation of emissions already during the combustion. The raw emissions can already be reduced in the combustion chamber and then no after treatment is necessary. Exhaust gas recirculation can reduce the formation of NO_x emissions during combustion. A portion of the exhaust gases is recirculated into the combustion chamber to replace the fresh intake air.

Because the exhaust gas consists mainly inert gases like nitrogen (N_2), carbon dioxide (CO_2) and water vapour (H_2O) and only a low percentage of oxygen(O_2), the recirculation of this exhaust gas lowers the concentration of oxygen in the combustion chamber and the heat capacity of the combustion mixture increases. As already explained in chapter 2, NO_x is formed under high temperature in an oxygen-rich environment. So lowering the oxygen content of the air-fuel mixture and increasing the heat capacity reduces the combustion temperatures and with that the formation of NO_x.

5.3. Disadvantages and difficulties of EGR

The working principle of exhaust gas recirculation is based on the reduction of the available oxygen in the cylinder. A smaller amount of oxygen in the combustion chambers leads to a bigger production of particulates. These particulates consist of fuel which has only been partially combusted. The trade-off between the emissions of NO_x on one hand and particulates on the other is often referred to as the "diesel dilemma". A schematic representation of this dilemma can be seen in figure 5.1. This trade-off has to be taken into account when EGR is implemented in an engine and measures have to be taken to control the emissions of the particulate matter. For example, this can be done by adding a particle filter to the EGR route.

Exhaust gas recirculation is operated by means of an EGR valve. This valve can not respond directly to changes and thus it will take time for the exhaust gases to flow around the EGR circuit. This will make the operation of the valve very complex during transient EGR behaviour. For this reason, the EGR valve is normally closed during transients and re-opened when a steady state is achieved again.

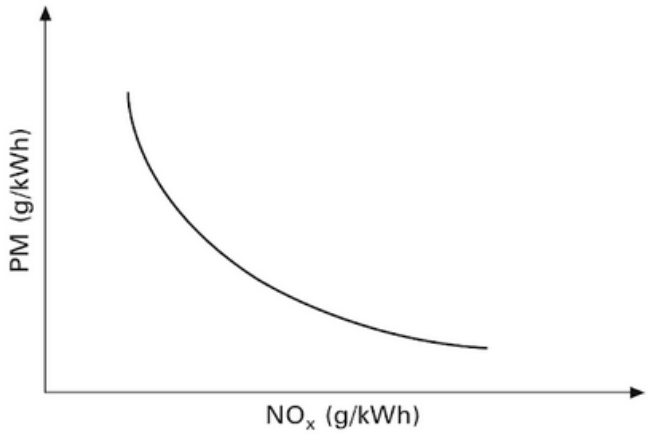

Figure 5.1: Schematic diagram of the 'Diesel dilemma' or PM (soot)-NO_x trade-off[68]

The gas that is recirculated will be introduced into the intake system of the engine and not directly into the cylinders. Despite the early mixing point, perfect mixing of the gas is not possible at all engine speeds and loads. Especially during transient operations the mixing is difficult. If common rail injection is used, the mixing process can continue there, but otherwise the cylinder-to-cylinder distribution of the EGR gas might not be equal. This can result in one cylinder receiving to much EGR gas, which will result in higher particulate emissions, while another cylinder receives not enough, what on its turn will result in higher NO_x emissions.

The biggest disadvantage of the implementation of EGR, as described by Wik and Niemi[62], is that it can only be used if the engine runs on fuel with a low-sulphur content. If residual products, like HFO, are used, this can lead to the formation of solid deposits, lubricating oil contamination and valve and cooler fouling. HFO can be used, but it requires the installation of effective cleaning equipment, which on its turn results in an increase in fuel consumption as high as 8%.

5.4. EGR configurations

This section will elaborate on the the different EGR configurations that are possible. The first distinction to be made is whether the used EGR strategy is internal or external. Codan et al.[14, 15] explains the difference: internal EGR is achieved adjusting the valve timing in such a way that a part of the exhaust gases remains in the cylinder. It can be achieved relatively easily, because no other components are needed. It is however difficult to cool the gas that remains in the cylinder and therefore more EGR is required for the same NO_x reduction level. It can potentially reduce NO_x emissions up to 20%.

External EGR recirculates the exhaust gases outside of the cylinder. A NO_x reduction potential is higher, because the possibility exist to cool the exhaust gases. Additional components are necessary to recirculate the exhaust gases. The second distinction is the difference between hot and cooled EGR. Hot EGR means that the exhaust gas is recycled to the intake directly, without being cooled. If the exhaust gas is cooled through an EGR cooler to condition the recirculated exhaust gas, it is called cooled EGR. Cooled EGR can be subdivided into Low-pressure Exhaust Gas Recirculation(LP-EGR) and High-pressure Exhaust Gas Recirculation(HP-EGR).

5.4.1. Low-pressure EGR

Because modern diesel engines are commonly turbocharged, the implementation of EGR is a bit more difficult than naturally aspirated engines. In order for EGR to work on a turbocharged engine, a positive differential pressure between the turbine outlet and compressor inlet is needed, this means $p_e - p_0 > 0$. If needed, the exhaust pressure p_e can be increased by partial throttling to ensure sufficient pressure for the EGR flow. The starting point of this configuration is after the turbine and the point where the exhaust gas flow re-enters the regular diesel engine cycle is before the compressor. This process, the so-called low-pressure EGR loop can be seen in figure 5.2.

Ueda[59] and Zheng et al.[69] have already described the most important downsides of the recirculation of exhaust gases for certain engine components. A downside is that conventional compressors and inter-coolers are not designed to withstand the temperature and the fouling of diesel exhaust gases. Therefore efforts have been made to reroute the EGR flow from the turbine exit directly to the inlet receiver, and thus bypassing the compressor. This solves the compressor fouling problem, but an independent EGR pump or blower is required to counteract the boost pressure. According to Reifarth[48] this special EGR pump needs to withstand the exhaust heat and fouling and of course needs substantial pumping power. The pumping power can either be provided mechanically from the crankshaft or electrically from an generator. Another option is to reroute the EGR flow upstream from the turbine to downstream of the compressor, this is high-pressure exhaust gas recirculation and will be discussed in section 5.4.2.[59, 69]

5.4.2. High-pressure EGR

The high-pressure EGR loop can be seen in figure 5.3 and lets the EGR flow start from upstream of the turbine to downstream of the compressor(or downstream of the inter-cooler). When this loop is used, the compressor and inter-cooler are not exposed to the hot and fouled exhaust gases. A downside of the high-pressure loop is that it can only be applied if the pressure upstream from the turbine is sufficiently higher than the boost pressure, $p_d - p_b > 0$. If the pressure difference cannot be overcome with the original turbocharger and the engine, which is the case most of the time, alterations have to made in order to overcome the pressure difference between the outlet receiver and inlet receiver.

An electrically driven blower can be used to pump the EGR flow to the inlet receiver to overcome the pressure gradient. The principle is the same as with a turbocharger, except instead of using a turbine to drive the compressor an electrical drive can be used. The electrical drive configuration will of course increase the weight complexity, space requirements the EGR implementation. Besides that, the EGR blower needs very high speeds and such machines are very expensive. According to Cavadini[11] the advantage of the configuration is that the flexibility of the system increases, since the EGR blower can be controlled independently of the engine speed and from the turbine.

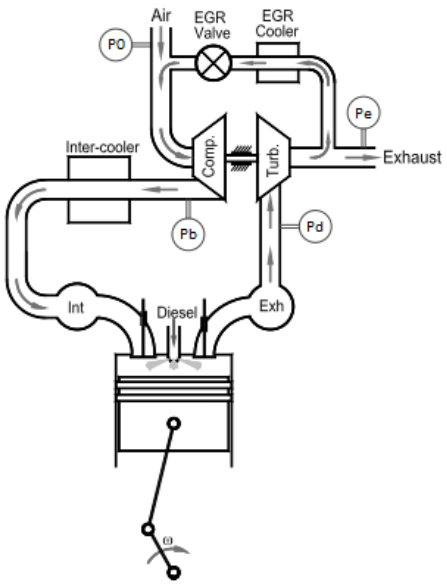

Figure 5.2: Low pressure loop EGR[69]

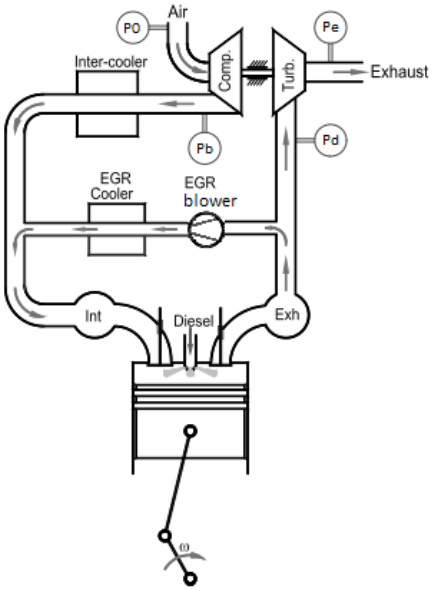

Figure 5.3: High pressure loop EGR[69]

An EGR valve is in between the blower and the mixing point. Andersson and Hedvall[2] give a short description on the behaviour of the EGR valve. The valve controls the amount of exhaust gases that are recirculated. The valve has a nonlinear behaviour due to the construction of the valve. A very small valve opening means that the recirculated gases can only flow through a small area of the pipe. But by opening the valve slightly further, the flow area increases considerably. For this research, the behaviour of the valve will

not be taken into account, because the behaviour of the total EGR system is more important. The valve is not shown in figure 5.3, but is placed before the EGR blower.

Both EGR configurations will be implemented into the Diesel A-M model, so that they can be compared. They will both have a positive influence on the reduction of NO_x emissions, but the question remains how big this reduction will be.

5.5. Implementation of the low-pressure EGR configuration

Now that both EGR configurations have been shortly discussed, it is time to implement them in the existing Diesel A-M model. The diesel model has already been calibrated with the available engine data and it agrees with the real engine quite well. The main problem with the implementation of EGR is that there is no emission or engine data for this engine with EGR implemented. This means that the results of the simulations with EGR equipped can not be compared to real data.

The Simulink environment in MATLAB is great for investigating large dynamic systems and all the physical diesel engine components can be modelled as separate blocks. This will make the implementation of the two exhaust gas recirculation configurations into the existing model a bit easier. The following section describes the implementation of the low-pressure EGR configuration into the diesel A-M model. It will start with a schematic representation of the implemented low-pressure configuration and after that, the changes in the diesel A-M model will be described. Section 5.6 will do the same for the implementation of the high-pressure EGR configuration.

5.5.1. A schematic representation of the low-pressure EGR configuration

To visualise the changes in the diesel A-M model with the implementation of the EGR configuration this section will elaborate a bit further on the schematic representation of the diesel A-M model that was already described and visualised in chapter 3 and figure 3.4. That same schematic representation will be used to describe the implementation of the low-pressure exhaust gas recirculation configuration.

The low-pressure configuration characterizes itself with the recirculation route starting downstream of the turbine and re-entering the cycle before the compressor. The route contains an EGR cooler to cool down the hot exhaust gases and an EGR valve to control the EGR rate. A schematic representation of this configuration can be seen in figure 5.4.

What can be seen in the figure is that an extra subsystem, or block, is added to the system. In this case, this is the EGR cooler. What is not shown in the figure is the EGR valve after the EGR cooler. This valve determines the EGR rate. A mass flow with a certain, temperature and air mass fraction flows from after the turbine to the EGR cooler. In the EGR cooler the temperature of the EGR flow is decreased to the desired temperature. After the EGR cooler, the cooled exhaust gases flow through the EGR valve to the inlet of the compressor, again with the desired temperature and air mass fraction. Thus it can be concluded that the most important parameters for the implementation of the low-pressure EGR configuration are the EGR mass flow $\dot{m}$, the temperature T and the air mass fraction x.

5.5.2. Changes in the diesel engine model

This subsection will describe the most important changes in the diesel A-M model needed to get the EGR working correctly. Because the low-pressure EGR route re-enters the engine before the compressor the explanation will start with the compressor block seen in figure 5.4. After that the changes in the in-cylinder process will be discussed and then the outlet receiver, turbine and eventually the EGR cooler will be discussed.

Changes in the compressor and inlet receiver

As already explained in chapter 3, the compressor(COM) and inlet receiver(IR) blocks are merged in the diesel A-M model. That is why these two blocks will be explained simultaneously.

Starting of with the most important part, namely the definition of the EGR ratio. Different definitions of the EGR rate or ratio are possible and a lot of times the CO_2 concentration or CO_2 volume fractions are used, like

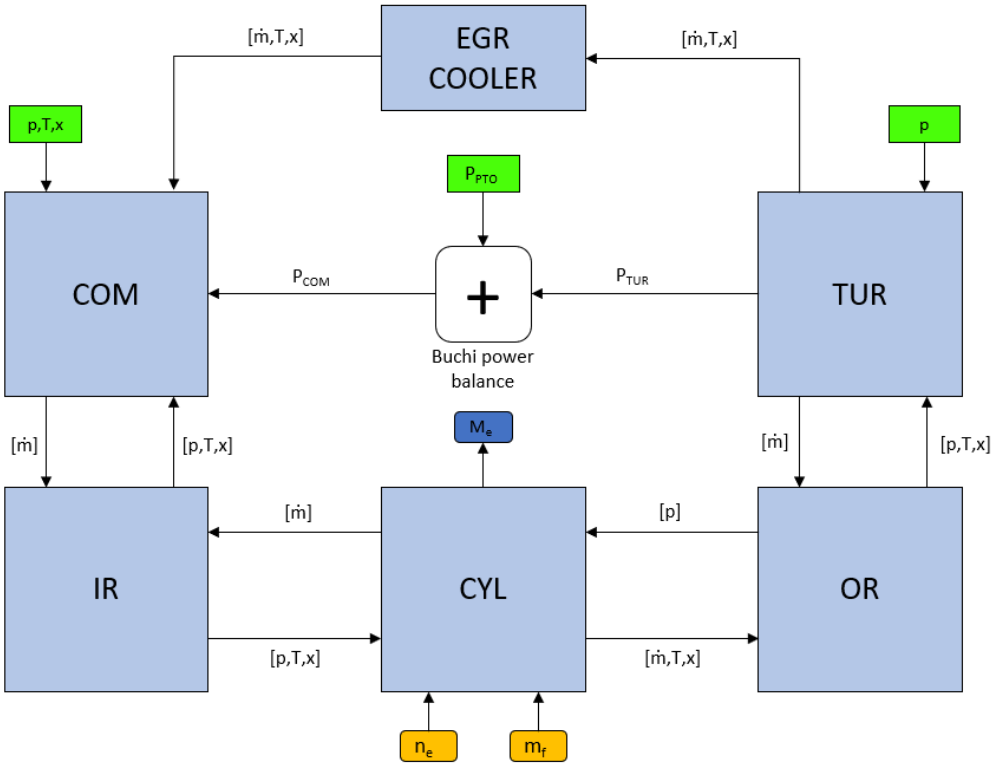

Figure 5.4: A schematic representation of Low-Pressure EGR configuration

described by for example Asano[5] and Yu[67] in equation 5.1:

$$EGR_{ratio} = \frac{CO_{2(in)} - CO_{2(amb)}}{CO_{2(exh)} - CO_{2(amb)}} \times 100(\%) \tag{5.1}$$

But in this case the data acquired from the FAT and EIAPP reports is limited and little is known about the CO_2 concentrations for the entire load case. Eventually the NO_x concentrations over the entire load case will be predicted and thus data has to be used that represents the entire load case. And thus, in this case a more general definition will be used. The EGR ratio will be defined as with the portion of exhaust gas that replaces the fresh air drawn into the cylinder. Thus the EGR ratio is the ratio of the mass flow of the recirculated exhaust gas over the total mass flow into the cylinder and can be seen in equation 5.2. The EGR ratio can be adapted in the MATLAB driver file.

$$EGR_{ratio} = \frac{\dot{m}_{EGR}}{\dot{m}_{in}} \times 100(\%) \tag{5.2}$$

As given by Abd-Alla[1]. This means that

$$\dot{m}_{EGR} = \dot{m}_{in} \cdot \frac{EGR_{ratio}}{100(\%)} \tag{5.3}$$

The next step in implementing the EGR configuration is making sure that the most important parameters for this configuration are defined correctly. As already explained in subsection 5.5.1 the important parameters for low-pressure EGR are the EGR mass flow $\dot{m}$, the temperature T and the air mass fraction x. The pressure p is of less importance, because the exhaust air can be directly channelled into the intake of the compressor and no pressure difference has to be overcome. In this model the pressure upstream of the turbine, p_e, and downstream of the compressor, p_a, are both equal to the atmospheric pressure of 100 kPa or 1 bar.

The recirculated exhaust gas mass flow $\dot{m}_{EGR}$ is mixed with the ambient intake air before the compressor, meaning that the characteristics of the mixed flow differ from the regular mass flow and the EGR mass flow. Figure 5.5 shows a schematic diagram of the mixing section where the two flows are combined.

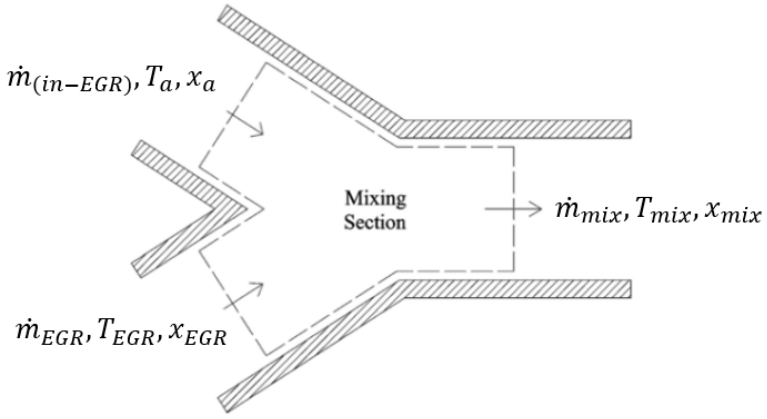

Figure 5.5: Schematic diagram of the mixing section of the exhaust gas and the intake air for LP EGR[61]

What can be seen in the figure is that there is a mass flow into the engine, $\dot{m}_{in}$, and the recirculated exhaust gas mass flow, $\dot{m}_{EGR}$. The most important parameters for this research are the temperatures and air mass fractions of these two flows. The temperature of the ambient intake air, T_a is constant at 20 °C or 293 K. The temperature of the EGR flow can be adjusted with the EGR cooler. For this research the temperature of the EGR flow is cooled to the ambient temperature, and thus equal to T_a.

The next factor is the air mass factor, x. Because the other important factors, temperature and pressure, are considered equal for the air flow and EGR flow, this factor will be of bigger influence on the operation of the EGR. The air mass fraction of the ambient intake air, x_a, equals 1, meaning that 100% of the intake air is air. The air mass fraction of the EGR flow, x_{EGR}, is dependent on the processes in the combustion chamber, which on its turn are dependent on the air mass fraction of the mixed gases. The air mass fraction of the mixed gases is defined by the following equation:

$$x_{mix} = \frac{\dot{m}_{EGR} \cdot x_{EGR} + \dot{m}_{(in-EGR)} \cdot x_a}{\dot{m}_{in}} \tag{5.4}$$

Where

$$\dot{m}_{(in-EGR)} = \dot{m}_{in} - \dot{m}_{EGR} \tag{5.5}$$

The equations above show that the air mass fraction is determined according to the ratio in mass flows. As mentioned above, the air mass fraction is changed during combustion and when recirculated is also dependent on itself. This results in an insolvable loop in the Simulink environment and thus a solution has to be invented to prevent this from happening. One way to do this in Simulink is by using a so-called memory block.

A memory block applies a one integration step delay and the output is the previous input value. The user has to define a certain initial condition which will be used for the first loop, meaning that the user needs to calculate this value or make an estimated guess. If the initial condition is selected carefully, unwanted behaviour can me minimized. But in the case of EGR implementation, the value of the memory block will change every time the EGR ratio changes. This means that both of the options are not ideal and will have an impact on the results. If the estimated initial differs too much from the real value, this can immediately be seen in the end result. The results that are partly dependent on the air mass fractions will show some deviations in the beginning of the simulation.

Figure 5.6 shows the air excess ratio as a function of the engine load. What can be seen in the figure is that the air excess ratio is displayed as it is expected, but at 10% engine load some deviations have occurred. It may not look like much, but the air excess ratio will also be used in further evaluation of the NO_x fits and therefore it has to be correct. MATLAB itself gives the tip to avoid using a memory block when

the input to the block changes during simulation, so one must look at a way to avoid using the memory block.

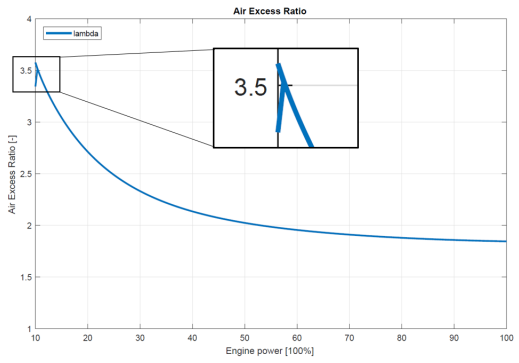

Figure 5.6: Air excess ratio versus engine load with Memory block

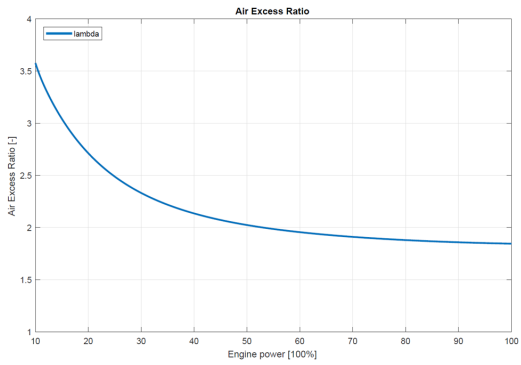

Figure 5.7: Air excess ratio versus engine load with Transfer funtion

MATLAB's Model Advisor suggests that the best way to break an algebraic loop is to use a continuous block. An example of such a block is a first order transfer function. Just like the memory block, the transfer function will introduce a new dynamic into the system. In order to not affect the dynamics of the system significantly, the trick is to make the time constant of the transfer function small enough[49]. A value of 1e-6 is suggested and is normally small enough to make sure the function does not affect the outcome to much. The result of using a transfer function instead of a memory block can be seen in figure 5.7. The air excess ratio is displayed as a smooth line without deviations and changing the EGR ratio also results in a graph without deviations.

Another factor that is influenced by the mixing of the two flows is the specific heat of the mixture. The specific heat of the mixture is needed to determine the temperature of the mixture after the compressor. The specific heat of the mixture is computed as defined in the same way as in chapter 3 in equation 3.28, where $c_{p,a}$ is the specific heat of air at constant pressure in J/kgK and $c_{p,g}$ is the specific heat of the stoichiometric combustion gas at constant pressure. More details of the computation of the specific heat and the specific heats during the combustion has already been given in chapter 3.

Changes in the in-cylinder process

Now that all the inlet receiver conditions of the engine are known, it is time to move on to the next part of the diesel engine, namely the air swallow and combustion process. Starting with the mass of the trapped air in the cylinder. The trapped mass at the start of compression was already given by equation 3.22 in chapter 3 and is defined as:

$$m_1 = \frac{p_1 \cdot V_1}{R \cdot T_1} \tag{5.6}$$

The pressure p_1 and temperature T_1 follow from the inlet receiver conditions, R is a constant and V_1 follows from engine geometry. Because the scavenge efficiency of the engine is assumed to be 100%, the total trapped mass consists purely of the fresh air drawn into the combustion chamber and the EGR part. One must keep in mind that the definition of the EGR ratio was defined as the ratio of the total mass drawn into the combustion chamber over the EGR mass flow. This means that the trapped mass is not equal to the mass drawn into the engine, because slip also occurs. The mass of the EGR flow has to be corrected with the slip flow, because also a part of the EGR flow slips through the engine.

This means that the model needs to be adjusted in order to let the model give the correct prediction of the EGR mass in the combustion chamber. It is known that the total mass flow drawn into the combustion chamber is defined as the trapped mass flow plus the slip flow. Besides that, the EGR ratio was already defined as a fraction of that total mass flow, meaning that part of the slip flow also consists of EGR gas. It will be assumed that the part of the slip flow consisting of EGR gas is the same as the EGR ratio and that will give the following definition of the slip flow part that consists of EGR gas:

$$\dot{m}_{slip,EGR} = \dot{m}_{EGR} \cdot \frac{EGR_{ratio}}{100(\%)} \tag{5.7}$$

The new EGR mass flow into the engine becomes:

$$\dot{m}_{1,EGR} = \dot{m}_{EGR} - \frac{EGR_{ratio}}{100(\%)} \cdot \dot{m}_{EGR} \tag{5.8}$$

The overall result of the trapped EGR mass being a bit smaller than first expected is that the part of fresh air in the combustion chamber will be slightly bigger. This will have some influence on quantity of fresh air drawn into the engine and on its turn this will have some influence on the air excess ratio. To get the mass, instead of the mass flow, of the EGR gas in trapped condition, one must divide the trapped EGR mass flow by the firing rate or cycle frequency of the engine:

$$f = \frac{i \cdot N}{k} \tag{5.9}$$

Where f is the firing rate in Hz, N is the nominal rotational speed of the engine in rev/s an k is the number of revolutions per cycle, where $k = 2$ for 4-stroke engines. The trapped EGR mass is then given by:

$$m_{1,EGR} = \frac{\dot{m}_{1,EGR}}{f} \tag{5.10}$$

One of the most important factors for the formation of NO_x is the amount of air available for combustion. The air excess ratio, λ, is a good way to describe the amount of excess air in the combustion chamber. Having already explained the definition of the trapped mass, λ (and λ^*, because $\eta_{scav} = 1$) becomes:

$$\lambda = \lambda^* = \frac{m_1 \cdot x_1}{m_f \cdot \sigma} \tag{5.11}$$

The following change is the change in air mass fraction during combustion, but this has already been thoroughly explained in section 3.5.

Changes in the outlet receiver and turbine

Following the in-cylinder process is the outlet receiver. This is where the flow out of the cylinder and the slip flow mix again. The most important change in the outlet receiver is the difference in the air mass fraction between the flow out of the cylinder and the slip flow. For the air mass fraction of the slip flow, x_{slip} it is assumed that it equals the air mass fraction of the trapped mass, $x_1 = x_c$. The computation of the total air mass fraction in the outlet receiver, x_{OR} has already been given in section 3.5.

The turbine does not require any massive changes for the EGR to be implemented correctly. No mixing or combustion takes place, so the air mass fraction stays the same and becomes x_{EGR}. This air mass fraction is already the same as in the outlet receiver and this will be the air mass fraction that will be recirculated to downstream of the compressor. The pressure of the EGR gas is the same as upstream of the turbine, namely equal to ambient: $p_{EGR} = p_e = p_a$. The final important part is the temperature of the recirculated gas. Because the recirculation starts after the turbine, the temperature of the EGR flow equals the temperature of the flow out of the turbine, and thus $T_{EGR} = T_e$.

The EGR cooler

The EGR cooler is a new part of the diesel engine and as the name already mentions it cools the recirculated exhaust gas. For the low-pressure EGR configuration, the EGR cooler cools the flow to ambient temperature in order to match the temperature of the fresh air drawn into the engine.

5.6. Implementation of the high-pressure EGR configuration

This section will elaborate further on the correct implementation of the high-pressure EGR configuration into the existing calibrated diesel A-M model. Just as with the low-pressure configuration, the high-pressure EGR configuration will be explained by using the schematic representation of the diesel engine model from chapter 3.

5.6.1. A schematic representation of the high-pressure EGR configuration

The high-pressure configuration has, as the name already mentions, a higher pressure than the other configuration. This is because the EGR flow already starts upstream of the turbine and re-enters the cycle after the compressor. Both of these points already have a higher pressure than in the low-pressure configuration case. Normally, the outlet receiver has a lower pressure than the inlet receiver, meaning that the EGR route will flow in the wrong direction if not an additional pump or blower is used. Figure 5.8 shows how the EGR cooler and blower are implemented in the existing diesel engine model.

The high-pressure EGR route starts upstream of the turbine, at the outlet receiver. The EGR flow is than pressurized to overcome the pressure difference between the in- and outlet receiver. After the blower, the EGR flow is cooled to the desired temperature in the EGR cooler. The flow then re-enters the diesel cycle downstream of the compressor in the outlet receiver. The most important parameters for this EGR route are, just as with the low-pressure configuration, the mass flow $\dot{m}$, the temperature T, the air mass fraction x and in the case of high-pressure EGR also the pressure p.

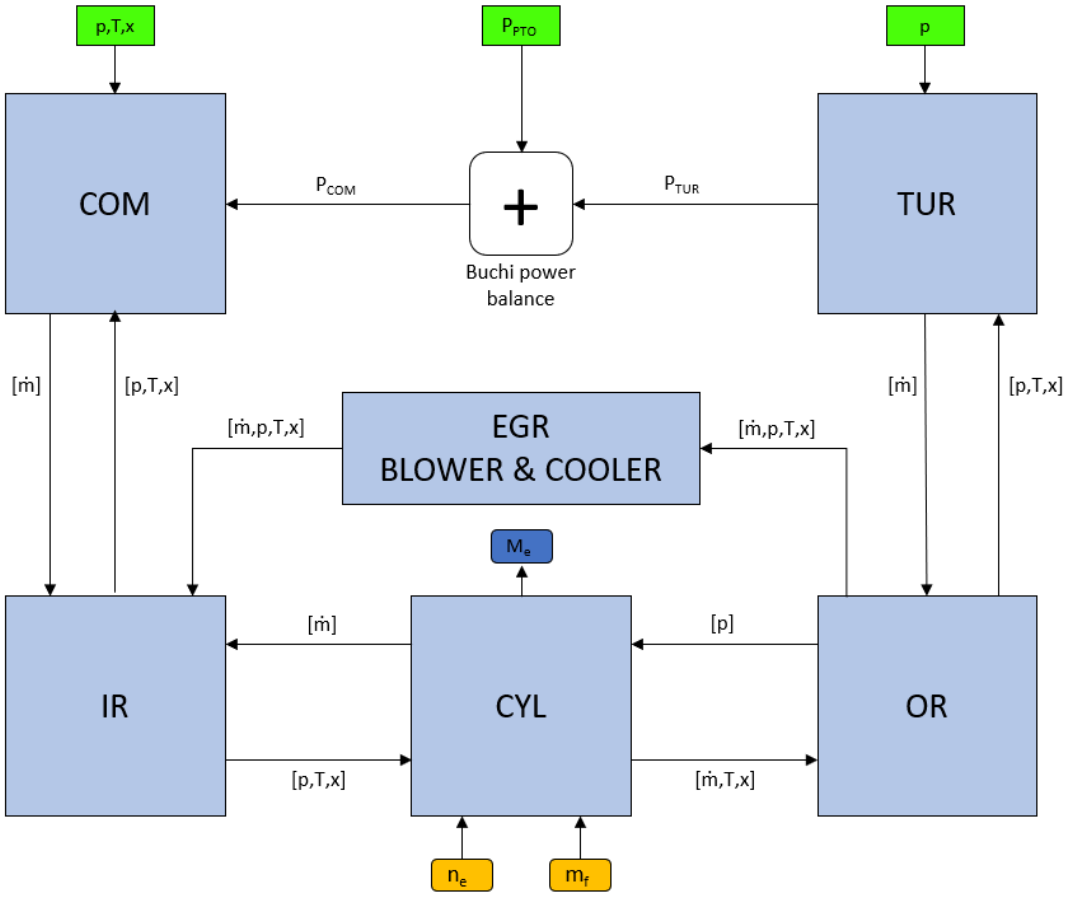

Figure 5.8: A schematic representation of High-Pressure EGR configuration

5.6.2. Changes in the diesel engine model

This subsection will describe the most important changes in the diesel A-M model needed to get the high-pressure EGR working correctly. Just as with the low-pressure configuration, the entire model and changes to it will be explained step by step, starting with the inlet receiver and compressor. After that, the cylinder process will be discussed, then the outlet receiver and the turbine and this section will be concluded with an explanation of the EGR cooler and blower.

Changes in the compressor and inlet receiver

The compressor and inlet receiver will be discussed simultaneously again, because in the MATLAB Simulink model of the engine, these two blocks are merged. The first important function to define is the EGR ratio

again. And just as with the low-pressure configuration, the EGR ratio is defined as the ratio of the ratio of the EGR mass flow over the ratio of the total mass flow into the cylinder.

But because the the high-pressure EGR configuration has another route than the low-pressure configuration, the rest of the changes to the model differ quite much. Let's start with the mixing of the exhaust gases and the ambient air again. For this configuration the recirculated exhaust gas flow $\dot{m}_{EGR}$ is mixed with the intake air after the compressor. Figure 5.9 shows a schematic diagram of the mixing section where the two flows are combined.

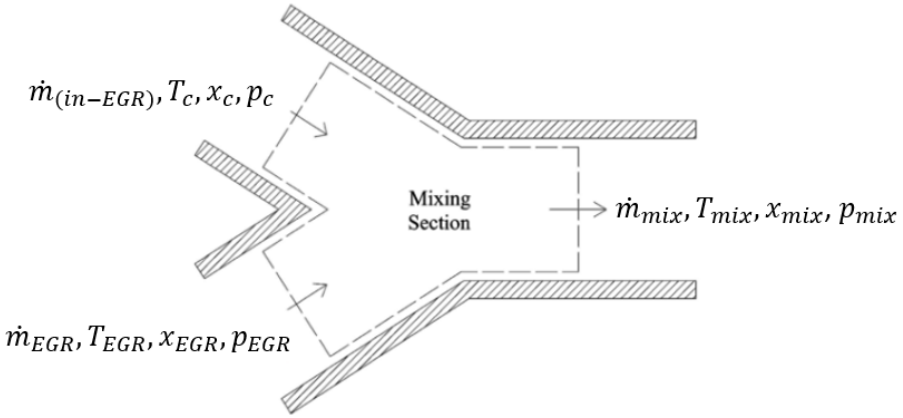

Figure 5.9: Schematic diagram of the mixing section of the exhaust gas and the intake air for HP EGR[61]

What can immediately be seen in comparison with the low-pressure variant is that pressure has much more of an influence for the high-pressure EGR configuration. The pressures for the low-pressure configuration are around ambient pressure, where the pressures for the high-pressure configuration are four to five times higher, between 4 and 5 bars. Just as with the low-pressure configuration the air mass fraction, x, is dependent on the EGR ratio. This can be seen in the following equation:

$$x_{mix} = \frac{\dot{m}_{EGR} \cdot x_{EGR} + \dot{m}_{(in-EGR)} \cdot x_a}{\dot{m}_{in}} \tag{5.12}$$

Because the regular flow into the engine and the EGR flow are mixed after the charge air cooler, the temperature after the cooler, T_c is also dependent on the EGR ratio. If the EGR cooler cools the EGR flow to another temperature than the charge air cooler temperature, the temperature in the inlet receiver becomes:

$$T_{mix} = \frac{\dot{m}_{EGR} \cdot T_{EGR} + \dot{m}_{(in-EGR)} \cdot T_c}{\dot{m}_{in}} \tag{5.13}$$

Another option for setting the temperature in the inlet receiver is to cool to EGR flow to the same temperature as the air flow into the engine. This way the temperatures are equal and T_c will be the constant inlet receiver temperature.
The low-pressure EGR also had a change in the specific heat, because the mixed flow is compressed in the compressor and the specific heat of the mixture has some influence on the functioning of the compressor. For the high-pressure EGR variant the mixed flow does not flow through the compressor and therefore there is no change in specific heat required yet. This is all done in the cylinder part of the model.

Changes in the in-cylinder process

This section will evaluate the changes in the air swallow and combustion processes. Because the mixing of the EGR flow and the regular flow into the engine already take place before the combustion chamber, the in-cylinder process has the exact same changes as the low-pressure configuration. What these changes are can be read in section 5.5.2.

Changes in the outlet receiver and turbine

In contrast with the low-pressure configuration, the outlet receiver and turbine required some big changes. For the high-pressure recirculation route, the starting point is between the outlet receiver and the turbine. The outlet receiver is the point where the flow out of the cylinder and the slip flow mix again. The definition of the air mass fraction at the starting point of the EGR route,x_{OR} has already been evaluated in section 3.5.

More important for this EGR configuration is the turbine block in the simulation model. Because the EGR starting point is before the turbine, the mass flow through the turbine changes and this has a big influence on the functioning of the turbine and with that also on the compressor. The turbine powers the compressor directly and if the mass flow through the turbine becomes lower, it will deliver less power. This means that there is also less power available for the compressor to compress the air drawn into the engine. This also influences the total mass drawn into the engine and with that the combustion. For this research it is important that the charge air pressure for every EGR ratio is the same to compare the results on the same basis. A more elaborate description of how this is done is added in appendix C.

The power delivered by the turbine is dependent on the mass flow through the turbine, $\dot{m}_{tur}$, the work of the turbine, w_{tur}, and the turbine Zinner coefficient β. Before the power of the turbine can be determined, the flow through the turbine has to be computed. $\dot{m}_{tur}$ is determined by the total constant effective turbine area based on nominal conditions, $A_{tur,eff}$, an inlet density term, the turbine mass flow function Ψ and the turbine Zinner coefficient α. Both Zinner coefficients, α and β, are equal to 1, because a constant pressure system is used. The turbine characteristic can then be defined as:

$$\dot{m}_{tur} = \alpha \cdot A_{tur,eff} \cdot \frac{p_d}{\sqrt{R_d \cdot T_d}} \cdot \Psi(\pi_{tur}) \tag{5.14}$$

Where Ψ is approximated by the following equation:

$$\Psi = \sqrt{1 - \left(\frac{1}{\pi_{tur}}\right)^f} \tag{5.15}$$

$f = 2$ is the so-called elliptic law. This approximation assumes flow similarity and a constant polytropic efficiency. This simplification has the advantage that the relation between flow and pressure can easily be inverted.

The turbine power can now be determined, but not before the actual mass flow is calculated. The actual mass flow into the turbine is given as the mass flow as determined in equation 5.14 minus the EGR flow, as can be seen in equation 5.16:

$$\dot{m}_{tur} = \dot{m}_{OR,out} - \dot{m}_{EGR} \tag{5.16}$$

The turbine power can then be defined as:

$$P_{tur} = \beta \cdot \dot{m}_{tur} \cdot w_{tur} \tag{5.17}$$

The turbine delivers its power directly to the compressor. Appendix C elaborates a bit further on the extra power that the turbine has to deliver to achieve the wanted charge air pressure.

The EGR blower and cooler

The final part of the high-pressure EGR system are the EGR blower and EGR cooler, combined in the EGR blower & cooler block in Simulink. In contrast to the low-pressure configuration, the high-pressure EGR configuration requires a blower to increase the pressure of the recirculated gas. Because the 9M 32C is a turbocharged engine, there is a pressure difference between the in- and outlet receiver. The blower is necessary to overcome this pressure difference.

The maximum pressure difference occurring between the in- and outlet receiver is $1bar$ or $100kPa$. The EGR mass flow ranges from 0 to $3.8kg/s$ for an EGR ratio of 50%. If a pressure difference of $1bar$ has to be overcome, a big compressor or blower is required. However, the pressure difference between the in- and outlet receiver decreases for increasing EGR rates, because the pressure in the outlet receiver increases. The inlet receiver pressure, or charge air pressure p_c remains constant for changing EGR ratios. The average

temperature in the outlet receiver is around 770 K or 500 °C, for which the density of the exhaust gas is around $0.7 kg/m^3$.

The different EGR mass flows and pressure difference result in different EGR blower powers to overcome the pressure difference. Despite the fact that the biggest mass flow is of course at 50% EGR, the pressure difference between the in- and outlet receiver is much smaller. The biggest power demand arises at only 20% EGR and is around 140 kW. This means that a EGR blower or compressor of around 150 kW is required to overcome the pressure difference.

Besides increasing the pressure, the recirculated flow also needs to be cooled down to a certain temperature. Therefore the recirculated flow is guided through the EGR cooler, to cool the mixture down to the charge air temperature.

5.7. Conclusion

The aim of this chapter was to explain the working principle of exhaust gas recirculation and which disadvantages it has. Therefore the trade-off between soot and NO_x, also called the "diesel dilemma" has to be kept in mind. Besides that, the fuel choice is also an important factor for the correct functioning of EGR.

Two EGR configurations were explained, low-pressure EGR and high-pressure EGR. The most important differences are, as the name already mentions, the pressure difference between the starting point and the mixing point of the EGR route. The low-pressure EGR route starts downstream of the turbine and is recirculated back to upstream of the compressor, where the pressures lie around ambient pressure. With high-presure EGR, the starting point of the EGR route is upstream of the turbine and the exhaust gases are mixed with the regular air taken into the engine after the compressor. The pressures, depending on the engine load, can go up to 5 bars.

The two sections after that have described the implementation of both configurations into the existing diesel engine model. The EGR routes are shown in schematic representations of the Simulink model and it was explained how the occurring difficulties were solved.

The following chapter will present the results of the implementation of the EGR configurations on the diesel AM model and the NO_x fits will be evaluated.

6 Results

6.1. Introduction

This section will elaborate on the effects of the implementation of exhaust gas recirculation on a 4-stroke marine diesel engine. For this research a mean value first principle diesel engine model was used. This model has already been calibrated to match the 9M 32C MaK engine, which is used aboard Jumbo Maritime's four newest vessels.

This research consisted of implementing two different EGR configurations into an existing diesel engine model: low-pressure and high-pressure exhaust gas recirculation. Chapter 5 explained the main differences between the two configurations and also described some necessary changes to make the model work correctly. This chapter will show the results of the implementation of both configurations. Special attention will be paid to the engine parameters that influence the formation of NO_x.

Once the effects of EGR on the engine have been discussed, the next step in this research was to predict the NO_x emissions when using exhaust gas recirculation. Exhaust gas recirculation should lower the combustion temperature and decrease the amount of oxygen available for combustion. In order to predict the NO_x emissions, chapter 4 first explained the origin of the NO_x emission data before discussing the engine parameters that influence the formation of NO_x. Subsequently, these parameters were used to make NO_x fits. The engine parameters that were used for the NO_x fits are influenced by the implementation of EGR and this means that the fits will also be affected. This way the fits can be used to predict the NO_x emissions.

This chapter will start with elaborating on the effects of the implementation of the two exhaust gas recirculation configurations on certain engine parameters. After that, the effects of EGR on the NO_x emission fits will be thoroughly presented and discussed.

6.2. The effects of the implementation of Exhaust Gas Recirculation

Chapter 2 introduced the main factors that influence the NO_x formation in diesel engines and the most important effects of exhaust gas recirculation are mentioned in section 5.2. The two main effects of exhaust gas recirculation are:

- Change in oxygen availability
- Lower combustion temperature

This section will elaborate further on these effects. The oxygen availability and combustion temperature might be the two most important effects, but they are certainly not the only effects that will be discussed. In order to compare both EGR configurations, low-pressure and high-pressure, each engine parameter will show two graphs, one for each configuration. The low-pressure configuration allows an EGR rate up to 50%, but the high-pressure variant only allows an EGR rate up to 40%. The reason for this will be explained below, but this must be kept in mind when comparing the two configurations.

6.2.1. Availability of oxygen

The first effect that will be evaluated is the availability of oxygen. The oxygen availability is an important factor when it comes to combustion of fuels. Without a sufficient amount of oxygen in the combustion chamber unstable combustion and misfiring will occur. The oxygen availability can be described in a number of ways, all with their own benefits and disadvantages. A couple of parameters that describe the oxygen availability in the diesel A-M model are the air excess ratio λ, the flow of fresh air into the engine $\dot{m}_{fresh}$, the air to fuel ratio afr and of course the mass of the trapped air in the combustion chamber m_1 in combination with the air mas fraction x.

This section will discuss the engine parameters that were used to create the NO_x emission fits. For this research that were the total mass flow of fresh air into the engine, $\dot{m}_{fresh,x}$ and the air excess ratio, λ. $\dot{m}_{fresh,x}$ requires two different engine parameters, namely the mass flow of fresh air drawn into the engine $\dot{m}_{fresh}$ and the air mass fraction x.

Impact of EGR on the air excess ratio, λ

The air excess ratio and its definition were already thoroughly discussed in chapter 3. This section will elaborate on the influence of both EGR configuration on the air excess ratio. It is expected that the air excess ratio will decrease because of the recirculated exhaust gas. The exhaust gas contains less oxygen than the fresh air drawn into the engine. When the EGR rate becomes higher, the air excess ratio should decrease. Figure 6.1 shows the air excess ratio for different EGR rates for the low-pressure configuration and figure 6.2 shows the air excess ratios for the high-pressure configuration.

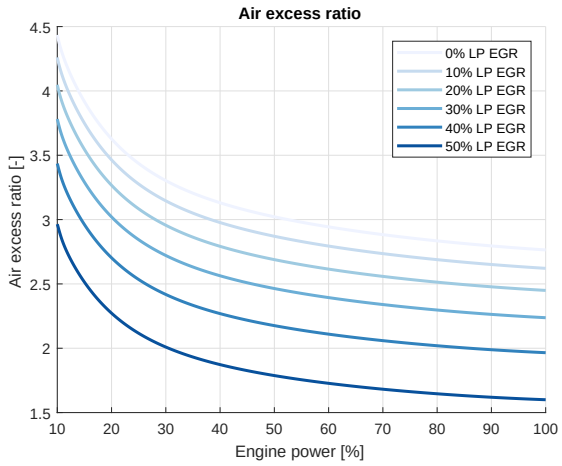

Figure 6.1: Influence of the low-pressure EGR rate on the air excess ratio

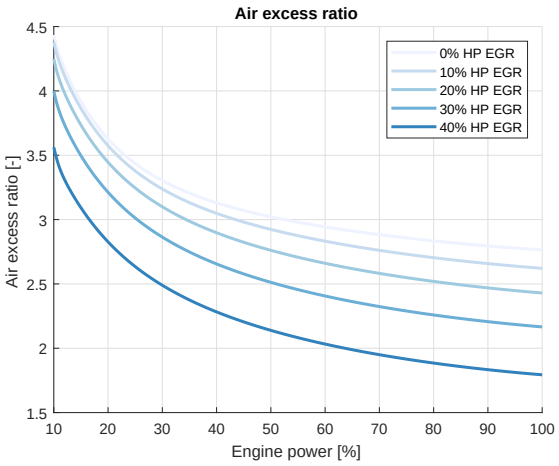

Figure 6.2: Influence of the high-pressure EGR rate on the air excess ratio

The horizontal axes of the graphs show the percentage of engine power, ranging from 10 to 100%. The maximum power of the engine is 4500 kW, meaning that this range extends from 450 to 4500 kW. The horizontal axis will be the same for this entire chapter due to the control strategy that is used for this research. The engine speed is constant at 600 rpm, but the load varies.

What can immediately be seen from both figures is that the air excess ratio decreases with increasing EGR ratio, as was expected. As already explained in chapter 4 the two different models have the same outputs when EGR is disabled (at 0% EGR). It can be seen that λ decreases from around 4.5 to 2.8. Then with each increase in EGR rate, the air excess ratio decreases. The air excess ratio for the high-pressure configuration seems to drop further than the low-pressure configuration. Why the drop in air excess ratio for the high-pressure configuration is bigger than the low-pressure configuration is because of the change in air mass fraction. The definition of the air excess ratio is as follows:

$$\lambda = \frac{m_1 \cdot x_1}{m_f \cdot \sigma} \tag{6.1}$$

The charge air pressure is kept equal for the different EGR ratios. An equal pressure also means an equal amount of mass that will be drawn into the combustion chamber. One of the important factors that changes due to EGR is the air mass fraction. The following section will elaborate a bit more on the effect of EGR on the air mass fraction.

What should also be noted is that the low-pressure configuration has an EGR ratio that goes up to 50%, where the high-pressure configuration goes up to a maximum EGR ratio of only 40%. The reason for this is already explained in chapter 3. If the EGR ratio increases, the air excess ratio decreases, but one must also keep the smoke limit in mind. If the smoke limit of an engine is reached, not all fuel will be burned completely, which causes smoke to come out the exhaust. The smoke limit of a common marine diesel engine is approximately between an air excess ratio of 1.5 to 1.7. The air excess ratio for the low-pressure EGR configuration already is in that range so that makes it a doubtful case. If an EGR ratio of 50% was to be set for the high-pressure configuration, the air excess ratio would definitely cross the smoke limit and for that reason it is not used in the comparison.

Impact of EGR on the air mass fraction, x

It is already known that the air mass fraction is an important factor in this research. Not only the air excess ratio is dependent on the air mass fraction, but also the specific heat of the mixture in the combustion chamber. The specific heats for both air and exhaust gas are assumed to be constant($c_{p,a} = 1005 J/kgK$, $c_{p,g} = 1100 J/kgK$), and the air mass fraction determines the distribution of these gases in the mixture and with that also the specific heat of the mixture. Figures 6.3 and 6.4 show the change in the air mass fractions for the different EGR ratios for both configurations.

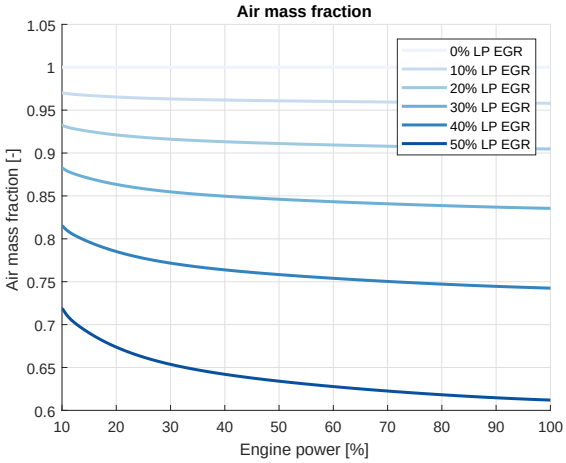

Figure 6.3: Influence of the low-pressure EGR rate on the air mass fraction

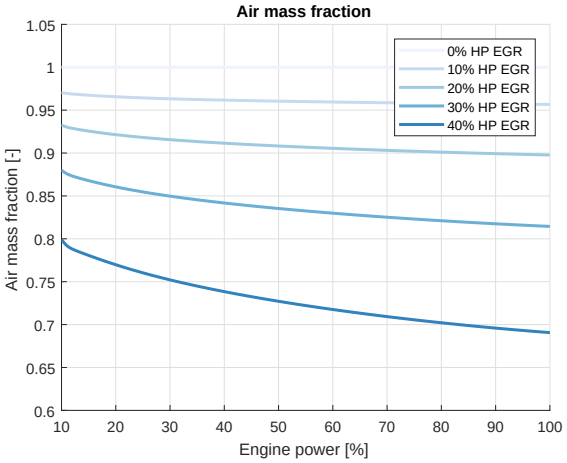

Figure 6.4: Influence of the high-pressure EGR rate on the air mass fraction

The vertical axes show the dimensionless air mass fraction ranging from 0.6 to 1.05. What can be seen is that the air mass fractions of the high-pressure configuration are slightly lower than the air mass fractions of the low-pressure variant. For an EGR rate of 40% the difference is about 5%. The shown air mass fractions are the air mass fractions at the start of combustion, so in the model they are called x_c or x_1. Both configurations use the same mixing methods and besides that, the charge air parameters are also the same for both configurations. This means that the difference originates from another part of the model. The main difference between the low-pressure and high-pressure configuration is of course the pressure, but besides that the recirculation flows have different starting points. The low-pressure flow starts downstream of the turbine and the high-pressure flow starts downstream of the outlet receiver upstream of the turbine. The obvious choice is to see how the air mass fractions in the outlet receiver and turbine of the engine is computed.

For the low-pressure EGR configuration, the air mass fraction through the turbine does not change and this means that the difference has to originate from the outlet receiver. Because the high-pressure configuration already starts downstream of the outlet receiver, the mass flow through the turbine is smaller than for the

low-pressure EGR loop. The turbine mass flow, m_{tur}, is the same as the mass flow out of the outlet receiver $m_{OR,out}$. And the outlet receiver air mass fraction is partly dependent on the mass flow out of the outlet receiver. For the high-pressure EGR loop the turbine mass flow m_{tur} is smaller and this results in the slightly lower air mass fraction in the outlet receiver.

Impact of EGR on the fresh air mass flow, $\dot{m}_{fresh,x}$

The next engine parameter that describes the amount of fresh air in the engine is the fresh air mass flow, or $\dot{m}_{fresh}$. Chapter 4 explained the difference between the regular fresh air mass flow, $\dot{m}_{fresh}$, and the one that is used when EGR is implemented, $\dot{m}_{fresh,x}$, but the differences between those two mass flows have not been showed yet. The main difference is that the regular $\dot{m}_{fresh}$ did not incorporate the oxygen available in the recirculated exhaust gas flow. Because not all oxygen is used for combustion, part of the unused oxygen is still in the exhaust gas flow. The following equation defines the fresh air mass flow when EGR is enabled:

$$\dot{m}_{fresh,x} = \dot{m}_1 \cdot x_c \tag{6.2}$$

Of course, when EGR is disabled, the air mass fraction is equal to 1 and $\dot{m}_{fresh,x} = \dot{m}_{fresh}$. And this means that this function also applies to 0% EGR. The previous section elaborated on the use of the air mass fraction and how it changes when EGR is enabled. Figures 6.5 and 6.6 show the regular fresh air mass flow into the engine.

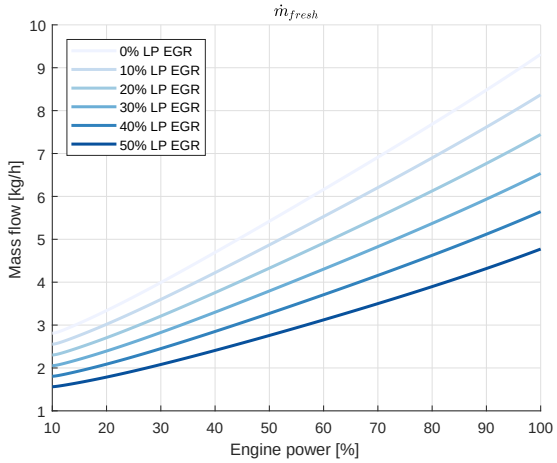

Figure 6.5: Influence of the low-pressure EGR rate on the fresh air mas flow

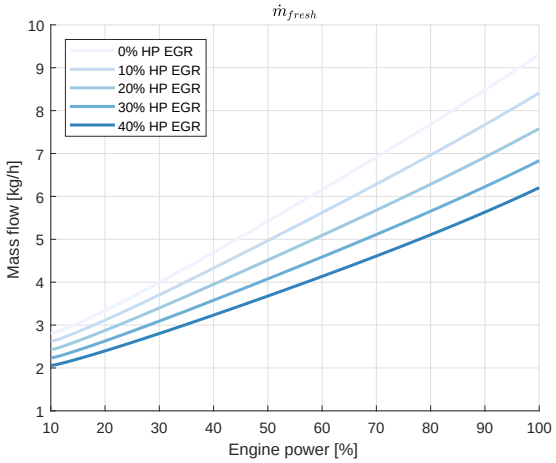

Figure 6.6: Influence of the high-pressure EGR rate on the fresh air mass flow

The figures show that the regular fresh air flow into the engine for the low-pressure EGR configuration is slighty lower than for the high-pressure EGR loop. Because this fresh air flow ($\dot{m}_{fresh}$) is not used to fit the NO_x data, it is time to see how much the air mass fraction is of influence on the fresh air mass flows. Figure 6.7 on the left shows the air flows for the low-pressure EGR configuration and on the right figure 6.8 shows the different mass flows for the high-pressure configuration.

As was to be expected, the fresh air mass flows do not change much. The vertical axes show the mass flow in kg/h and where the regular fresh air mass flow, $\dot{m}_{fresh}$, ranges from 4.8 to 9.3 kg/h, the fresh air mass flow that incorporates the air mass fraction($\dot{m}_{fresh,x}$) ranges from 5.8 to 9.3 kg/h. This is of course because the only fresh air that is not taken into account in $\dot{m}_{fresh}$, is the fresh air in the exhaust gas that did not take part in the combustion. And that is only a small part of the exhaust gas. The 0% EGR mass flows stay the same, but for every higher EGR rate, the fresh air mass flow lines move a bit closer to the 0% EGR mass flow lines.

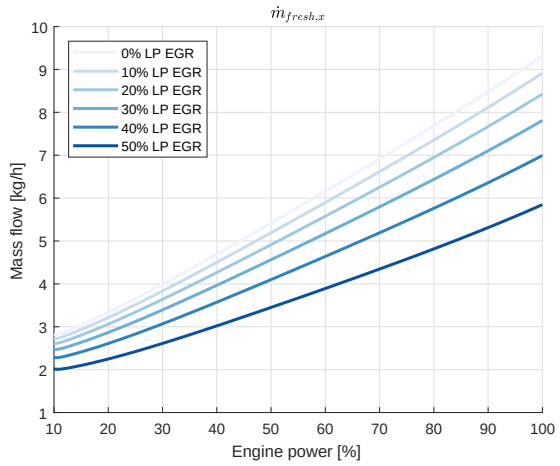

Figure 6.7: Influence of the low-pressure EGR rate on the total fresh air mas flow

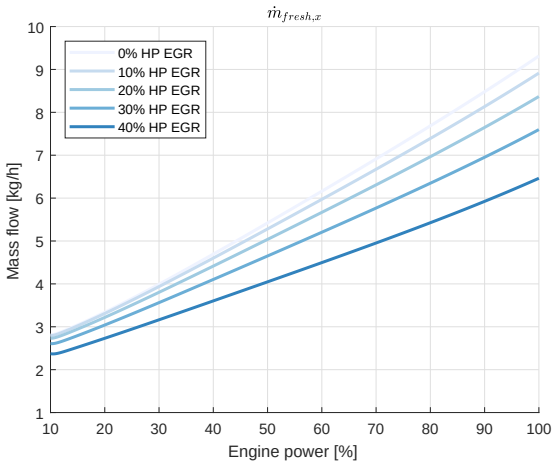

Figure 6.8: Influence of the high-pressure EGR rate on the total fresh air mass flow

Altogether the reductions in the oxygen related engine parameters for increasing EGR rate look really promising for the abatement of the NO_x emissions. How this will affect the NO_x emission fits will be discussed later on in this chapter.

6.2.2. Combustion temperature

Now that all the oxygen related engine parameters have been discussed, it is time to take a look at the other important parameter, namely the combustion temperature. Chapter 4 elaborated on the maximum combustion temperature, which is reached in steps 4 and 5 of the Seiliger cycle. because $T_4 = T_5 = T_{max}$ the figures below show the maximum average combustion temperatures. The figure on the left, 6.9, shows the temperatures for different low-pressure EGR rates and figure 6.10 shows the temperatures for the high-pressure EGR loop.

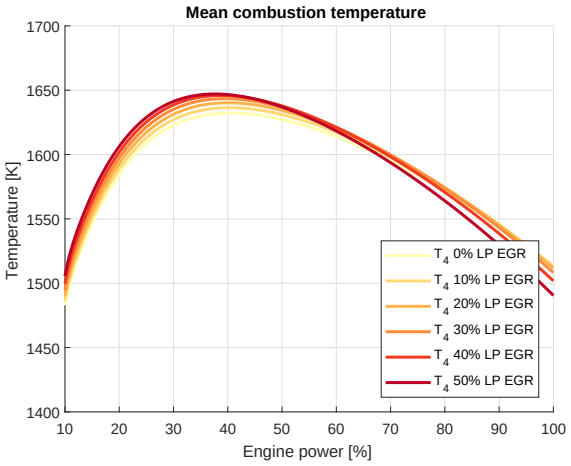

Figure 6.9: Influence of the low-pressure EGR rate on the maximum combustion temperature

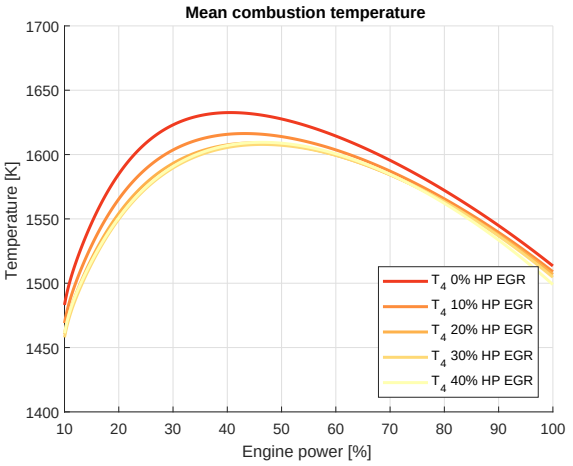

Figure 6.10: Influence of the high-pressure EGR rate on the maximum combustion temperature

What can immediately be seen in both figures is how small the temperature differences are. The horizontal axes show the engine power and the vertical axes show the temperature in Kelvin. The starting temperatures, for a 0% EGR rate, are exactly the same and have their peak at around 40% engine power at 1630 Kelvin. The low-pressure configuration on the left shows a small temperature increase for increasing EGR rates and the figure on the right shows a small decrease in temperature for the high-pressure EGR loop. But what applies for both EGR configurations is that the maximum deviation in temperature is less than 20 Kelvin, and on a scale of more than 1600 that is much less than was expected.

Because part of the working principle of EGR is based on an increase in the heat capacity of the combustion mixture, it was expected that the maximum combustion temperature would decrease for both EGR configurations. This means that it has to be checked why there is a difference between the two configurations, increase versus decrease, and besides that why the temperature change is only this small.

Because the specific heat of the combustion mixture is an important factor for EGR, the change in specific heats shall be checked first. The following figures show the changes in specific heats for both EGR configurations.

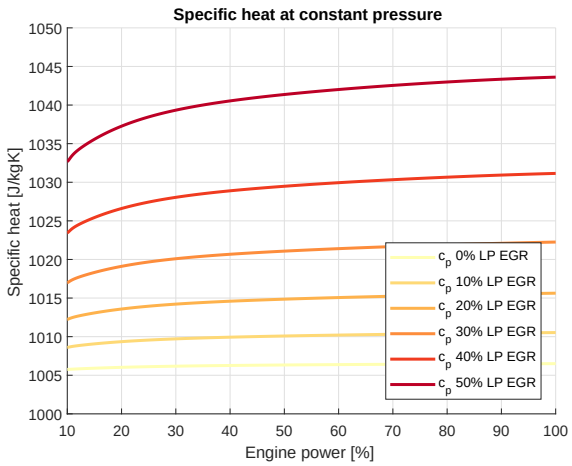

Figure 6.11: Influence of the low-pressure EGR rate on the specific heat

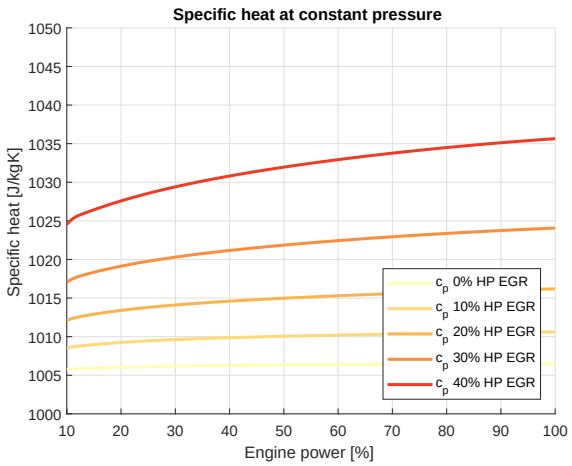

Figure 6.12: Influence of the high-pressure EGR rate on the specific heat

Figure 6.11 shows the specific heat (in J/kgK) of the low-pressure EGR configuration and figure 6.12 shows the changes in specific heat for the different high-pressure EGR ratios. What both figures show is that the specific heat (at constant pressure) increases with increasing EGR ratio. However, the increase in specific heat is a little higher for the high-pressure EGR configuration. This is the result of the slightly lower air mass fraction(seen in figures 6.3 and 6.4): a lower air mass fraction means that the mixture contains a little more exhaust gas. The higher specific heat of the exhaust gas causes the higher specific heat of the combustion mixture for the high-pressure loop.

However, this does still not explain the increase in maximum combustion temperature. A higher specific heat should result in a lower maximum combustion temperature. The next step in this analysis is to take a look at the heat release at constant pressure. Only a higher heat release could explain a rise in temperature when the specific heats become higher. The following figures show the heat release at constant pressure (isobaric combustion and expansion). This step in the heat release is used because this determines the heat release to achieve the maximum combustion temperature.

The figures show characteristics which are similar to the temperature graphs, but this time the vertical axes show the heat release at constant pressure given in kJ/kg. Figure 6.13, the low-pressure configuration, shows an increase in heat release for increasing EGR rates and figure 6.14 shows a decrease in heat release for increasing high-pressure EGR rates. This is the same trend as the temperatures show and the heat release might declare the different changes to the combustion temperature. However, this still does not explain why the heat release increases for the low-pressure configuration and decreases for the high-pressure EGR loop.

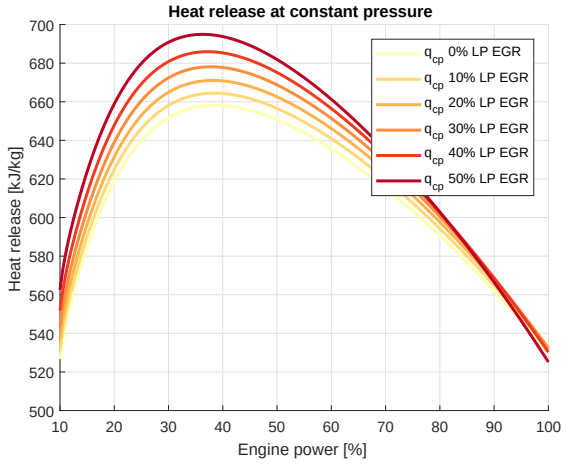

Figure 6.13: Influence of the low-pressure EGR rate on the heat release at constant pressure

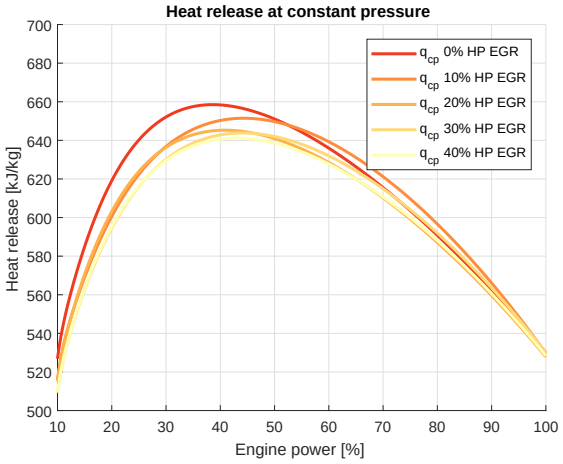

Figure 6.14: Influence of the high-pressure EGR rate on the heat release at constant pressure

An explanation for the rise in heat release might be that there is change in fuel injection to reach the desired power. The nominal engine power is 4500 kW at 600 rpm. With EGR enabled it was expected that there would be a small decrease in power, but the simulation model is controlled via speed and load. Because the engine in question runs in generator mode, the speed is kept constant at the nominal point of 600 rpm and the load is varied from a certain point to the maximum power output. This means that, despite the implementation of EGR, the engine still reaches its nominal power of 4500 kW. This is achieved by injecting more fuel in order to reach the engines' maximum power output.

The next step in the analysis of the combustion temperature is to check how the fuel injection is affected by the implementation of exhaust gas recirculation. The following graphs show the amount of fuel injected for both EGR configurations:

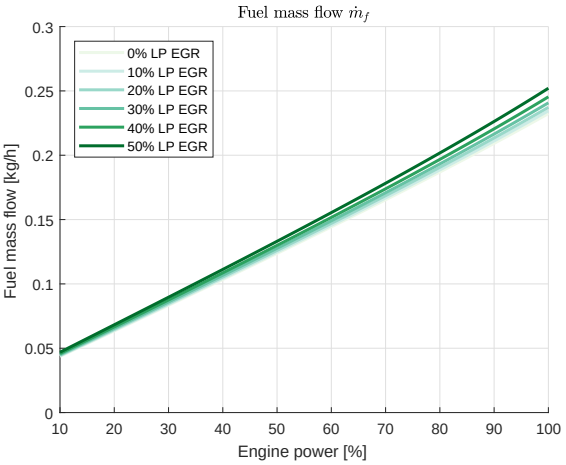

Figure 6.15: Influence of the low-pressure EGR rate on the fuel mass flow $\dot{m}_f$

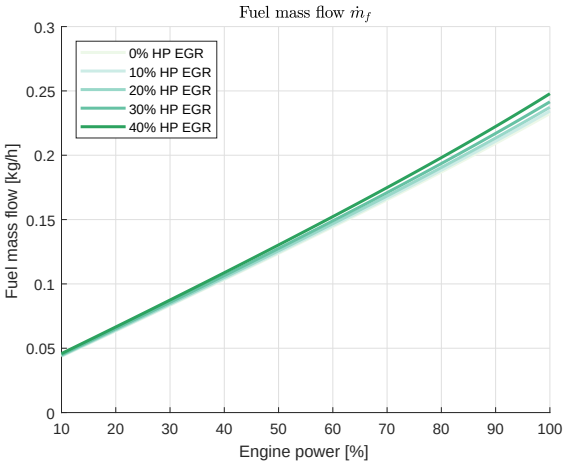

Figure 6.16: Influence of the high-pressure EGR rate on the fuel mass flow $\dot{m}_f$

Figure 6.15 shows the flow of fuel for the low-pressure EGR loop and figure 6.16 shows the amount of fuel injected for the high-pressure configuration. The vertical axes show the amount of fuel injected in kg/h. Again similar trends can be seen between the low-pressure and high-pressure loops. The amount of fuel injected increases linearly with the engine load for both configurations. Besides that the amount of fuel injected also increases with increasing EGR rate. This explains the rise in heat release for the low-pressure EGR configuration: the increase in specific heat is too small to overrule the increase in heat release. So despite the fact that the specific heat increases from around 1005 J/kgK to 1045 J/kgK, the amount of fuel injected

increases from 0.23 kg/s to 0.25 kg/s. A higher amount of fuel means that more fuel can be burned and this causes an increase in the heat release.

6.2.3. Brake specific fuel consumption

It is already known that one of the downsides of exhaust gas recirculation is that the specific fuel consumption will be slightly higher. Due to EGR an amount of excess air is declined to the combustion chamber which causes the slight loss in fuel economy. The excessive charge dilution probably leads to unstable combustion and misfiring, which on its turn results in power loss and a higher specific fuel consumption.[29]

The figures below, 6.17 and 6.18, show the brake specific fuel consumption for respectively the low-pressure and high-pressure EGR configurations. What can be seen are to almost similar figures. The brake specific fuel consumptions increases with increasing EGR rate, and the increases are for both EGR configurations are about even. As already explained in the previous section, extra fuel is injected to reach the desired engine power. It was expected that the implementation of EGR would cause a decrease in power, but the control strategy of the engine ensures that, despite the implementation of EGR, the desired power output of 4500 kW is still reached.

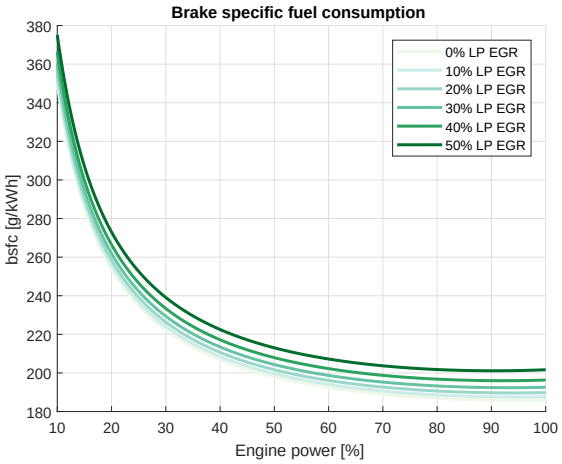

Figure 6.17: Influence of the low-pressure EGR rate on the brake specific fuel consumption

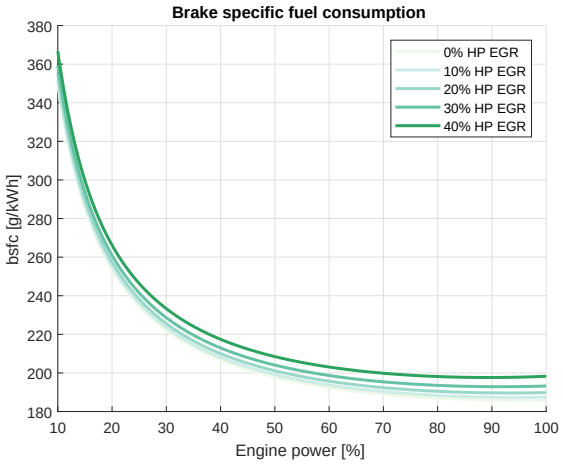

Figure 6.18: Influence of the high-pressure EGR rate on the brake specific fuel consumption

6.3. Prediction of the NO_x emissions

Chapter 4 introduced the origin of the NO_x data and discussed how the data was going to be used. After that, the most important factors influencing the formation of NO_x were shortly discussed. And the chapter was concluded with the actual NO_x emission fits with the units kg/h and g/kWh. This section will elaborate on those fits and will show how the implementation of the two EGR configurations influences the fits and with that, the prediction of the NO_x emissions.

6.3.1. kg/h emission predictions

The same structure as chapter 4 will be used, meaning that the kg/h fits will be reviewed first, followed by the g/kWh fits. Two of the four kg/h fits are shown in this chapter. The remaining NO_x predictions can be seen in appendix D. This chapter will show the prediction of the NO_x emissions using the 'basic' NO_x fit (only $\dot{m}_{fresh,x}$) and the more extended NO_x fit (with $\dot{m}_{fresh,x}$, T_{max}/T_3 and λ). Figure 6.19 shows all of the kg/h NO_x fits once more before the resulting predictions are showed.

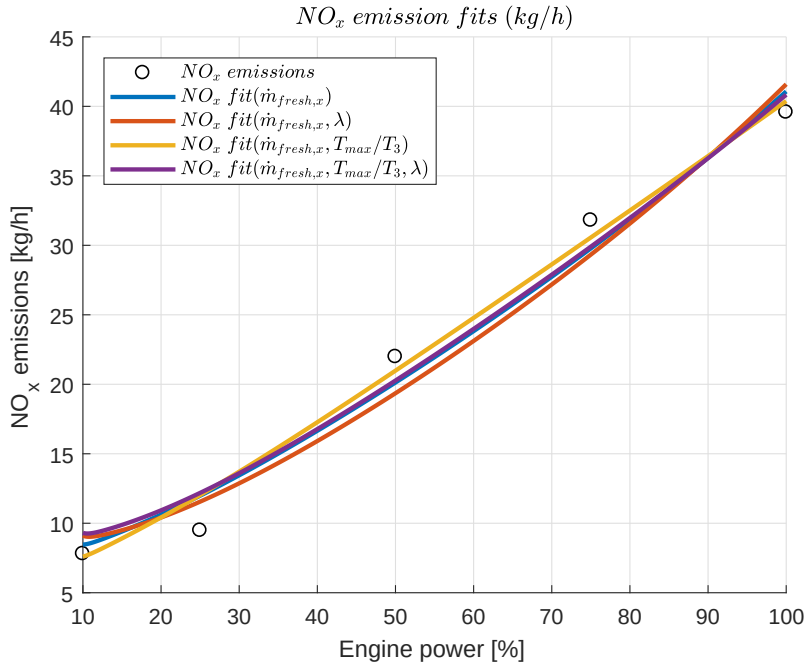

Figure 6.19: NO_x emissions fits (kg/h)

kg/h NO_x prediction using $\dot{m}_{fresh,x}$

The 'basic' NO_x fit is designed to meet the kg/h unit requirements of the emissions. The NO_x emissions were given in kg/h which means that an engine parameter with those units was chosen as a basis for all the fits. Figure 6.21 shows the original NO_x fit and the NO_x emission predictions for increasing EGR rates.

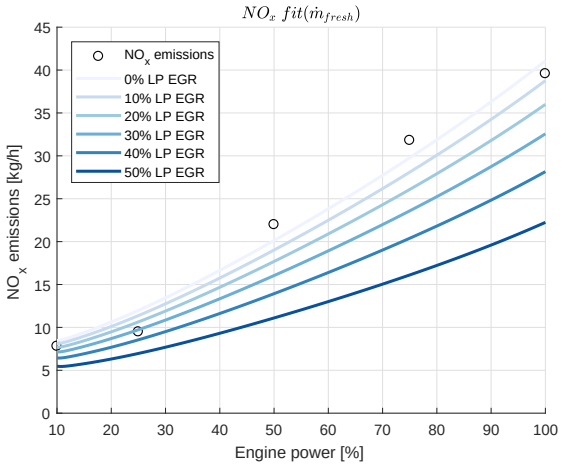

Figure 6.20: kg/h NO_x emission prediction as a function of $\dot{m}_{fresh,x}$

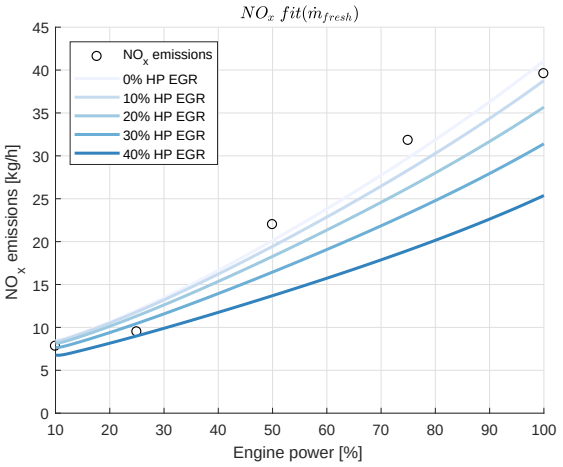

Figure 6.21: kg/h NO_x emission prediction as a function of $\dot{m}_{fresh,x}$

The fit is fully dependent on the total fresh air mass flow into the combustion chamber and that is why it follows the same trend as the $\dot{m}_{fresh,x}$ for increasing EGR rates (Figure 6.7). If the emissions predictions for 0% and 50% EGR are compared it can be seen that for maximum engine power the NO_x emissions are almost cut in half. What can also be seen is the difference between the EGR rates. The step from 40% EGR to 50% EGR is bigger than the step from 30% to 40%. This also applies to the lower EGR ratios.

The high-pressure EGR differs a little from the low-pressure variant. This can of course be explained by the influence of the high-pressure EGR on $\dot{m}_{fresh,x}$. The fresh air flow into the engine, and therefore also the NO_x prediction are partly dependent on the lower air mass fractions of the high-pressure EGR loop. Figure 6.21

shows that an EGR ratio of 40% also causes the NO_x emissions to go down by 40%. This is, of course, logical if the emission prediction is purely dependent on the amount of fresh air drawn into the engine.

kg/h NO_x prediction using $\dot{m}_{fresh}$, T_{max}/T_3 and λ

The following prediction is substantiated by more than one engine parameter. For this prediction the temperature and air excess ratio are also taken in to account. The fits where the temperature and air excess ratio are used independently are attached in appendix D. Figure 6.22 shows the prediction for the low-pressure EGR configuration and figure 6.23 shows the emission predictions for the high-pressure EGR loop.

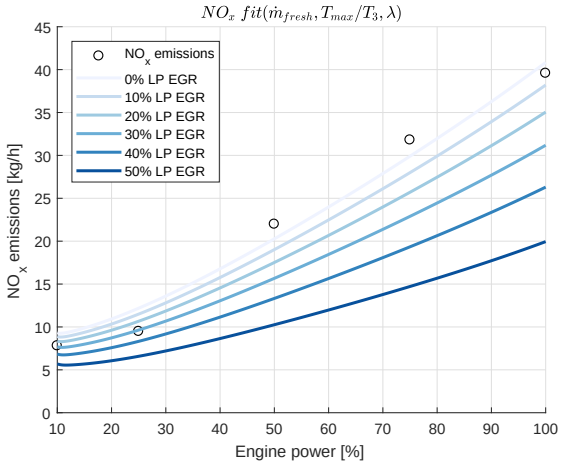

Figure 6.22: kg/h NO_x emission prediction as a function of $\dot{m}_{fresh,x}$, T_{max}/T_3 and λ

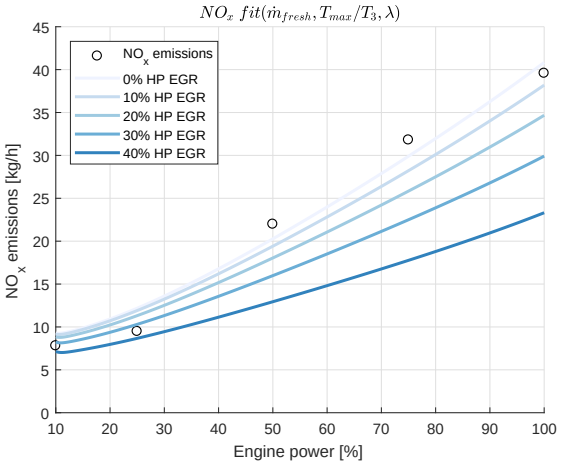

Figure 6.23: kg/h NO_x emission prediction as a function of $\dot{m}_{fresh,x}$, T_{max}/T_3 and λ

Both figures look a lot like the prediction where only $\dot{m}_{fresh,x}$ is used, but there are some small deviations. Because when both the temperature and air excess ratio are used in the fits, the predicted NO_x emissions are slightly lower than for the $\dot{m}_{fresh,x}$ prediction. The temperature is not of much influence, because the temperature changes are only small, but the air excess ratio is of more influence. Figures 6.1 and 6.2 showed that the air excess ratio decreases up to 50% for 50% EGR, where the maximum temperature changes are only 2%.

Of course, as long as no NO_x emission data is available for the 9M 32C diesel engine, these predictions cannot be validated. Different studies however report that EGR can achieve NO_x emission reductions up to 60%. This means that the predictions are already in the right range.

6.3.2. g/kWh emission predictions

Just as with the kg/h prediction, this section will elaborate on the g/kWh emission predictions for two of the four fits. Again the base fit ($\dot{m}_{fresh,x}$ and P_B) and a more extensive fit ($\dot{m}_{fresh,x}$, P_B, T_{max}/T_3 and λ) are shown. As a reminder, figure 6.24 shows all of the emission fits once more before the predictions are discussed.

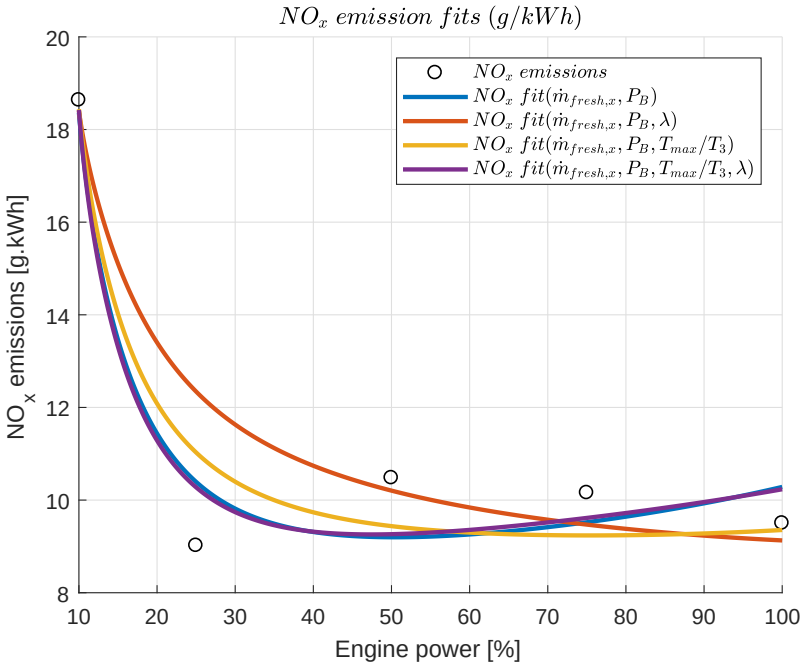

Figure 6.24: NO_x emissions fits (g/kWh)

g/kWh NO_x prediction using $\dot{m}_{fresh,x}$ and P_B

The base fit of the g/kWh also incorporates the brake power of the engine besides $\dot{m}_{fresh,x}$. This is of course needed to meet the specific emissions units of g/kWh. Figures 6.25 and 6.26 show the NO_x predictions of the low-pressure and high-pressure EGR loop respectively.

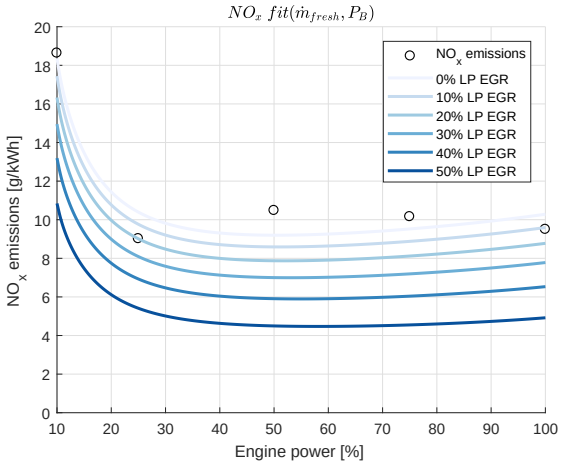

Figure 6.25: g/kWh NO_x emission prediction as a function of $\dot{m}_{fresh,x}$ and P_B

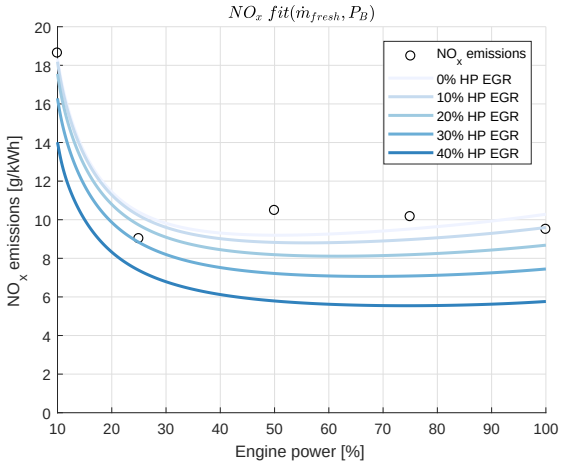

Figure 6.26: g/kWh NO_x emission prediction as a function of $\dot{m}_{fresh,x}$ and P_B

This g/kWh predictions show the same trend as the basis kg/h predictions. The specific NO_x emissions decrease incrementally for increasing EGR rates: the decrease in NO_x is slightly bigger for each increasing EGR rate. And again, the decreases for the high-pressure configuration are slightly larger than for the low-pressure variant. NO_x emission reductions up to 50% are predicted for an EGR rate of 50%.

g/kWh NO_x prediction using $\dot{m}_{fresh,x}$, P_B, T_{max}/T_3 and λ

Again, the fits dependent on the temperature ratio T_{max}/T_3 and λ (and $\dot{m}_{fresh,x}$ and P_B) are enclosed in appendix D. The figures below, 6.27 and 6.28, show the emission predictions derived from $\dot{m}_{fresh,x}$, P_B, T_{max}/T_3 and λ.

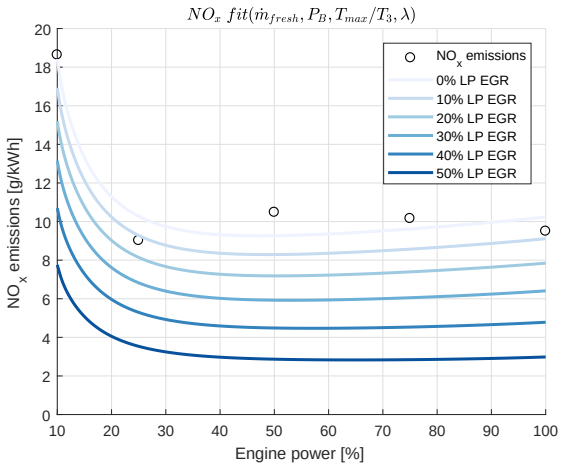

Figure 6.27: g/kWh NO_x emission prediction as a function of $\dot{m}_{fresh,x}$, P_B, T_{max}/T_3 and λ

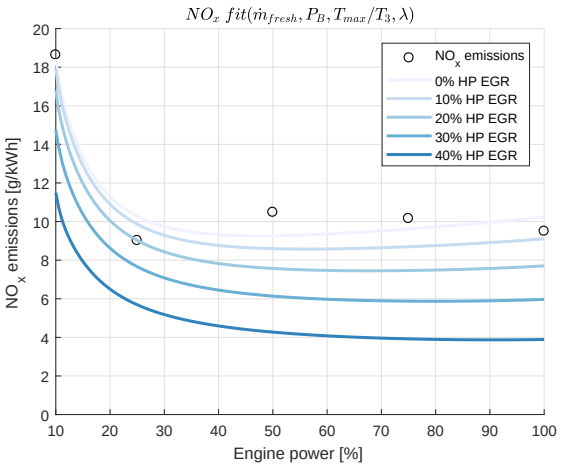

Figure 6.28: g/kWh NO_x emission prediction as a function of $\dot{m}_{fresh,x}$, P_B, T_{max}/T_3 and λ

What can be seen is that, again the predicted NO_x emissions decrease for increasing EGR rates. What catches the eye is that the decrease in emissions is big compared to the kg/h emission predictions. The low-pressure prediction decreases from around 10 g/kWh to less than 4 g/kWh for 50% recirculated exhaust gas. And for the high-pressure configuration, the same thing occurs. For 40% EGR rate, the specific emissions prediction decreases from 10 g/kWh to 4 g/kWh.

Another observation is that the newly predicted NO_x emissions seem to increase less and less for higher EGR rates. For the lower EGR rates, the emission prediction rises slightly from around 50% engine power. For the higher EGR rates the prediction flatten out more, which shows more similarities with the original NO_x emission data.

In conclusion it can be said that the predicted emissions reductions are in the right range and in general 10% less NO_x is emitted for each 10% increase in EGR rate. The following chapter will show a short recap of this research and conclusions and recommendations for future research will be given.

7

Conclusions and recommendations

7.1. Introduction

The main objective of this thesis was to gain insight in the behaviour of a 4-stroke marine diesel engine when exhaust gas recirculation is implemented. Besides that a research was conducted on how the NO_x emissions of this engine might be predicted. The first step in this research was to define a problem definition and a set up a list of research objectives. The problem definition, as it was already mentioned in chapter 1 is stated as:

How can the NO_x emissions of a 4-stroke marine diesel engine be predicted after the implementation of exhaust gas recirculation and with the use of a mean value simulation model?

In order to find a solution for this problem the following set of research objective had to be accomplished:

- Investigate the NO_x formation in diesel engines and determine the most important factors that influence the formation.
- Determine which engines are used on Jumbo Maritime's vessels and select an appropriate simulation model which can be calibrated with the available engine data.
- Evaluate the available NO_x emission data and use certain engine parameters to fit this data.
- Explain the working principle of exhaust gas recirculation and implement multiple EGR configurations into the calibrated diesel engine model.
- Evaluate the effects of the implementation of the different EGR configurations on the diesel engine model.
- Use the developed NO_x fits to predict the NO_x emissions of the diesel engine equipped with EGR and analyse the results.

This chapter will shortly describe how the research objectives were accomplished and how the stated problem was solved. After shortly recapturing the entire research, this thesis will be concluded and recommendations for future research will be given.

This research started with the investigation of the formation of NO_x in diesel engines. After discussing the reaction kinetics, the most important factors influencing the formation of NO_x were determined: the combustion temperature (including hot spots) and the amount of oxygen available for combustion. It was then decided that this research would focus on the 9M 32C MaK marine diesel engine, which is used aboard four of Jumbo Maritime's newest vessels. Matlab and Simulink were used to calibrate a mean value first principle simulation model with the available engine data.

The next step was to fit the NO_x emission data. The available NO_x emission data (extracted from an EIAPP report) was evaluated and the factors influencing the formation of NO_x were discussed again. Subsequently the engine parameters representing the influence factors and a nonlinear regression model were used to fit

the NO_x emission data. Fits were made for the kg/h and g/kWh NO_x emissions.

The following chapter explained the working principle of exhaust gas recirculation and introduced two EGR configurations: low-pressure and high-pressure exhaust gas recirculation. The differences between the two configurations were explained and the required changes to the model were discussed. After the successful implementation of both EGR configurations, the effects of EGR on the diesel engine model were presented. The final step in this research was to predict the NO_x of the diesel engine equipped with EGR with the help of the NO_x fits.

7.2. Conclusions

Now that this entire research has been shortly summarized, it is time to draw some conclusions. The most important parts to be discussed are:

- The modelling approach
- The effects of exhaust gas recirculation
- The prediction of the NO_x emissions

7.2.1. Modelling approach

This research was first started to investigate the behaviour of a marine diesel engine equipped with EGR and the influence on EGR on the NO_x emissions. It soon became clear that the formation of NO_x in a diesel engine is a difficult and not fully understood process which raises a lot questions. Many researches into the formation of NO_x in diesel engines have already been conducted, but did not give the desired results. Therefore it was decided that a different approach would be used for this thesis.

The main issue with the prediction of the amount of NO_x formed is determining the maximum temperature during combustion and then especially the local temperatures of the hot spots. The used model is a mean value simulation model, which is also not able to predict the local temperatures in the combustion chamber. This approach focusses on the mean temperature during combustion. It can be assumed that when the mean temperature in the combustion chamber is lower, it is easier for the hot spots to transfer their heat to the surrounding area, causing the temperature of the hot spots to be lower. A lower temperature means that less NO_x will be formed. Besides the temperature, the other main contributor to the formation of NO_x is the availability of oxygen and that can also be described really well in this model.

Chapter 3 showed that the model matches the 9M 32C MaK diesel engine very well. A comparison with data from the EIAPP report and FAT records showed that the majority of all data points is well within a 5% margin of the model's data. Altogether it can be concluded that the model is a good representation of the actual engine and can be used for the implementation of EGR and further research.

A drawback of the model is that it is not generic, meaning that the performed analysis is purely meant for the engine used in this specific research, namely the 9M 32C MaK diesel engine. If the emissions of another engine need to be predicted, this model has to be calibrated with that engine first. Certain engine parameters have to be tuned to match the bench data for that particular engine. The implementation of EGR will not be affected when a different engine is used.

On to the next point, namely the control strategy of the model. With the used model a different control strategies were possible. Because the engine runs in generator mode to propel a controllable pitch propeller, it was decided that the speed control would be used. This, combined with load control, means that the engine runs at a constant rpm, but with varying load. This is also how the actual motor management system aboard Jumbo's vessel operates. When the model had to be tuned to match the engine, the results were great and the model simulated the engine very well.

However, after calibration of the model the next step was to implement the two different EGR configurations. This caused changes in the fuel injection. Because the fuel injection adapts with the desired load, more fuel is injected when the desired load cannot be reached. Implementing EGR resulted in a loss in power which is made up for with the injection of more fuel. The injection of more fuel results in more heat release, which

on its turn results in a higher power output. This means that the output power of the engine remained the same as when EGR is disabled, but this is at the expense of a higher fuel consumption. The engines aboard Jumbo's vessels work according to this principle, but this makes it difficult to determine the power losses due to the implementation of EGR. If power losses have to be taken into account the control strategy of the model needs to be adapted.

In conclusion it can be said that the control strategy for the diesel engine model without EGR is appropriate and gave excellent results, but changes are required if power losses need to be taken into account. A desired control strategy would then be the combination of speed and fuel control.

7.2.2. Effects of EGR

Now that the modelling approach has been discussed, it is time to evaluate the effects of exhaust gas recirculation on the diesel engine. The two most important factors influencing the formation of NO_x are the combustion temperature and the availability of oxygen.

What became clear when presenting the results was that, for the low-pressure EGR configuration, the maximum temperature during combustion rose slightly for increasing EGR rate, where it was expected that this temperature would drop. A part of the temperature change is dependent on the specific heat of the mixture in the combustion chamber. The results showed that the specific heat of the mixture only rose by 40 J/kgK from 1005 J/kgK to 1045 J/kgK. On the other hand, an increase in heat release also occurred and this is of bigger influence on the temperature than the change in specific heat. The change in heat release is due to the fact that the model is load controlled, as already mentioned above. This means that more fuel is injected if the desired load is not reached. If more fuel is combusted, more heat will be released. If the fuel injection would remain the same, the output power of the engine would decrease slightly, but it would also result in a lower combustion temperature.

The high-pressure EGR configuration reacted a bit different: the combustion temperature decreased for increasing EGR rate. In comparison with the low-pressure configuration, at the same EGR rate, the specific heats are slightly higher and the heat release is lower. Those two parameters combined result in lower combustion temperatures for increasing EGR rate. The temperature decrease would even be bigger if the control strategy of the model could be adapted to speed and fuel control.

Altogether it can be said that the mean combustion temperature did not react to the implementation of EGR as was first expected. The changes are a lot smaller and this means that the influence of the temperature on the prediction of the NO_x emissions will only be small. The influence on the prediction will be explained in the following section.

Then continuing with the oxygen content, it can be concluded that EGR does indeed decrease the amount of oxygen available for combustion. With EGR enabled, a certain amount of fresh intake air, depending on the EGR rate, is replaced by exhaust gas. The amount of air is described by the air mass fraction, which on its turn forms the basis for the air excess ratio and the fresh air mass flow. The fresh air mass flow is reduced by almost for 50% at a 50% EGR rate. The air excess ratio decreases from 2.8 to 1.6 at full engine load at 50% EGR. One must keep in mind that the air excess ratio does not cross the smoke limit, which is situated around an air excess ratio of 1.6.

In general it be concluded that the implementation of EGR has a different effect than was first expected. The availability of oxygen in the combustion chamber, described by both the air excess ratio and the fresh air mass flow into the engine decrease as expected, but the temperature does not decrease as expected. It is expected that changing the control strategy of the model to speed and fuel control would result in the desired decrease in temperature.

7.2.3. Prediction of NO_x emissions

The purpose of this research was to gain an insight in the behaviour of a marine diesel engine equipped with exhaust gas recirculation. Another important research objective was to try and predict the NO_x emissions of the engine equipped with EGR. Multiple steps were required to make an estimation of the NO_xemissions.

What has to be mentioned first is that this is an exploratory research to find a way to predict the NO_x emissions of marine diesel engines. There is no emission data available for this specific engine when it is equipped with EGR. The made predictions are estimates on how the engine might react to the implementation of EGR. This means that the results cannot be validated until emission data becomes available for this specific engine, or a similar engine, equipped with EGR.

The process of predicting the emissions started with an evaluation of the available NO_x emission data. It can be concluded that the data set is quite limited and it contains an outlier at 25% engine load. However, it remains unclear why the NO_x emissions at 25% load are this low. There are no outliers in the engine parameters at this point. Besides that, all new marine diesel engines are subjected to a strict test protocol and the results of that test, the EIAPP certificate, confirms that there is no question of variable injection timing or variable valve timing. Those where two options which might have influenced the emissions at that point. The outlier has been accepted as a valid data point and will be used in the emission fits and predictions.

What also has to be mentioned is that the engine manufacturer does not recommend to operate at those lower engine loads. This results in a higher fuel consumption, lower efficiency and higher polluting emissions. The recommended operating range for the 9M 32C engine is therefore set to 70-100%. The commercial department of Jumbo Maritime complies with this recommendation by selling voyages at an engine load between 75% and 95% engine load, mostly dependent on the schedule and the weather.

The emission fits have been made using a nonlinear regression model. This type of model uses a combination of different engine parameters dependent on one or more independent variables to fit observational data to a function. The goodness of fit statistics show that, despite the outlier in the emission data, the fits can represent the data quite well with R-square values of over 90%. This means that the fits explain over 90% of the total variation in the data about the average. It can be concluded that the use of a nonlinear regression model is a good method to fit multiple parameters to observational data.

Another benefit of using a nonlinear regression model is that the model can also be tuned by hand. This means that if the model cancels out an engine parameter, because it does not fit the function properly, the user can manually add a value to the variable. This might be needed if the user needs a certain engine parameter to influence the fit more. Most of the time this results in a small decrease in the goodness of fit statistics.

The emissions fits were of course dependent on the engine parameters relevant to the formation of NO_x. The two most important factors were the air mass fraction and maximum temperature, but other parameters were used as well to meet the unit requirements (kg/h and g/kWh) of the emission data. An example of such a parameter is the brake power of the engine to cope with the g/kWh emissions. Because the changes in temperature were really small, the effect of the temperature on the emissions fits is also small in comparison with for example the fresh air mass flow and the air excess ratio.

The predictions of the NO_x emissions are based on a set of engine parameters that change with changing EGR rate. The predictions show that a NO_x emission reduction up to 60% (for 50% EGR rate) can be achieved. However, this differs per engine fit. Some fits, like the g/kWh fit based on the fresh air mass flow $\dot{m}_{fresg}$ and the brake power P_B only achieves a 40% reduction. This is of course fully dependent on which engine parameters are used for the fits and how they are affected by the EGR rate. As already mentioned above, these predictions are only estimates and are based on the hypothesis that the NO_x emissions are dependent on the above mentioned engine parameters. The main issue is that the predicted emissions cannot be compared to observational data. If observational data of an engine equipped with EGR is available, the diesel engine model could be calibrated to match that specific engine and the nonlinear regression model could also be tuned to match the NO_x emissions.

Altogether it can be concluded that the use of a nonlinear regression model is an excellent method for the fitting of data which is dependent on multiple independent parameters. The made predictions are only estimates, but if observational data of an engine equipped with EGR is available, the model could be improved and tuned to match the NO_x emissions.

7.3. Recommendations

This section will elaborate on the recommendations which can be used for future research. This thesis investigated the behaviour and the NO_x emissions of a marine diesel engine equipped with exhaust gas recirculation. The conclusions of this research showed the potential of the implementation of exhaust gas recirculation and the use of a nonlinear regression model to fit the emission data.

Starting with the control strategy of the model: the used model showed a good representation of the tested engine, but the power losses due to EGR cannot be taken into account. The motor management system ensures that the desired power is reached at the expense of a slightly higher fuel consumption. If one wants to analyse the effect of EGR on power losses in the engine it is recommended that the control strategy of the model is adapted from speed and load control to speed and fuel control. This way the rpm could be kept constant at 600 rpm and the fuel injection could be adapted manually. This might give a better overview of how much power is lost due to the implementation of EGR and it would also result in the desired lower combustion temperature. This way, the temperature will also be of bigger influence on the NO_x emission prediction.

Another part of the model that can be improved is the turbocharger. Due to the use of exhaust gas recirculation, in particular the high-pressure configuration, a part of the exhaust gas is already recirculated before it reaches the turbine and mixed with the fresh air after the compressor. This means that the mass flows through both the compressor and turbine decrease for increasing EGR rate. For this research the delivered turbine power was adjusted in such a way that the desired charge air pressure was reached. For further investigation of the influence of EGR it is recommended that the model is expanded with a variable geometry turbocharger or VGT. A VGT is designed to allow the effective aspect ratio of the the turbocharger to be altered if the conditions change. This way the desired compressor power would be automatically controlled for changing EGR rates.

The final recommendation for the model is the use of gas properties: the gas properties that are used in the model are now only dependent on their species(i.e. the air mass fraction) and not on the temperature. Because temperature is an important factor when it comes to the formation of NO_x, one should check how much using temperature dependent gas properties will affect the model and with that, the NO_x emissions.

To continue with the effects of the implementation of exhaust gas recirculation: the results show a decrease in the NO_x emissions for increasing EGR rate. If the data is compared to data from literature, the achieved results are in the same range. However as already mentioned above, there is no way to validate the achieved results. In order to do a validation, the results need to be compared to the emission data of (similar) marine diesel engines equipped with EGR. The model can then be tuned the match that specific engine and the predictions can then be validated. But altogether the first predictions look promising.

Bibliography

[1] G.H. Abd-Alla. Using exhaust gas recirculation in internal combustion engines: a review. *Energy Conversion and Management*, 43(8):1027–1042, 2002. ISSN 01968904. doi: 10.1016/S0196-8904(01)00091-7.

[2] H. Andersson and M. Hedvall. *Model based control of Air and EGR into a Diesel Engine*. Master thesis, Chalmers University of Technology, 2008. URL http://publications.lib.chalmers.se/records/fulltext/68134.pdf.

[3] A. Andreasen and K. Braüner Nyggard. Water-in-fuel emulsion as marine engine fuel for reduced NOx and particulate emissions. (1380), 2011.

[4] C Argachoy and A P Pimenta. Phenomenological Model of Particulate Matter Emission from Direct Injection Diesel Engines. *Journal of the Brazilian Society of Mechanical Sciences and Engineering*, XXVII (3):266–273, 2005. ISSN 16785878. doi: 10.1590/S1678-58782005000300008. URL http://www.scielo.br/scielo.php?script=sci{_}arttext{&}pid=S1678-58782005000300008{&}lng=en{&}nrm=iso{&}tlng=en.

[5] I. Asano. Measurement Systems for Diesel Exhaust Gas and Future Trends. pages 12–16, 2010. URL http://www.horiba.com/uploads/media/RE03-03-012-600.pdf.

[6] W. Balachandran, R. Beleca, N. Manivannan, and M. Abbod. Non-thermal Plasma System for Marine Diesel Engine Emissions Control. (January):1–9, 2014.

[7] A. Betz and G. Woschni. Energy conversion rate and rate of heat release of turbocharged diesel engines under transient conditions. *MTZ Motortechnische Zeitschrift*, 47(7-8):263–267, 1986.

[8] Caterpillar Motoren GmbH & Co. KG. M 32 C Low Emission Engine. Technical report, Caterpillar Motoren GmbH & Co. KG, Kiel, 2009. URL http://marine.cat.com/cda/files/953489/7/Brochure-MaKM32CLowEmissionEngine.pdf.

[9] Caterpillar Motoren GmbH & Co. KG. M 32 C Project Guide - Propulsion. Technical report, Caterpillar Motoren GmbH & Co. KG, Kiel, 2010. URL http://www.bmgs.com.tr/doc/GucSistemleri/Marin/Mak/M32CPropulsion.pdf.

[10] Caterpillar Motoren GmbH & Co. KG. Engine International Air Pollution Prevention Certificate, 2013.

[11] M. Cavadini. *1-D Simulations of EGR on a Marine Diesel Engine using GT-Power*. Master thesis, Swiss Federal Institute of Technology (ETH) Zurich, 2014. URL http://e-collection.library.ethz.ch/eserv/eth:47747/eth-47747-01.pdf.

[12] CIMAC Working group "Exhaust Emissions Control". Guide to Diesel Exhaust Emissions Control of NOx, SOx, Particulates, Smoke and CO2. 2008.

[13] E Codan and I Vlaskos. Turbocharging medium speed diesel engines with extreme Miller timing. *Proceedings of the 9th Turbocharging Conference, Dresden, Germany, September*, pages 23–24, 2004.

[14] E. Codan and J Wüthrich. Turbocharging solutions for EGR on large diesel engines. *ABB Download Center*, pages 1–22, 2013.

[15] E. Codan, S. Bernasconi, and H. Born. IMO III Emission Regulation: Impact on the Turbocharging System. 2010.

[16] N. De Nevers. *Air Pollution Control Engineering*. McGraw-Hill, New York, 2nd edition, 1995. ISBN 0071132732.

[17] DNV GL. IMO NOx Tier III requirements, 2015. URL https://www.dnvgl.com/news/imo-nox-tier-iii-requirements-to-take-effect-on-january-1st-2016-51970.

[18] K.G. Evangelos. *Emission Abatement Techniques for Marine Diesel Engines*. Dissertation thesis, National and Technical University of Athens, 2012.

[19] V. Eyring, H. W. Köhler, A. Lauer, and B. Lemper. Emissions from international shipping: 2. Impact of future technologies on scenarios until 2050. *Journal of Geophysical Research D: Atmospheres*, 110(17): 183–200, 2005. ISSN 01480227. doi: 10.1029/2004JD005620.

[20] S. Galindo López. *Three-Zone in-cylinder process model for DI diesel engines*. Master thesis, Delft University of Technology, 2014. URL https://repository.tudelft.nl/islandora/object/uuid{%}3A3eba6c98-1945-4c61-99bb-3af0f2a0ca4a?collection=education.

[21] R.D. Geertsma. *Diesel Engine A3 model*. Working paper, Delft University of Technology, 2016.

[22] A.A. Hairuddin, A.P. Wandel, and T. Yusaf. An Introduction to a Homogeneous Charge Compression Ignition Engine. *Journal of Mechanical Engineering and Sciences*, 7(February):1042–1052, 2014. ISSN 22894659. doi: 10.15282/jmes.7.2014.3.0101. URL http://jmes.ump.edu.my/images/Volume{_}7/3Hairuddinetal.pdf.

[23] G.S. Hebbar. NOx from diesel engine emission and control strategies - a review. *International Journal of Mechanical Engineering and Robotics Research*, 3(4):471–482, 2014.

[24] J.B. Heywood. *Internal combustion engines fundamentals*. McGraw-Hill series in Mechanical Engineering, New York, 1st edition, 1988. ISBN 0-07-028637-x.

[25] M. Imperato. *Studies on the reduction of nitrogen oxides emission in a large-bore diesel engine*. Doctoral thesis, Aalto University, 2016.

[26] International Maritime Organisation. Nitrogen Oxides (NOx) - Regulation 13, 2016. URL http://www.imo.org/en/OurWork/environment/pollutionprevention/airpollution/pages/nitrogen-oxides-(nox)-\T1\textendash-regulation-13.aspx.

[27] H. Jääskeläinen and M.K. Khair. Exhaust Gas Recirculation, 2016. URL https://www.dieselnet.com/tech/engine{_}egr.php.

[28] Jumbo Maritime. Jumbo Maritime Company. URL https://www.jumbomaritime.nl/en/company/.

[29] C. Kannan and T. Vijayakumar. Influence of Exhaust Gas Recirculation, and Injection Timing on the Combustion, Performance and Emission Characteristics of a Cylinder Head Porous Medium Engine. *Journal of Thermodynamics*, 2015:1–10, 2015. ISSN 16879252 16879244. doi: 10.1155/2015/927896. URL http://dx.doi.org/10.1155/2015/927896.

[30] A. Kedzierski. Sulphur in Marine Fuels, jan 2012. URL https://www.transportenvironment.org/publications/sulphur-marine-fuels.

[31] H. Klein Woud and D. Stapersma. *Design of Propulsion and Electric Power Generation Systems*. IMarEST, London, reprint 20 edition, 2002.

[32] M. I. Lamas and C. G. Rodríguez. Emissions from marine engines and NOx reduction methods. *Journal of Maritime Research*, 9(1):77–82, 2012. ISSN 16974840.

[33] Y. Linden. *NO-emission prediction in a Diesel Engine: using a two zone in-cylinder model*. Master thesis, Delft University of Technology, 2017. URL https://repository.tudelft.nl/islandora/object/uuid{%}3Aa67734ee-bb18-4be7-b746-15510b5a0164?collection=education.

[34] X. Llamas and L. Eriksson. A Model of a Marine Two-Stroke Diesel Engine with EGR for Low Load Simulation. In *9th EUROSIM Congress*, page 6, Linköping, 2016. Linköping University, Sweden, Department of Electrical Engineering. URL http://urn.kb.se/resolve?urn=urn:nbn:se:liu:diva-136804.

[35] Lloyd's Register. Understanding exhaust gas treatment systems - Guidance for shipowners and operators. Technical report, Lloyd's Register, London, 2012.

[36] Lloyd's Register of shipping. Emissions of Nitrogen Oxides from Marine Diesel Engines. 2002. URL papers2://publication/uuid/E40342D4-15C1-4C90-97E8-D0794DD63C2A.

[37] M.A. Loonstijn. *Diesel A-M (A-Modular) Model Proposal: Expanding the Diesel A model for advanced turbocharging capabilities*. Working paper, Delft University of Technology, Delft, 2017.

[38] MAN Diesel & Turbo. Humid Air Motor - Technology for green profits. 2011.

[39] MAN Diesel & Turbo. MAN B&W Two-stroke Marine Engines: Emission Project Guide for Marpol Annex VI Regulations. Technical report, MAN Diesel & Turbo, Copenhagen, 2017.

[40] Marine Environment Protection Committee. Annex 14 - MEPC.177(58) - Amendments to the NOx Technical Code 2008, 2010.

[41] M. Marissal and M. Andreasen. *Implementation of Exhaust Gas Recirculation for Double Stage Waste Heat Recovery System on Large Container Ship*. Master thesis, Aalborg University School of Engineering and Science, 2014.

[42] MathWorks. Statistics and Machine Learning Toolbox- User's Guide R2018a. Technical report, The MathWorks, Inc., Natick, 2018.

[43] G. Merker, C. Schwarz, G. Stiesch, and F. Otto. *Simulating Combustion - Simulation of combustion and pollutant formation for engine-development*. Springer-Verlag Berlin Heidelberg, 1st edition, 2006. ISBN 9780874216561. doi: 10.1007/s13398-014-0173-7.2.

[44] K. Muric. *Modeling of NOx formation in heavy duty engines*. Master thesis, Lund University, 2011.

[45] D. Nam. *How to reduce emission of nitrogen oxides [NOx] from marine diesel engines in relation to Annex VI*. Dissertation, World Maritime University Malmö, 2000.

[46] H. Patel Sagar, P. Gaurav Rathod, and M. Patel Tushar. Experimental investigation of diesel engine with water injection system on emission parameters \n. *IOSR Journal of Mechanical and Civil Engineering (IOSR-JMCE)*, 11(2):47–51, 2014. URL http://www.iosrjournals.org/iosr-jmce/papers/vol11-issue2/Version-8/H011284751.pdf.

[47] J. Plester. Dirty diesel: why ships are the worst offenders, may 2017. URL https://www.theguardian.com/uk-news/2017/may/18/dirty-diesel-ships-worst-offenders-pollutionwatch.

[48] S. Reifarth. *EGR-Systems for Diesel Engines*. Licentiate thesis, KTH Royal Institute of Technology in Stockholm, 2010.

[49] G. Rouleau. Why you should never break a continuous algebraic loop with a Memory block, 2015. URL https://blogs.mathworks.com/simulink/2015/07/18/why-you-should-never-break-an-algebraic-loop-with-with-a-memory-block/.

[50] P.J.M. Schulten. *The Interaction Between Diesel Engines, Ship And Propellers During Manoevring*. Doctoral thesis, Delft University of Technology, 2005. URL https://repository.tudelft.nl/islandora/object/uuid{%}3A4989126e-ca6f-44e0-9cde-317584567680?collection=research.

[51] P.J.M. Schulten and D. Stapersma. Mean Value Modelling of the Gas Exchange of a 4-stroke Diesel Engine for Use in Powertrain Applications. *SAE 2003 World Congress & Exhibition*, (2003-01-0219), 2003. doi: https://doi.org/10.4271/2003-01-0219.

[52] C. Schwerdt. *Modelling NOx-Formation in Combustion Processes*. Master thesis, Lund University, 2006.

[53] Ibrahim S. Seddiek and Mohamed M. Elgohary. Eco-friendly selection of ship emissions reduction strategies with emphasis on SOx and NOx emissions. *International Journal of Naval Architecture and Ocean Engineering*, 6(3):737–748, 2014. ISSN 20926790. doi: 10.2478/IJNAOE-2013-0209. URL http://dx.doi.org/10.2478/IJNAOE-2013-0209.

[54] L.C. Stan and D.E. Mitu. Simplified mechanism used to estimate the NOx emission of Diesel engine. In *2nd International Conference on Manufacturing Engineering, Quality and Production Systems*, pages 61–64, 2010. ISBN 9789604742202. URL http://www.wseas.us/e-library/conferences/2010/Constantza/MEQAPS/MEQAPS-11.pdf.

[55] D Stapersma. *Diesel Engines Volume 1 Performance Analysis*, volume 1. Netherlands Defence Academy & Delft University of Technology, 8th edition, 2010. ISBN 0693485000.

[56] D Stapersma. *Diesel Engines Volume 4 Emissions and Heat transfer*, volume 4. Netherlands Defence Academy & Delft University of Technology, 6th edition, 2010. ISBN 0693485000.

[57] D Stapersma. *Diesel Engines Volume 6: Thermodynamical Principles II*, volume 6. 2010. ISBN 0693485000.

[58] S.R. Turns. *An Introduction to Combustion: Concepts and Applications*. McGraw-Hill series in Mechanical Engineering, 2nd edition, 2000. ISBN 0072300965.

[59] T. Ueda. Development of Low Pressure Exhaust Gas Recirculation System for Exhaust Gas Emission Control of Mitsubishi UE Diesel Engine. *Journal of the JIME*, 50(06):1–12, 2015.

[60] M.A.J. van Riet. *The Reduction of NOx and SOx emissions in Marine Diesel Engines: A literature study*. Research thesis, Delft University of Technology, 2017.

[61] S. Verhelst, J. Vancoillie, K. Naganuma, M. De Paepe, J. Dierickx, Y. Huyghebaert, and T. Wallner. Setting a best practice for determining the EGR rate in hydrogen internal combustion engines. *International Journal of Hydrogen Energy*, 38(5):2490–2503, 2013. ISSN 03603199. doi: 10.1016/j.ijhydene.2012.11.138.

[62] C. Wik and S. Niemi. Low emission engine technologies for future tier 3 legislations - options and case studies. *Journal of Shipping and Trade*, 1(1):3, 2016. ISSN 2364-4575. doi: 10.1186/s41072-016-0009-z. URL http://jshippingandtrade.springeropen.com/articles/10.1186/s41072-016-0009-z.

[63] H. Winnes and E. Fridell. Particle emissions from ships: Dependence on fuel type. *Journal of the Air and Waste Management Association*, 59(12):1391–1398, 2009. ISSN 21622906. doi: 10.3155/1047-3289.59.12.1391.

[64] D. Woodyard. *Pounder's Marine Diesel Engines and Gas Turbines*. Elsevier Butterworth-Heinemann, Oxford, 8th editio edition, 2004. ISBN 0750689846. doi: 10.1016/B978-0-7506-8984-7.00027-8.

[65] E. A. Yfantis, T. C. Zannis, Ioannis Katsanis, Roussos G. Papagiannakis, Petros Siritoglou, and Athanasios Lamprou. Miller Cycle Application in Marine Diesel Engines for NOx Reduction : A Review. *ASHRAE International Conference on Energy and Environment in Ships*, 2015.

[66] E. A. Yfantis, T. C. Zannis, E. G. Pariotis, J. S. Katsanis, and I. Roumeliotis. NOx Reduction Technologies for Marine Diesel Engines - Operational, Environmental and Economical Aspects. In *International Conference "Green transportation 2016"*, page 45, Athens, 2016.

[67] X.C. Yu, Z.C. Liu, Z.S. Wang, and H.L. Dou. Effects of EGR Rate and Excess Air Ratio on the Combustion Characteristics of Compressed Natural Gas Engine. In X.C. Yu, Z.C. Liu, Z.S. Wang, and H.L. Dou, editors, *International Conference on Transportation, Mechanical, and Electrical Engineering, TMEE 2011*, pages 1177–1180, Changchun, 2011. ISBN 9781457717017. doi: 10.1109/TMEE.2011.6199415.

[68] H. Zhao. *Advanced Direct Injection Combustion Engine Technologies and Development*. Woodhead Publishing, 1st edition, 2009.

[69] M. Zheng, G.T. Reader, and J.G. Hawley. Diesel engine exhaust gas recirculation - A review on advanced and novel concepts. *Energy Conversion and Management*, 45(6):883–900, 2004. ISSN 01968904. doi: 10.1016/S0196-8904(03)00194-8.

A

Engine description

The following pages show the most important data extracted from the Acceptance Test Record and the EIAPP report of the parent engine of the 9M 32 C marine diesel engine from Caterpillar Motoren GmbH & CO. KG.

The following records are shown:

- Figure A.1:Emission Test Report (Engine Family/Group information)
- Figure A.2: Emission Test Report (Engine information)
- Figure A.3:Diesel Engine Acceptance Test Record
- Figure A.4: Emission Test Report M32C Ambient and Gaseous Emissions Data
- Figure A.5: Emission Test Report M32C Engine Test Data

Emission Test Report No. M32C-LE

Engine Family / Group Information

Engine Group Information	
Combustion cycle	4 - stroke
Cooling medium	water
Individual cylinder displacement	38,60 ltr.
Cylinder number and configuration	6, 8, 9 inline
Method of air aspiration	pressure charged
Fuel type	destillate
Combustion chamber type	open chamber
Nominal compression ratio	16,8
Fuel system type	single element
Miscellanous features	
Electr. injection control	no
Variable injection timing	no
Variable turbocharger geometrie	no
Variable valve timing	no
Charge cooling system	yes
Exhaust gas recirculation	no
Water injection / emulsion	no
Air injection	no
Exhaust aftertreatment	no
Exhaust aftertreatment type	-
Dual fuel	no

Engine Group Information	
Family / Group Identification	M32C-LE2
Method of pressure charging	single line
Charge air cooling system	water
Max. rated power per cylinder	500 kW
Max.permitted range of derating	80%of max rated power per cylinder
Rated speed	600 rpm
max. rated speed	620 rpm
Start of delivery (fuelpump)	5,5 (-1,0) ° CA BTDC

Figure A.1: Emission Test Report (Engine Family/Group information)[10]

Emission Test Report **No. M32C-LE**

Engine Information

Engine		
Manufacturer	Caterpillar Motoren GmbH	
Engine type	6 M 32 C	
Group identification	M32C-LE2	
Serial number	38729	
Rated speed	600	rpm
Rated power	3000 / 2880	kW
Intermediate speed	-	rpm
Max. torque at intermediate speed	-	Nm
Cylinder number and configuration	6,8,9 inline	
Bore	320	mm
Stroke	480	mm
Mean effective pressure at ratet power	25,9 / 24,8	bar
Max. cylinder pressure at ratet power	204	bar
Auxiliaries	2 pumps	

Specified ambient conditions		
Max. Seawater temperature	38	°C
Max. Charge air temperature, if applicable	45	°C
Cooling system spec., intermediate cooler	yes	
Cooling system spec., charge air stages	2 stage	
Low / high temp.cooling system setpoints	30 / 90	°C
Maximum inlet depression	25	mbar
Maximum exhaust backpressure	30	mbar
Fuel oil specification	Gas oil	
Fuel oil temperature	40	°C
Lubricating oil specification	see engine documentation, chapter "Operating Media"	

Application / Intendet for	
Customer	
Final application/ installation, Ship	
Final application/ installation, Engine	main

Emissions test results				
Cycle		D 2	E 2	
NOx	600 1/min	9,8	9,6	g/kWh

Figure A.2: Emission Test Report (Engine information)[10]

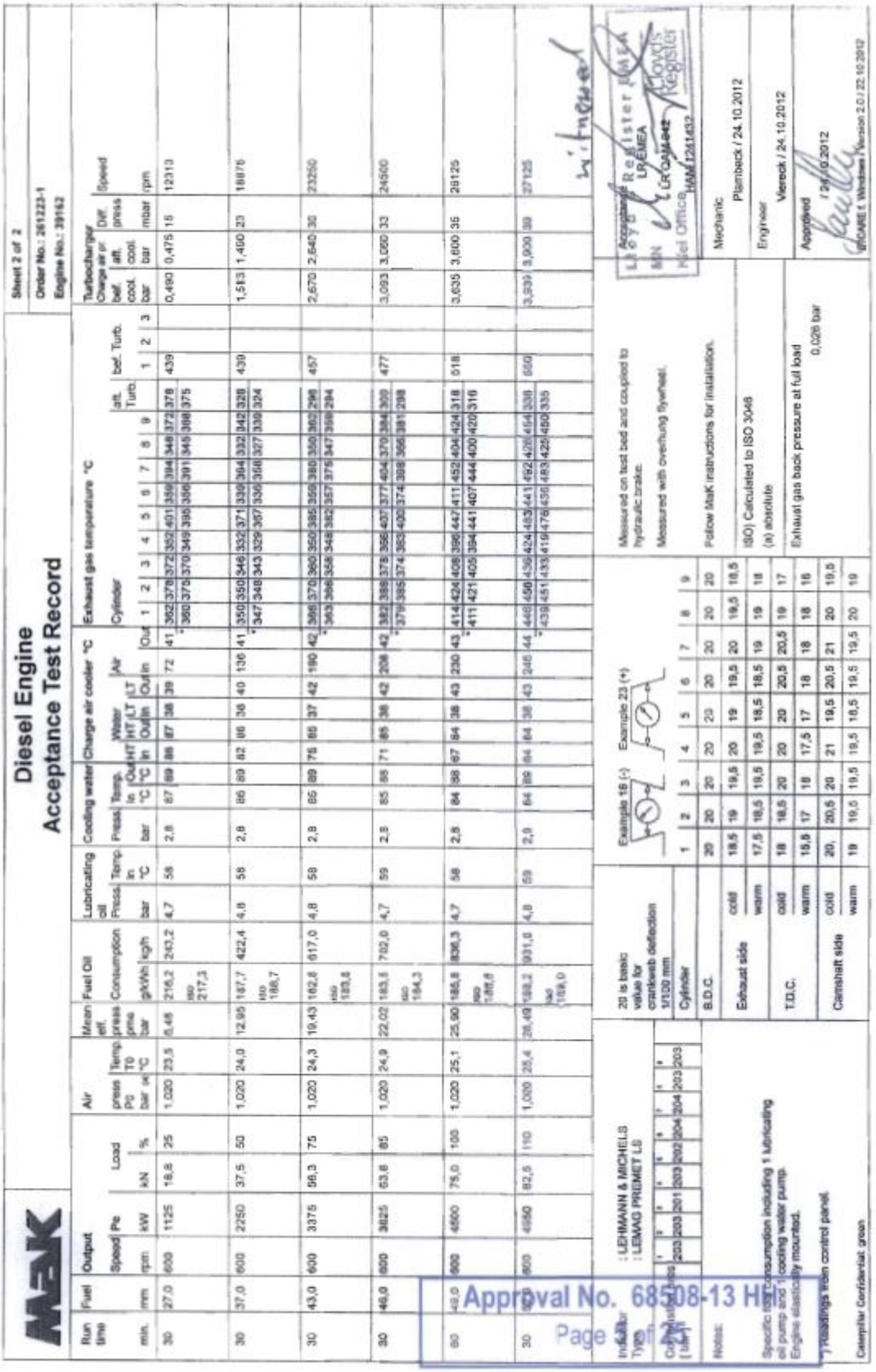

Figure A.3: Diesel Engine Acceptance Test Record[10]

Emission Test Report M32C LE Ambient and Gaseous Emissions Data

Mode		1	2	3	4	5
Power / Torque	%	100	75	50	25	10
Speed	%	100	100	100	100	100
Time at beginning of mode		14:28	14:47	15:08	15:28	15:47
Ambient Data						
Atmosph. pressure	mbar	1021	1021	1022	1021	1021
Intake air temp.	°C	30,7	31,9	32,4	32,3	31,5
Intake air humidity	%	19,4	18	17,5	17,5	18,4
Atmospheric factor (fa)		1,013	1,018	1,021	1,020	1,016
Gaseous Emissions Data						
NOx conc. wet	ppm	875,9	898,7	913	681,6	822,3
CO conc. dry	ppm	43,4	38,9	39,5	87,4	132,5
CO2 conc. dry	%	5,84	5,63	5,66	5,48	4,11
O2 conc. dry	%	12,92	13,20	13,16	13,41	15,31
HC conc. wet	ppm	143,2	152,2	215,1	264,9	266
NOx hum.corr.factor		0,959	0,966	0,971	0,973	0,969
Dry/wet corr.factor		0,948	0,95	0,95	0,951	0,963
NOx mass flow	kg/h	26,383	21,199	14,653	6,319	5,20
CO mass flow	kg/h	0,787	0,55	0,377	0,482	0,507
CO2 mass flow	kg/h	1664	1249,5	850	475,2	247,2
O2 mass flow	kg/h	2675	2129,2	1437	845	669,3
HC mass flow	kg/h	1,358	1,122	1,074	0,762	0,524
SO2 mass flow	kg/h	-	-	-	-	-
NOx specific	g/kWh	9,55	10,157	10,479	9,018	18,634

Figure A.4: Emission Test Report M32C Ambient and Gaseous Emissions Data[10]

Emission Test Report No. M32C LE Engine Test Data

Mode		1	2	3	4	5
Power / Torque	%	100	75	50	25	10
Speed	%	100	100	100	100	100
Time at beginning of mode		14:28	14:47	15:08	15:28	15:47
Engine Data						
Speed	rpm	600	600	600	600	600
Power	kW	2880	2160	1440	720	288
Mean eff. pressure	bar	24,87	18,65	12,43	6,22	2,49
Fuel rack	mm	48,4	44,3	39,8	31,7	25,1
Uncorr.spec.fuel cons.	g/kWh	184,3	184,5	189	211,1	275
Fuel flow	kg/h	530,7	398,5	271,5	152,0	79,2
Air flow	kg/h	-	-	-	-	-
Firing pressure	bar	201	-	-	-	-
End of needlelift (Noz)	° CA	-	-	-	-	-
Charge air pressure	bar	3,51	2,48	1,4	0,51	0,14
Turbo speed	rpm	31040	27520	22400	15280	10040
Exhaust flow (gexhw)	kg/h	19800	15392	10421	6006,5	4115
Exhaust temp.	°C	291	294	321	335	259
Exhaust backpress.	mbar	25				
LT Coolant temp. in	°C	37	37	38	38	38
LT Coolant temp. out	°C	40	39	39	38,5	39
HT Coolant temp. in	°C	75	80	84	87	87
HT Coolant temp. out	°C	87	87	87	87	87
Cyl.Coolant pressure	bar	3,7	3,7	4	3,6	3,7
Temp. intercooled air	°C	43	41	40	39	38
Lubricant temp.	°C	56	54	54	56	53
Lubricant pressure	bar	4,4	4,4	4,4	4,5	4,5
Inlet depression	mbar	-	-	-	-	-

Figure A.5: Emission Test Report M32C Engine Test Data[10]

B

Goodness-of-Fit Statistics

This appendix provides some information on the Goodness-of-Fit statistics that are used in chapter 3. The created fits have to evaluated on certain aspects. MATLAB provides a toolbox and functions for fitting curves and surfaces to data. With this Curve Fitting Tool different analyses can be conducted using linear and non-linear models. After fitting the data with one or more models the so-called goodness-of-fit needs to be evaluated. Of course, the first step in this is a visual examination of the plotted curve, but this also needs to be quantified. This is where the goodness-of-fit statistics come in. The following goodness-of-fit statistics can be used for the fits:

- The sum of squares due to error (SSE)
- R-square
- Adjusted R-square
- Root mean squared error (RMSE)

These four statistics will further be evaluated in the following sections.

B.1. The sum of squares due to error (SSE)

The Sum of Squares due to Error is a statistic that measures the total deviation of the response values from the fit to the actual response values. It can also be called summed square of residuals and can be labelled as SSE. It is described as in equation B.1:

$$SSE = \sum_{i=1}^{n} w_i (y_i - \hat{y}_i)^2 \tag{B.1}$$

The sum of squares due to error can take values from 0 to infinity, where a value closer to 0 indicates that the model has a smaller random error component, meaning that the fit will be more useful for prediction. So the aim is to get the SSE value as close to 0 as possible, while also maintaining acceptable values in the other goodness-of-fit statistics.

B.2. R-Square

The R-square statistic measures how successful the fit is in explaining the variation of the data. This means that the R-square is the square of the correlation between the response values and the fitted response values and can also be called the square of the multiple correlation coefficient and the coefficient of multiple determination. It is defined as the ratio of the sum of squares of the regression (SSR) and the total sum of squares (SST), so these will be defined first in equations B.2 and B.3. The definition of R-square can be seen in equation B.4.

$$SSR = \sum_{i=1}^{n} w_i (\hat{y}_i - \bar{y})^2 \tag{B.2}$$

$$SST = \sum_{i=1}^{n} w_i (y_i - \bar{y})^2 \tag{B.3}$$

$$R - square = \frac{SSR}{SST} = 1 - \frac{SSE}{SST} \tag{B.4}$$

The values that R-square can take are limited to any value between 0 and 1. If the value is closer to 1 it indicates that a greater proportion of variance is accounted for by the model. As an example, if R-square takes on a value of 0.91 it means that the fit explains 91% of the total variation in the data about the average. A way to increase the value of R-square the number of fitted coefficients in the model need to be increased. This is of course not always possible with the given data and it may also not improve the fit in a practical sense. To avoid this from happening, one can use the degrees of freedom adjusted R-square method, which will be described below.

B.3. Degrees of freedom Adjusted R-Square

This goodness-of-fit statistic uses the R-square statistic as it is defined above and adjusts it based on the residual degrees of freedom. These residual degrees of freedom can be defined as the number of response values n minus the number of fitted coefficients m estimated from the response values. The residual degrees of freedom are defined in equation B.5:

$$\upsilon = n - m \tag{B.5}$$

υ describes the number of independent pieces of information involving the n data points that are required to calculate the sum of squares. The adjusted R-square statistic is a good indicator of the fit quality when to nested models are compared. Nested means a series of models each of which adds additional coefficients to the previous model. The adjusted R-square statistic is described by equation B.6

$$adjusted\ R - square = 1 - \frac{SSE(n-1)}{SST(\upsilon)} \tag{B.6}$$

This statistic can take on any value less than or equal to 1. Just as with the regular R-square statistic a value closer to 1 indicates a better fit.

B.4. Root Mean Squared Error (RMSE)

The Root Mean Squared Error is also known as the fit standard error and the standard error of the regression. It is an estimate of the standard deviation of the random component in the data and it can be described by equation B.7

$$RMSE = s = \sqrt{MSE} \tag{B.7}$$

where MSE is the mean square error or the residual mean square.

$$MSE = \frac{SSE}{\upsilon} \tag{B.8}$$

Like with the SSE, an MSE value that is closer to 0 indicates a better fit that is more useful for prediction.

C

Simulation errors

The following pages give a more profound explanation of the first simulation results. These were not as expected, because the maximum combustion temperature increased for increasing EGR rate, while it should actually decrease with increasing EGR rate. The temperature should decrease, because exhaust gas is recirculated back into the engine and exhaust gas has a higher specific heat than the regular intake air of an engine. A higher specific heat means that more energy is needed to warm up a certain amount of mass by a certain temperature difference. This has already be mentioned in section 3.5.3.

When first implementing the EGR configuration into the existing diesel engine model the the low-pressure configuration showed an unexpected change in maximum combustion temperature. This can be seen in figure C.1.

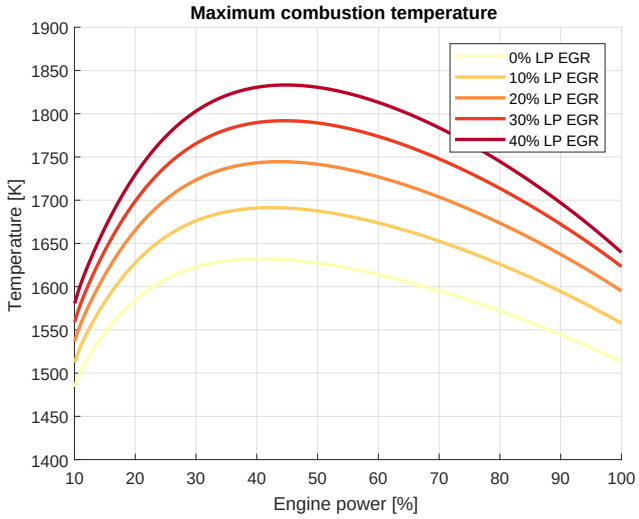

Figure C.1: Maximum combustion temperature versus engine power [K]

The figure shows the maximum combustion temperature, T_4, plotted against the engine power. The shown temperatures are for different EGR ratios, varying from 0% EGR to 40%. The working principle of EGR is based on the decrease of the oxygen concentration and an increase in the heat capacity of the mixture in the combustion chamber. Therefore the temperature is expected to decrease instead of increase.

To make the model work correctly it should be investigated why the temperature changes the way it does and this will be done by retracing the steps prior to the final computation of the combustion temperature. One of the most important factors that influences the temperature in the combustion chamber are the heat release rates. The heat release rate is divided in three parts, namely the heat release at constant volume, heat release

at constant pressure and heat release at constant temperature. All of these heat release rate are dependent on the trapped mass at the start of compression, m_1. On its turn, the trapped mass is dependent on the charge air temperature, T_c, and the charge air pressure, p_c, as can be seen in the equation below:

$$m_1 = \frac{p_1 \cdot V_1}{R \cdot T_1} \tag{C.1}$$

Where it is assumed that $p_1 = p_c$, $T_1 = T_c$ and R, the gas constant, is a constant. The temperature T_c is already prescribed and set to a certain value, in this case 315K. This means that both the regular intake flow and the recirculated exhaust gas flow are both cooled down to that temperature, meaning that the charge temperature is also considered constant. The only thing left that could be of influence for the trapped was is the charge air pressure. The charge air pressure is plotted in figure C.2:

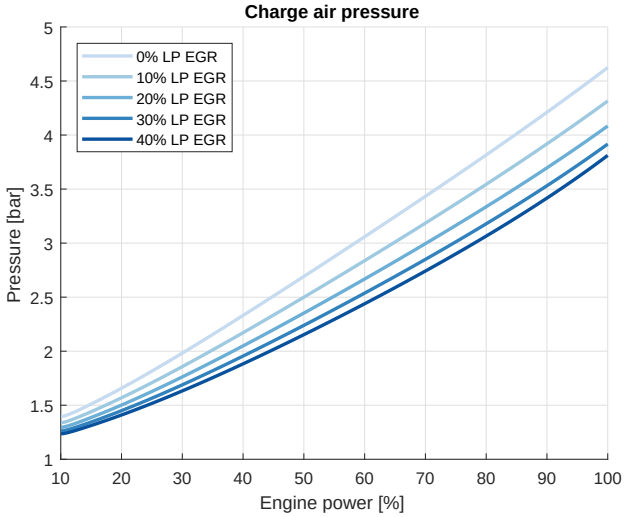

Figure C.2: Charge air pressure versus engine power [bar]

What can immediately be seen in the figure is that the charge air pressure changes for different EGR rates. For 40% EGR the charge air pressure is almost 1 bar lower than for 0% EGR. This of course has a huge influence on the trapped mass m_1, but also on the maximum combustion pressure and the pressure in the outlet receiver. A lower charge air pressure results in a lower combustion pressure and also a lower outlet receiver pressure. The reason for the lower combustion pressure and lower outlet receiver pressure is that with a lower charge air pressure, a lower amount of mass is drawn into the combustion chamber.

The reason for the higher combustion temperature can be traced back to the amount of trapped mass in the combustion chamber. A part of the released heat will of course be absorbed by the surrounding mixture of gases. But if the amount of mass in the combustion chamber is smaller, due to the lower charge air pressure, the released heat will be absorbed by a smaller amount of mixture. Therefore the temperature of the mixture will be higher, despite the slightly higher heat capacity.

In order to compare the different EGR rates on the same basis and evaluate their influence on the maximum combustion temperature, one must make sure that all the bases for the comparison are the same. The first solution is to ensure that the charge air pressure is the same for the different EGR rates.

The charge air pressure is dependent on the amount of power that the compressor can deliver. The compressor receives its power directly from the turbine. How the power of turbine is computed has already been introduced in section 5.6.2. One of the main factors influencing the mass flow through the turbine and thus also the power delivered by the turbine is the pressure ratio over the turbine. Figure C.3 shows the pressure ratios of both the compressor and turbine.

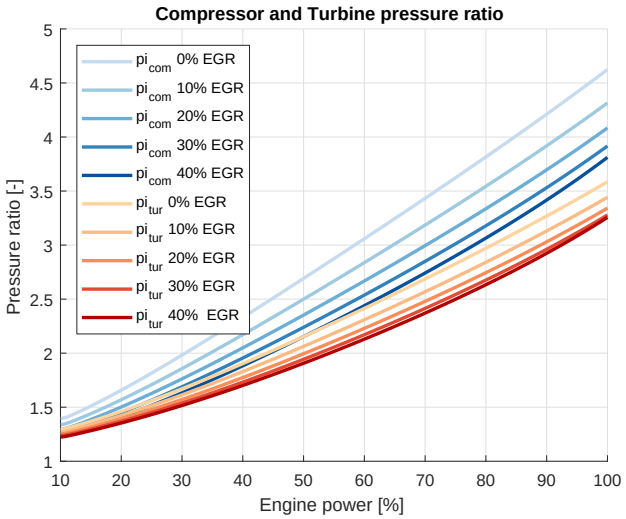

Figure C.3: Compressor and Turbine pressure ratio's versus engine power for different EGR rates [-]

The pressure ratio over the compressor is defined as the pressure after the compressor, p_b or p_c, over the pressure before the compressor, the ambient pressure p_a in this case. For the turbine the same rule applies, the ratio is given as p_d over p_e, where p_e is equal to the ambient pressure. So what is seen in the figure is to be expected: the ambient pressure is a constant and both the charge air pressure and outlet receiver pressure decrease for increasing EGR rates, resulting in lower pressure ratios.

What is required for maintaining a high compression ratio is more power to achieve this higher pressure. Because the compressor receives its power directly from the turbine a solution would be to increase the power of the turbine. Because the rest of the simulation needs to remain the same, it has been decided that the only thing to be altered is the output power of the turbine. Because an increasing turbine power is necessary with increasing EGR ratio, the amount of extra power is made dependent on the EGR ratio, as can be seen in the following equation:

$$P^*_{tur} = P_{tur} \cdot \left(1 + \frac{EGR_{ratio}}{100\%}\right) \tag{C.2}$$

Where the EGR ratio can vary between 0% and 40%. After that the air excess ratio λ comes to close to the smoke limit of the engine. The effect of the increased turbine power on the charge air pressure can be seen in figure C.5. In order to compare the old model results with the new model results, the old results have been placed next to the new results. The graphs on the left show the old results and the graphs on the right show the new improved results.

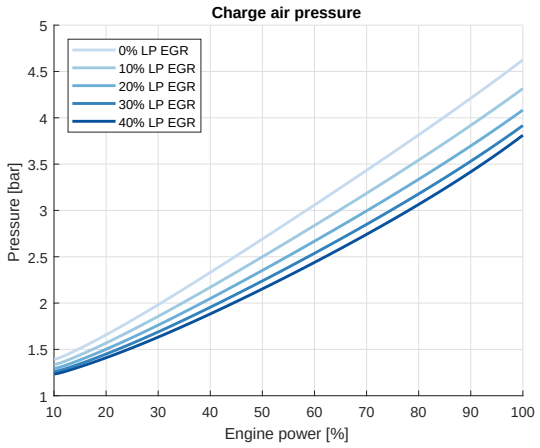

Figure C.4: Charge air pressure versus engine power [bar]

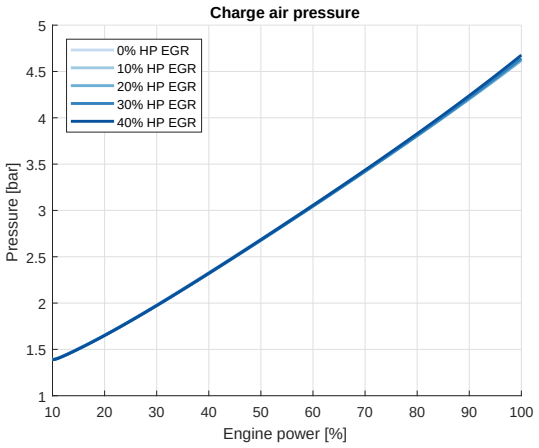

Figure C.5: Charge air pressure versus engine power [bar]

What can immediately be seen is that the charge air pressure is almost constant for all the different EGR ratios. The graphs are only diverging a little at the higher engine loads. Where the deviation was almost 20% at first, the improved model brought it down to just 1%. Now that the pressure is almost constant for the different ratios it is time to look at the influence of this pressure on the maximum combustion temperature T_4, which can be seen in figure C.7:

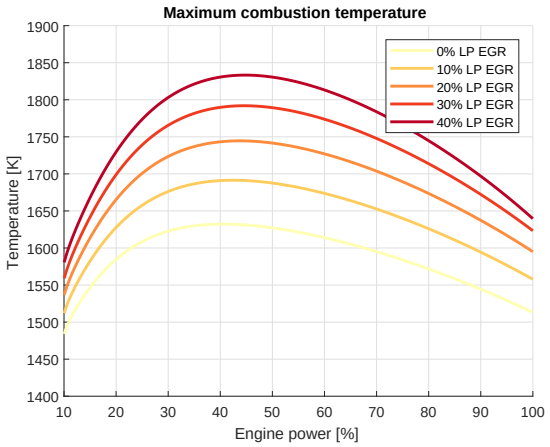

Figure C.6: Maximum combustion temperature versus engine power [K]

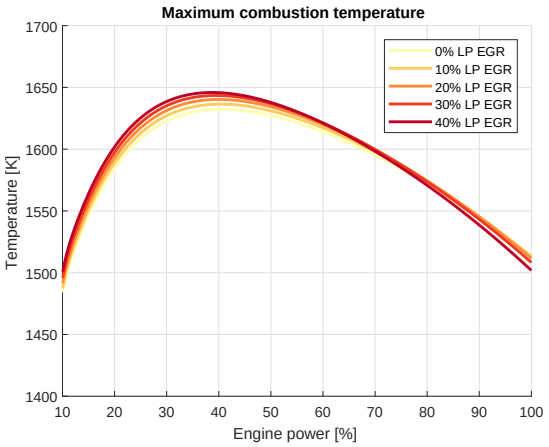

Figure C.7: Maximum combustion temperature versus engine power [K]

Just as with the charge air pressure, the temperature difference deviates much less than before. Where the temperature deviated more than 11% at first, the new improved model reduced the deviation to less than 1%. However, this is still not what was expected to happen, because the maximum combustion temperature was expected to decrease. However, this will be a part of the results and will therefore be evaluated in chapter 6

D

Additional NO_x emission predictions

Because the results chapter (6) otherwise would have become to long, it has been decided that a part of the NO_x emission predictions was to be enclosed in the appendices. This appendix shows the predicted emissions for a couple of the NO_x fits. The same structure is maintained as in chapter 6, meaning that the kg/h fits will be discussed first, followed by the g/kWh fits.

D.1. kg/h emission predictions

The two remaing kg/h emission predictions are derived from the fits that are dependent on the base parameter $\dot{m}_{fresh,x}$ and λ and the other one is based on $\dot{m}_{fresh,x}$ and T_{max}/T_3.

kg/h NO_x prediction using $\dot{m}_{fresh,x}$ and λ

The first prediction to be discussed is with λ. The figures below, D.1 and D.2, show the NO_x emission predictions.

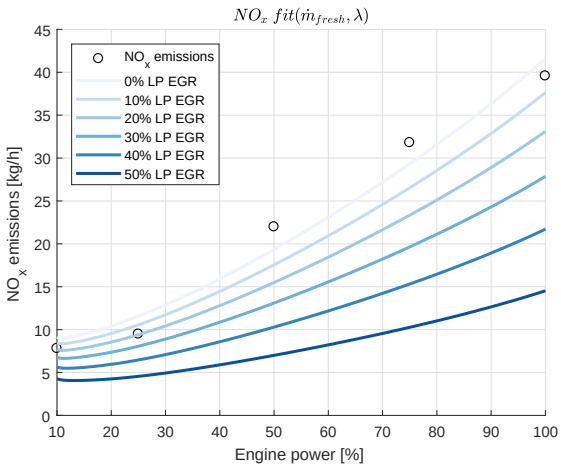

Figure D.1: kg/h NO_x emission prediction as a function of $\dot{m}_{fresh,x}$ and λ

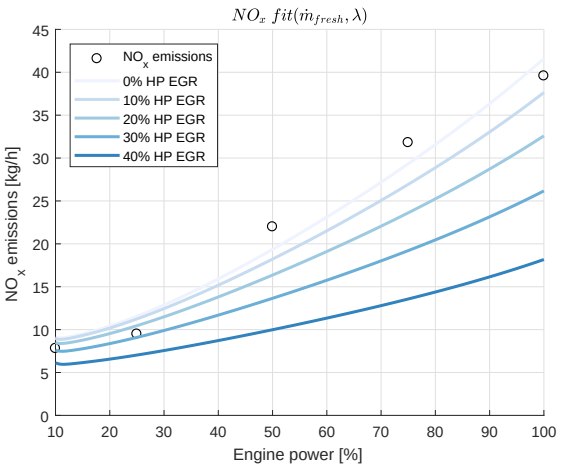

Figure D.2: kg/h NO_x emission prediction as a function of $\dot{m}_{fresh,x}$ and λ

What can be noticed from these predictions, in comparison with the prediction dependent only on $\dot{m}_{fresh,x}$, is that the decrease in NO_x emissions is bigger. For a low-pressure EGR rate of 50%, the emissions decrease from over $40kg/h$ to less than $15kg/h$. The same occurs for the high-pressure configuration. The decrease is more than 50% for a 40% EGR rate.

kg/h NO_x prediction using $\dot{m}_{fresh,x}$ and T_{max}/T_4

The following prediction is dependent on $\dot{m}_{fresh,x}$ and T_{max}/T_4 and can be seen in figures D.3 and D.4 for the low-pressure and high-pressure EGR configuration respectively.

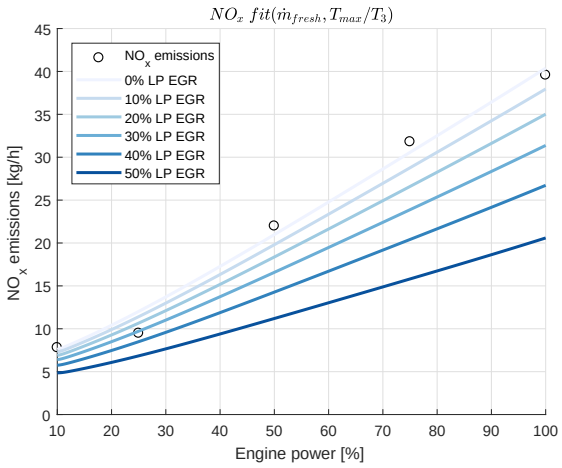

Figure D.3: kg/h NO_x emission prediction as a function of $\dot{m}_{fresh,x}$ and T_{max}/T_3

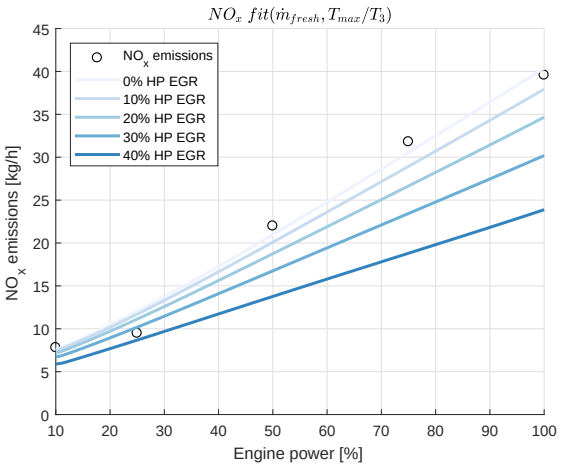

Figure D.4: kg/h NO_x emission prediction as a function of $\dot{m}_{fresh,x}$ and T_{max}/T_3

The effect of the temperature on the NO_x prediction is smaller than the effect of λ, because the decrease in emissions is around 50%. Chapter 6 already showed that the variance in temperature for increasing EGR rates is really small, compared to the decrease in air excess ratio. So this explains the slightly higher NO_x prediction when the temperature ratio is used.

D.2. g/kWh emission predictions

Following the two kg/h emission predictions, the g/kWh emission predictions are next. Just as the kg/h predictions, the predictions that still need to be discussed are those dependent on $\dot{m}_{fresh,x}$, P_B and λ and on the other hand $\dot{m}_{fresh,x}$, P_B and T_{max}/T_4.

g/kWh NO_x prediction using $\dot{m}_{fresh,x}$, P_B and λ

The first emission fits to be shown are the g/kWh fits dependent on $\dot{m}_{fresh,x}$, P_B and λ. The results of the predictions can be seen in the following figures.

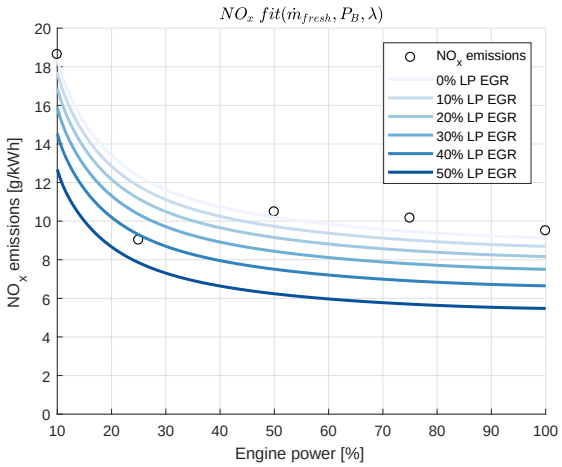

Figure D.5: g/kWh NO_x emission prediction as a function of $\dot{m}_{fresh,x}$, P_B and λ

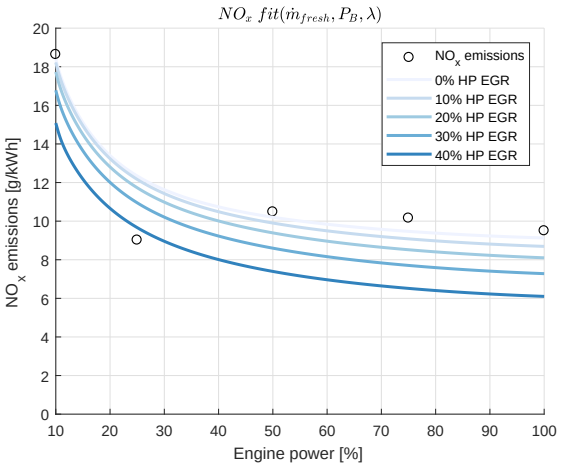

Figure D.6: g/kWh NO_x emission prediction as a function of $\dot{m}_{fresh,x}$, P_B and λ

g/kWh NO_x prediction using $\dot{m}_{fresh,x}$, P_B and T_{max}/T_3

The final predictions are done with $\dot{m}_{fresh,x}$, P_B and the temperature ratio T_{max}/T_3 as engine parameters. The resulting predictions are shown in figures D.7 and D.7.

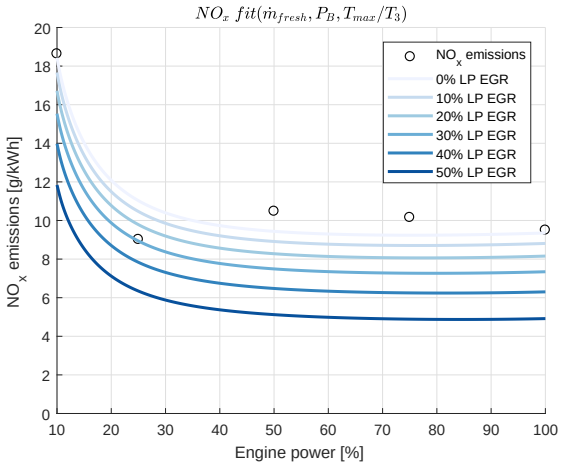

Figure D.7: g/kWh NO_x emission prediction as a function of $\dot{m}_{fresh,x}$, P_B and T_{max}/T_3

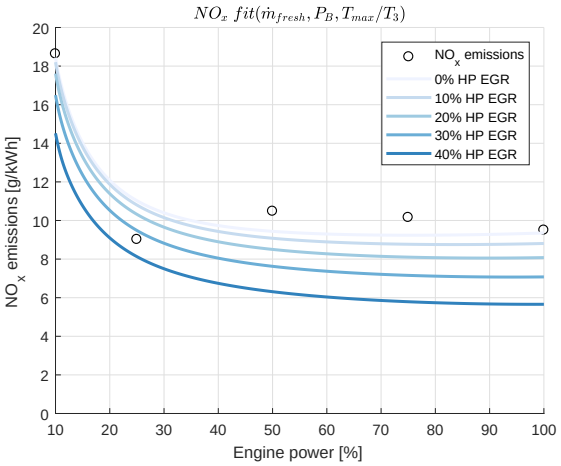

Figure D.8: g/kWh NO_x emission prediction as a function of $\dot{m}_{fresh,x}$, P_B and T_{max}/T_3